Viscous Dissipation and Joule Heating Effects on MHD Combined Heat and Mass Transfer Flow through a Porous Medium in a Rotating System

A Thesis

Submitted for the Partial Fulfillment of the Degree of

MASTER OF PHILOSOPHY
in
Mathematics

By

Md. Delowar Hossain

Roll No. 0651551, July 2006

To

Department of Mathematics
Khulna University of Engineering & Technology
Khulna-9203, Bangladesh

June, 2008

We the Examination committee do here by recommend that the thesis prepared by Md. Delowar Hossain, Roll No. 0651551, Session: July-2006 to be accepted as the partial fulfillment of the requirement of the Master of Philosophy (M. Phil.) degree in Mathematics.

Examination Committee

1. Professor Dr. Mohammad Arif Hossain
   Supervisor
   Department of Mathematics
   Khulna University of Engineering & Technology
   Khulna-9203

2. Professor Dr. Mohammad Arif Hossain
   Head
   Department of Mathematics
   Khulna University of Engineering & Technology
   Khulna-9203

3. Dr. Md. Abul Kalam Azad
   Associate Professor
   Department of Mathematics
   Khulna University of Engineering & Technology
   Khulna-9203
   Member 22/6/08

4. M. M. Touhid Hossain
   Assistant Professor
   Department of Mathematics
   Khulna University of Engineering & Technology
   Khulna-9203
   Member 22/6/08

5. Professor Dr. M. Shamsul Alam Sarkar
   Examiner (External)
   Department of Applied Mathematics
   Rajshahi University
   Rajshahi
   Member (External) 22.06.08

Contents

Declaration

I hereby declare that the thesis entitled "Viscous dissipation and joule heating effects on MHD combined heat and mass transfer flow through a porous medium in a rotating system" submitted for the partial fulfillment for the Master of Philosophy degree is done by myself under the supervision of Professor Dr. Mohammad Arif Hossain as a supervisor and is not submitted elsewhere for any other degree or diploma.

M. Delowar Hossain

(Md. Delowar Hossain)
Roll No. 0651551, Session: July 2006

Counter signed by

Arif 6/5/08

Supervisor

Professor Dr. Mohammad Arif Hossain
Head
Department of Mathematics
Khulna University of Engineering & Technology
Khulna-920300

Abstract

Viscous dissipation and *Joule* heating effects on MHD combined heat and mass transfer flow through a porous medium in a rotating system has been studied numerically. *Nacthsheim-Swigert* iteration technique is used as the main tool for the numerical approach.

The studies of the flow features mentioned above are made in different sections taking different aspects of the flow that are of practical importance. These studies are mainly based on the similarity approach. The similarity solutions have been obtained for the one dimensional unsteady MHD combined heat and mass transfer flow past an infinite vertical porous plate in a rotating system taking into account the viscous dissipation and *Joule* heating effects. Impulsively started plate moving in its own plane is considered. Similarity equations of the corresponding momentum, energy and concentration equations are derived by introducing a time dependent length scale which in fact plays the role of a similarity parameter. The suction velocity is taken to be inversely proportional to this parameter. The momentum, energy and concentration equations are solved numerically by applying the method of *Swigert* iteration technique. The above flow problem has further been considered in a steady two dimensional problem. The similarity solutions of the governing equations are obtained by employing the usual similarity technique based on large suction. The effects of the various important parameters, entering into the problems on the velocity, temperature, concentration, skin-friction, *Nusselt* and the *Sherwood* numbers are separately discussed for each problem with the help of graphs and tables.

Introduction

The aim of this dissertation is to make some numerical calculations on MHD combined heat and mass transfer flow which is of interest to the engineering community and to the investigators dealing with the problems in geophysics and astrophysics. The analyses so produced in fact arouse out of the natural tendency to investigate a subject that may be said to relate to some academic types of problems of solving the equations of the fluid mechanics. The results of this investigation may not have direct practical applications but are relevant to the problems mentioned above. It is however to be mentioned that the thermal instability investigations of MHD natural convection flows have direct application to problems in geophysics and astrophysics. The natural convection process involving the combined mechanism of heat and mass transfer are encountered in natural process, industrial applications and chemical processing systems. In our analyses the combined buoyancy effect arising from the simultaneous diffusion of thermal energy and chemical species are considered on the flow of electrically conducting fluid under the action of transversely applied magnetic field.

Considering various aspects of on MHD combined heat and mass transfer flow, the analyses presented here, as mentioned above, is classified mainly as *Swigert* iteration technique for solving the nonlinear ordinary differential equations.

In **Chapter 1**, literature review regarding MHD combined heat and mass transfer flows along with various effects are summarized and discussed from both analytical and numerical point of view. In **Chapter 2**, the basic governing equations related to the problems considered thereafter are shown in standard form. In **Chapter 3**, the calculation technique is discussed. In **Chapter 4,** a specific problem of the one dimensional unsteady MHD combined heat and mass transfer flow through a porous medium near an infinite vertical porous plate in a rotating system taking into account the viscous dissipation and Joule heating effects are considered. In **Chapter 5**, we have considered a steady two dimensional problem of the MHD combined heat and mass transfer flow through a porous medium near semi-infinite vertical porous plate in a rotating system taking into account the viscous dissipation and *Joule* heating effects based on large suction.

List of figures

Unsteady case

Steady case

List of Tables

Unsteady case

Steady case

Chapter 1

Physical Basis

1.1. Magnetohydrodynamics

Magnetohydrodynamics (MHD) is that branch of continuum mechanics which deals with the flow of electrically conducting fluids in electric and magnetic fields. Probably the largest advance towards an understanding of such phenomena came from the field of astrophysics. It has long been suspected that most of the matter in the universe is in the plasma or highly ionized gaseous state, and their studies provide much of the basic knowledge in the area of electromagnetic fluid dynamics.

As a branch of plasma physics, the field of MHD consists of the study of a continuous, electrically conducting fluid under the influence of electromagnetic fields. Originally, MHD included only the study of strictly incompressible fluid, but today the terminology is applied to studies of partially ionized gases as well. The essential requirement for problems to be analyzed under the laws of MHD is that the continuum approach be applicable.

Many natural phenomena and engineering problems are susceptible to MHD analysis. It is useful in astrophysics. Geophysicists encounter MHD phenomena in the interactions of conducting fluids and magnetic fields that are present in and around heavenly bodies. Engineers employ MHD principles in the design of heat exchangers, pumps and flow meters, in space vehicle propulsion control and re-entry, in creating novel power generating systems, and in developing confinement schemes for controlled fusion.

The most important application of MHD is in the generation of electrical power with the flow of an electrically conducting fluid through a transverse magnetic field. Recently, experiments with ionized gases have been performed with the hope of producing power on a large scale in stationary plants with large magnetic fields. Cryogenic and superconducting magnets are required to produce these very large magnetic fields. Generation of MHD power on a smaller scale is of interest for space applications.

It is generally known that, to convert the heat energy into electricity, several intermediate

transformations are necessary. Each of these steps mean a loss of energy. This naturally limits the overall efficiency, reliability and compactness of the conversion process. Methods for direct conversion to energy are now increasingly receiving attention. Of these, the fuel cell converts the chemical energy of fuel directly into electrical energy, fusion energy utilizes the energy released when two hydrogen nuclei fuse into a heavier one and thermoelectrical power generation uses a thermocouple. Magnetohydrodynamic power generation is another important new process that is receiving worldwide attention.

Faraday (1832) carried out experiments with the flow of mercury in glass tubes placed between poles of a magnet, and discovered that a voltage was induced across the tube due to the motion of the mercury across the magnetic fields, perpendicular to the direction of flow and to the magnetic field. He observed that the current generated by this induced voltage interacted with the magnetic field to slow down the motion of the fluid and this current produced its own magnetic field that obeyed Ampere's right hand rule and thus, in turn distorted the magnetic field.

The first astronomical application of the MHD theory occurred in *1899* when *Bigalow* suggested that the sun is a gigantic magnetic system. *Alfven (1942)* discovered MHD waves in the sun. These waves are produced by disturbances which propagate simultaneously in the conducting fluid and the magnetic field.

1.2. The Dimensionless Parameters

Reynolds number R_e

It is the most important parameter of the fluid dynamics of a viscous fluid. It is defined as the ratio of the inertia force to viscous force and is represented as

$$R_e = \frac{\text{Inertia force}}{\text{Viscous force}} = \frac{\rho U^2 / L}{\mu U / L^2} = \frac{UL}{\upsilon}$$

where U, L, ρ and μ are the characteristic values of velocity, length, density and coefficient of viscosity of the fluid respectively. When the Reynolds number of the system is small the viscous force is predominant and the effect of viscosity is important in the whole velocity field. When the Reynolds number is large the inertia force is predominant, and the effects of viscosity is important only in a narrow region near the solid wall or other restricted region which is known as boundary layer. If the Reynolds numbers is enormously large, the flow becomes turbulent.

Prandtl number P_r

The *Prandtl* number is the ratio of kinematics viscosity to thermal diffusivity and may be written as follows $P_r = \dfrac{\text{Kinematic viscosity}}{\text{Thermal diffusivity}} = \dfrac{\upsilon}{\dfrac{k}{\rho C_p}}$

The value of υ shows the effect of viscosity of the fluid. The smaller the value of υ is, the narrower is the region which is affected by viscosity and which is known as the boundary layer region when υ is very small. The value of $\dfrac{k}{\rho C_p}$ shows the thermal diffusivity due to heat conduction. The smaller the value of $\dfrac{k}{\rho C_p}$ is, the narrower is the region which is affected by the heat conduction and which is known as thermal boundary layer when $\dfrac{k}{\rho C_p}$ is small. Thus the *Prandtl* number shows the relative importance of heat conduction and viscosity of a fluid. For a gas the *Prandtl* number is of order of unity.

Schmidt number S_c

This the ratio of the viscous diffusivity to the chemical molecular diffusivity and is defined as

$$S_c = \frac{\text{Viscous diffusivity}}{\text{Chemical molecular diffusivity}} = \frac{\upsilon}{D_m}$$

Nusselt number N_u

The local dimensionless coefficient of heat transfer is known as *Nusselt* number and is defined as

$$N_u = \frac{-1}{\Delta T}\left(\frac{\partial T}{\partial y}\right)_{y=0}$$

Sherwood number S_h

The local dimensionless coefficient of mass transfer is known as *Sherwood* number and is defined as

$$S_h = \frac{-1}{\Delta C}\left(\frac{\partial C}{\partial y}\right)_{y=0}$$

Local Grashof number G_r

This is defined as $G_r = \dfrac{2x^3 g\beta(T_w - T_\infty)}{\upsilon^2}$ and is a measure of the relative importance of the buoyancy forces and viscous forces.

Local Modified Grashof number G_m This is defined as $G_m = \frac{2x^3 g\beta^*(C_w - C_\infty)}{\upsilon^2}$

Soret number S_0 This is defined as $S_0 = \frac{k_T(T_w - T_\infty)}{T_m(C_w - C_\infty)}$

Dufour number D_f This is defined as $D_f = \frac{D_m k_T \rho}{c_s K} \frac{(C_w - C_\infty)}{(T_w - T_\infty)}$

Eckert number E_c This is defined as $E_c = \frac{U_0^2}{c_p(T_w - T_\infty)}$

Magnetic parameter M This is defined as $M = \frac{2xB_0{}^2\sigma'}{\rho U_0}$

Rotation parameter R This is defined as $R = \frac{\Omega\sigma'^2}{\upsilon}$

Permeability parameter K This is defined as $K = \frac{2x\upsilon}{K'U_0}$

Suction number f_w This is defined as $f_w = v_0\sqrt{\frac{2x}{U_0\upsilon}}$

1.3 Suction and Injunction

For ordinary boundary layer flows with adverse pressure gradients, the boundary layer flow will eventually separate from the surface. Separation of the flow causes many undesirable features over the whole field; for instance if separation occurs on the surface of an airfoil, the lift of the airfoil will decrease and the drag will enormously increase. In some problems we wish to maintain laminar flow without separation. Various means have been proposed to prevent the separation of the boundary layer flows, suction and injection are two of them.

The stabilizing effect of the boundary layer development has been well known for several years and it is still the most of efficient, simple and common method of boundary layer control. Hence, the effect of suction on hydromagnetic boundary layer is of great interest in astrophysics. It is often necessary to prevent separation of the boundary layer to reduce the drag and attain high lift values.

Many authors have made mathematical studies on these problems, especially in the case of steady flow.

Among them the name of *Cobble (1977)* may be cited who obtained the conditions under which similarity solutions exist for hydromagnetic bounder layer flow past a semi-infinite vertical plate with or without suction. Following this, *Soundalgeker and Ramanamurthy (1980)* analyzed the thermal boundary layer. Then *Singh (1980)* studied this problems for large values of suction velocity employing asymptotic analysis in the spirit of *Nanbu (1971). Singh and Dikshit (1988)* have again adopted the asymptotic method to study the hydromagnetic effect on the boundary layer development over a continuously moving plate. In a similar way *Bestman (1990 a)* studied the boundary layer flow past a semi-infinite heated porous plate for a two component plasma.

On the other hand, one of the important problems faced by those who are engaged in high speed flow is the cooling of the surface to avoid the structural failures as a result of frictional heating and other factors. In these respect, the possibility of using injection at the surface is a measure to cool the body in the high temperature fluid.

Injection of secondary fluid through porous walls is of practical importance in film cooling of turbine blades in combustion chambers. In such applications injection usually occurs normal to the surface and the injection fluid may be similar to or different from the primary fluid. In some recent applications, however, it has been recognized that the cooling efficiency can be enhanced by vectored injection at an angle other than 90^0 to the surface. A few workers including *Inger and Swearn (1975)* have theoretically proved this feature for a linear boundary layer. In addition, most previous calculations have been limited to injection rates ranging from small to moderate. *Rapits et al. (1980)* studied the free convection effects on the flow field of an incompressible viscous dissipative fluid past an infinite vertical porous plate which is accelerated in its own plane. The fluid is subjected to a normal velocity of suction/injection proportional to time $\left(\frac{1}{\sqrt{t}}\right)$, and the plate is perfectly insulated, i.e. there is no heat transfer between the fluid and the plate. *Hasimoto (1957)* studied the boundary layer growth on an infinite vertical plate. Starting at time $t = 0$, with uniform suction or injection, exact solutions of the *Navier-Stokes* equations of motion were derived for the case of uniform suction and injection which was taken to be steady or proportional to time $\left(\frac{1}{\sqrt{t}}\right)$. Numerical calculations are also made for the case of impulsive motion of the plate. In the case of injection, velocity profiles have injection points. The qualitative natures of the flow in both the suction and injection cases are the same which are obtained from the results of the corresponding studies on steady boundary layer, so far obtained.

1.4. Free and Forced Convection

In nature a number of practical situations involve convective heat transfer which is neither "forced" nor "free". The circumstances arise when a fluid is forced to flow over a heated

surface at a rather low velocity. Coupled with the forced flow velocity there is a convective velocity which is generated by the buoyancy forces resulting from a reduction in fluid density near the heated surface. The heating of rooms and building by the use of radiators is a familiar example of heat transfer by free convection. Heat losses from hot pipes, ovens etc., surrounded by cooler air, are at least in part, due to free convection. However, the mixed types of problems are very important and have many industrial and technological applications.

Pohlhausen (1921) first studied the steady thermal boundary layer flow past a semi infinite vertical plate using the momentum integral method. Similarity solution to this problem was given by *Ostrach (1953). Siegel (1958)* first studied the transient free convective flow past a semi-infinite vertical plate by an integral method.

A summary of the combined free and forced convection effects in tubes has been given by *Metais and Eckert (1964).* Since then many papers have been published on forced and free convection flow past a semi infinite vertical plate. Some of them are due to *Sparrow and Gregg (1959), Szewczyk (1964), Merkin (1969), Mori (1961), Eshghy (1964)* and *Acrivos (1958). Sparrow* and *Gregg, Szewczyk, Merkin* and *Mori* all have used numerical solutions to the similarity equations, whereas *Eshghy* and *Acrivos* both used an integral method for solving the forced and free convection problem. In recent past *Soundalgekar et. al. (1981)* studied the combined free and forced convection flow past a vertical porous plate.

On the other hand the flow through very porous media is very prevalent in nature and therefore the study of flow through porous medium has become of principal interest in many scientific and engineering applications. The investigation of flow streaming into a porous and permeable medium with arbitrary but smooth surfaces was done by *Yamamoto and Iwamura (1976).* Further analysis for a free convection in a porous medium bounded by an infinite plate was made by *Raptis (1983, 1985), Raptis and Perdikis (1982,1985a,b),Raptis* et.al. *(1981).* Latter, *Bestman (1990 a,b)* made analytical efforts to study the free- convection flow in a very porous medium, respectively, with mass transfer and chemical reaction with finite *Arrhenius* activation energy. However, *Raptis and Perdikis (1988)* made a numerical study of the combined free and forced convective flow through a very porous medium bounded by a semi-infinite vertical porous plate. In addition to other effects their results display the effect of the permeability parameter on the velocity and temperature field. Although the analytical solutions of *Bestman (1990 a),* a complement to the work of *Raptis and Perdikis (1988),* are valid for large suction.

Following the work of *Raptis and Perdikis (1988), Sattar (1992)* obtained an analytical solution to the same problem by perturbation technique adopted by *Singh and Dikshit (1988).* The solutions of *Sattar* are however concise. He obtained the solutions in the form of zeroth

order and first order respectively for temperature and velocity distributions. These solutions are valid for the *Prandtl* number P_r other than one.

1.5. MHD Boundary Layer

Boundary layer phenomena occurs when the influence of a physical quantity is restricted to small regions near confining boundaries. This phenomena occurs when the non-dimensional diffusion parameters the Reynolds number, and the *Peclet* number or the magnetic *Reynolds* number are large. The boundary layers are then the velocity and thermal or magnetic boundary layers and each thickness is inversely proportional to the square root of the associated diffusion number. *Prandtl* fathered classical fluid dynamic boundary theory by observing, from experimental flows, that for large Reynolds number, the viscosity and thermal conductivity appreciably influenced the flow only near a wall. When distant measurements in the flow direction are compared with a characteristic dimension in that direction, transverse measurements compared with the boundary layer thickness, and velocities compared with the free stream velocity, the *Navier-Stokes* and energy equations can be considerably simplified by neglecting small quantities. The number of component equations is reduced to those in the flow direction and pressure changes across the boundary layer are negligible. The pressure is then only a function of the flow direction and can be determined from the inviscid flow solution. Also the number of viscous term is reduced to the dominant term and the heat conduction in the flow direction is negligible.

MHD boundary layer flows are separated into two types by considering the limiting cases of a very large or a negligible small magnetic Reynolds number. When the magnetic field is oriented in an arbitrary direction relative to a confining surface and the *magnetic Reynolds number* is very small, the flow direction component of the magnetic interaction and the corresponding Joule heating is only a function of the transverse magnetic field component and local velocity in the flow direction. Changes in the transverse magnetic field component and pressure across the boundary layer are negligible. The thickness of the magnetic boundary layer is very large and the induced magnetic field is negligible. However, when the magnetic Reynolds number is very large, the magnetic boundary layer thickness is small and is of nearly the same size as the viscous and thermal boundary layers and then the MHD boundary layer equations must be solved simultaneously, in this case, the magnetic field moves with the flow and is called frozen mass.

1.6. Heat and Mass Transfer

Combined heat and mass transfer problems are of importance in many processes and have therefore received a considerable amount of attention. In many mass transfer processes, heat transfer considerations arise owing to chemical reaction and are often due to the nature of the process. In processes such as drying, evaporation at the surface of water body, energy transfer in a wet cooling tower and the flow in a desert cooler, heat and mass transfer occur simultaneously. In many of these processes, the interest lies in the determination of the total energy transfer, although in processes such as drying, the interest lies mainly in the overall mass transfer for moisture removal. Natural convection processes involving the combined mechanisms are also encountered in many natural processes, such as evaporation, condensation and agricultural drying, in many industrial applications involving solutions and mixtures in the absence of an externally induced flow and in many chemical processing systems. In many processes such as the curing of plastics, cleaning and chemical processing of materials relevant to the manufacture of printed circuitry, manufacture of pulp-insulated cables etc., the combined buoyancy mechanisms arise and the total energy and material transfer resulting from the combined mechanisms, has to be determined.

The basic problem is governed by the combined buoyancy effects arising from the simultaneous diffusion of thermal energy and of chemical species. Therefore the continuity, momentum, energy and concentration equations are coupled through the buoyancy terms alone, if the other effects, such as the *Soret* and *Dufour* effects are neglected.

Mathers et al. (1957) treated a problem in which uniform temperature and uniform species concentration at the surface be assumed and the obtained results are expected to be valid for P_r and S_c values around 1.0 with one buoyancy effect being small compared to each other as a boundary layer flow for low species concentration, neglecting inertia effects. Results were obtained numerically for $P_r = 1.0$ and S_c varying from 0.1 *to* 10. *Lowell and Adams (1967)* and *Gill et al. (1965)* also considered this problem, including additional effects such as appreciable normal velocity at the surface and comparable species concentrations in the mixture. Similar solutions were investigated by *Lowel and Adams (1967)* and by *Adams and Lowell (1968). Light foot (1968)* and *Saville and Churchill (1970)* considered some asymptotic solutions. *Adams and McFadden (1966)* presented experimental measurements of heat and mass transfer parameters, with opposed buoyancy effects. *Gebhart and Pera(1971)* studied laminar vertical natural convection flows resulting from the combined buoyancy mechanisms in terms of similarity solutions. Similar analyses have been carried out by *Pera and Gebhart(1972)* for flow over horizontal surfaces and by *Mollendrof and Gebhart(1974)* for

axisymetric flows, particularly for the axisymetric plume.

Boura and Gebhart (1976), Hubbell and Gebhart (1974) and *Tenner and Gebhart(1971)* have studied buoyant free boundary flows in a concentration-stratified medium. *Agrawal et al.(1977,1980)* have studied the combined buoyancy effects on the thermal and mass diffusion on MHD natural convection flows, and it is observed that, for the fixed G_r and P_r the value of Xt (dimensionless length parameter) decreases as the strength of the magnetic parameter increases. *Georgantopoulos et al. (1981)* discussed the effects of free convective and mass transfer in a conducting liquid, when the fluid is subjected to a transverse magnetic field. *Haldavnekar and Soundalgekar (1977)* studied the effects of mass transfer on free convective flow of an electrically conducting viscous fluid past an infinite porous plate with constant suction and transversely applied magnetic field. An exact analysis was made by *Soundalgekar et al.(1979)* of the effects of mass transfer and the free convection currents on the MHD Stokes (Rayleigh) problem for the flow of an electrically conducting, incompressible viscous fluid past an impulsively started vertical plate under the action of a transversely applied magnetic field. The heat due to viscous and Joule dissipation and induced magnetic field are considered. During the course of discussion, the effects of heating $G_r < 0$ of the plate by free convection currents, G_m (modified Grashof number), S_c and M on the velocity and the skin friction are studied. *Nanousis and Goudas (1979)* have studied the effects of mass transfer on free convective problem in the Stokes problem for an infinite vertical limiting surface. *Georgantopolous and Nanousis (1980)* have considered the effects of the mass transfer on free convection flow of an electrically conducting viscous fluid (e.g of a stellar atmosphere) past an impulsively started infinite vertical limiting surface(e.g of star) in the presence of transverse magnetic field. Solution for the velocity and skin friction in closed form are obtained with the help of the *Laplace* transform technique, and the results obtained for the various values of the parameters (S_c, P_r and M) are given in graphical form. *Raptis and Kafoussias (1982)* presented the analysis of free convection and mass transfer steady hydromagnetic flow of an electrically conducting viscous incompressible fluid, through a porous medium, occupying a semi-infinite region of the space bounded by an infinite vertical and porous plate under the action of transverse magnetic field. Approximate solution have been obtained for the velocity, temperature, concentration field and the rate of heat transfer. The effects of different parameters on the velocity field and the rate of heat transfer are discussed for the case of air (*Prandtl number* $P_r = 0.71$) and the water vapour (*Schmidt number* $S_c = .60$). *Raptis and Tzivanidis(1983)* considered the effects of variable suction /injection on the unsteady two dimensional free convective flow with mass transfer of an electrically conducting fluid past a vertical accelerated plate in the presence of transverse

magnetic field. Solutions of the governing equations of the flow are obtained with the power series. An analysis of two dimensional steady free convective flow of a conducting fluid, in the presence of a magnetic field and a foreign mass, past an infinite vertical porous and unmoving surface is carried out by *Raptis (1983)*, when the heat flux is constant at the limiting surface and the magnetic Reynolds number of the flow is not small. Assuming constant suction at the surface, approximate solutions of the coupled nonlinear equations are derived for the velocity field, the temperature field, the magnetic field and for their related quantities. *Agrawal et al. (1987)* consider the steady laminar free convection flow with mass transfer of an electrically conducting liquid along a plane wall with periodic suction.

1.7. Rotation

In 1950's, considerable progress has been made in the general theory of rotating fluids because of its application in cosmic and geophysical sciences as pionted out by *Greenspan (1968)*. The steady and unsteady *Ekman* layers of an incompressible fluid have been investigated as basic boundary layers in a rotating fluid appearing in the oceanic, atmospheric, cosmic fluid dynamics and solar Physics or geophysical problems. It is well known that, in a rotating fluid near a flat plate, an *Ekman* layer exists where the viscous and Coriolis forces are of the same order of magnitude. The *Ekman* layer flow on a horizontal plate has been studied by *Batchelor(1970). Greenspan and Howard(1963)* have analyzed an unsteady rotating flow past an impermeable or permeable plate under the assumption of rigid body rotation. The effect of a uniform transverse magnetic field on such a layer was investigated by *Gupta(1972). Mazumder et al.(1976a, b)* have studied the flow and heat transfer in a hydromagnetic *Ekman* layer on a porous plate with *Hall* effects. It was observed that, with increasing *Hall* parameter, axial shear stress decreases and the transverse shear stress reaches a maximum and then decreases when M is constant. For M fixed, the *Ekman* layer thickness increases with increase of *Hall* parameter and decreases with increasing M when *Hall* parameter is constant. The energy equation has also been solved, and it has been observed that the asymptotic solution is possible for the case of suction only. Without *Hall* current, this problem has been solved by *Gupta and Soundalgekar(1975)*. These studies ware concerned with channel flow. *Debnath(1972,1975)* has made a major contribution to the study of unsteady hydromagnetic and hydrodynamic boundary layer flows in a rotating viscous fluid system. *Soundalgekar and Pop(1979)* have studied the free convection effects in rotating viscous fluid past an infinite vertical porous plate. *Murty and Ram(1978)* have studied a steady asymptotic solution for the temperature distribution in the case of flow past a porous plate in a rotating frame of reference. In particular,

the temperature distribution for an MHD *Ekman* layer on a porous plate is obtained. It was seen that a steady asymptotic solution is possible for suction, but no steady temperature field is possible for blowing. Further, it was observed from the results that suction and magnetic field have opposing influences on the rate of heat transfer. *Debnath and Mukherjee(1977)* obtained the solution for *Ekman* and *Hartmann* layers on a porous plate with variable suction or blowing. *Mazumder(1977)* studied the combined effects of *Hall* current and rotation on hydromagnetic flow over an oscillating porous plate. *Bathaiah(1978)* considered forced oscillations of an enclosed rotating fluid under a uniform magnetic field. *Bhattacharya and Jain(1977)* discussed the stability of an infinite horizontal layer of electrically conducting incompressible fluid which lost heat throughout its volume, and at constant rate, when the fluid was in a state of uniform rotation and in the presence of a magnetic field. The value of the critical *Rayleigh* number R_a was found to decrease with an increase in the rate of heat loss, showing that the layer becomes less stable. It was observed that the destabilizing effect of the heat source parameter is more prominent for small values of the magnetic field parameter and the *Taylor* number. *Debnath et at. (1979)* studied the effect of *Hall* current on unsteady hydromagnetic flow past a porous plate in a rotating fluid system.

Raptis et al. (1981) studied the effects of a transverse magnetic field on the hydromagnetic free convective flow in a rotating fluid system. Exact solutions for the velocity and temperature field have been derived. The effects of M on the flow characteristics were discussed. An exact solution of the temperature profile in the MHD flow in a rotating straight channel is derived by *Bhat(1982)*. It was observed that the rate of heat transfer decreases with increasing magnetic parameter M when k is small, but at large values of k it increases with increasing M. Unsteady hydromagnetic flow of an electrically conducting viscous incompressible fluid in a rotating system under the influence of a transverse magnetic field was investigated by *Seth et al. (1982)*. It was found that the shear stress components due to the primary flow to decreases whereas that due to the secondary flow to increase with the increase in rotations parameter. *Seth and Jana(1981)* have studied the unsteady hydromagnetic flow past a porous plate in a rotating medium with time independent free stream.

1.8. Thermal and Mass Diffusions

In the above mentioned studies, heat and mass transfer occur simultaneously in a moving fluid where the relations between the fluxes and the driving potentials are of more intricate nature. In general, the thermal diffusion effects is of a smaller order of magnitude than the effects described by *Fourier's* or *Fick's* laws and is often neglected in heat and mass transfer process. However, exceptions are observed therein. The thermal diffusion (*Soret*) effect, for instance, has been

utilized for isotope separation and in mixtures between gases with very light molecular weight (H_2, H_e) and of medium molecular weight (N_2, air), the diffusion- thermo (*Dufour*) effect was found to be of order of considerable magnitude such that it cannot be ignored *(Eckert and Drake, 1972)*.

In view of the importance of above mentioned effects, *Jha and Singh (1990)* and *Kafoussias and Williams (1995)* studied *Soret* and *Dufour* effects on mixed free-forced convective and mass transfer boundary layer flow with temperature dependent viscosity. *Anghel et al.(2000)* investigated the *Dufour* and *Soret* effects on free convection boundary layer flow over a vertical surface embedded in a porous medium. Recently, *Postelnicu(2004)* studied numerically the influence of a magnetic field on heat and mass transfer by natural convection from vertical surfaces in porous media considering *Soret* and *Dufour* effects. Quite recently, *Alam and Rahman (2006)* investigated the *Dufour* and *Soret* effects on mixed convection flow past a vertical porous flat plate with variable suction.

Chapter 2

The Basic Governing Equations

The *Navier-Stokes* equation, energy equation and concentration equation, together with the Maxwell equations, form the basis for studying Magnetofluid Dynamics (MFD). In MFD, we consider a conducting fluid that is approximately neutral; the charge density in the Maxwell equations must then be interpreted as an excess charge density which is not large. If we disregard the excess charge density, then we must disregard the displacement current. In most problems, the displacement current, excess charge density, excess charge body force and the current due to convection of the excess charge are small. The electrodynamics equations to be used are then pre-Maxwell equations and the complete set becomes

$$\nabla.\mathbf{D} = 0 \tag{2.1}$$

$$\nabla.\mathbf{J} = 0 \tag{2.2}$$

$$\nabla.\mathbf{B} = 0 \tag{2.3}$$

$$\nabla \wedge \mathbf{H} = \mathbf{J} \tag{2.4}$$

$$\nabla \wedge \mathbf{E} = -\frac{\partial \mathbf{B}}{\partial t} \tag{2.5}$$

$$\mathbf{D} = \varepsilon \mathbf{E} \tag{2.6}$$

$$\mathbf{B} = \mu_e \mathbf{H} \tag{2.7}$$

$$\mathbf{J} = \sigma' \left(\mathbf{E} + \mathbf{q} \wedge \mathbf{B}\right) \tag{2.8}$$

where $\mathbf{D}$ is the electric displacement, $\mathbf{J}$ is the current density, $\mathbf{B}$ is the magnetic induction, $\mathbf{H}$ is the magnetic field strength, $\mathbf{E}$ is the electrostatic field, ε is the electrical permeability, σ' is the electrical conductivity, $\mathbf{q}$ is the velocity, μ_e is the magnetic permeability.

The continuity equation for a viscous compressible electrically conducting fluid in vector form is

$$\frac{\partial \rho}{\partial t} + \nabla.(\rho \mathbf{q}) = 0 \tag{2.9}$$

where ρ is the density of the fluid and $\mathbf{q}$ is the fluid velocity.

For incompressible fluid, the equation (2.9) becomes

$$\nabla.\mathbf{q} = 0 \tag{2.10}$$

In three-dimensional Cartesian coordinate system the equation (2.10) becomes

$$\frac{\partial u}{\partial x}+\frac{\partial v}{\partial y}+\frac{\partial w}{\partial z}=0 \tag{2.11}$$

where u, v and w are the velocity components in the x, y and z direction respectively.

The *Navier-Stokes* equation for viscous compressible fluid in vector form is

$$\frac{d\mathbf{q}}{dt}=\mathbf{F}-\frac{1}{\rho}\nabla P+\frac{\upsilon}{3}\nabla(\nabla.\mathbf{q})+\upsilon\nabla^2\mathbf{q} \tag{2.12}$$

where $\mathbf{F}$ is the body force per unit mass, P is the fluid pressure and υ is the kinematic viscosity. For incompressible fluid, the equation (2.12) becomes

$$\frac{d\mathbf{q}}{dt}=\mathbf{F}-\frac{1}{\rho}\nabla P+\upsilon\nabla^2\mathbf{q} \tag{2.13}$$

When the system rotates with constant angular velocity $\mathbf{\Omega}$, the equation (2.13) becomes

$$\frac{d\mathbf{q}}{dt}=\mathbf{F}-\frac{1}{\rho}\nabla P+\upsilon\nabla^2\mathbf{q}-2\mathbf{\Omega}\wedge\mathbf{q} \tag{2.14}$$

When the fluid moves through a porous medium, the equation (2.14) becomes

$$\frac{d\mathbf{q}}{dt}=\mathbf{F}-\frac{1}{\rho}\nabla P+\upsilon\nabla^2\mathbf{q}-2\mathbf{\Omega}\wedge\mathbf{q}-\frac{\upsilon}{K'}\mathbf{q}, \tag{2.15}$$

where K' is the permeability of the porous medium.

When electrically conducting fluid moves through a magnetic field of intensity $\mathbf{H}$ ($\mathbf{B}=\mu_e\mathbf{H}$, where $\mathbf{B}$ is the magnetic field), then the equation (2.15) becomes the MHD equation in the following form,

$$\frac{d\mathbf{q}}{dt}=\mathbf{F}-\frac{1}{\rho}\nabla P+\upsilon\nabla^2\mathbf{q}-2\mathbf{\Omega}\wedge\mathbf{q}-\frac{\upsilon}{K'}\mathbf{q}+\frac{1}{\rho}\mathbf{J}\wedge\mathbf{B}, \tag{2.16}$$

where $\mathbf{J}\wedge\mathbf{B}$ is the force on the fluid per unit volume produced by the interaction of the electric and magnetic field (called *Lorentz* force).

We have $$\frac{d\mathbf{q}}{dt}=\frac{\partial\mathbf{q}}{\partial t}+(\mathbf{q}.\nabla)\mathbf{q} \tag{2.17}$$

then the equation (2.16) becomes

$$\frac{\partial\mathbf{q}}{\partial t}+(\mathbf{q}.\nabla)\mathbf{q}=\mathbf{F}-\frac{1}{\rho}\nabla P+\upsilon\nabla^2\mathbf{q}-2\mathbf{\Omega}\wedge\mathbf{q}-\frac{\upsilon}{K'}\mathbf{q}+\frac{\mu_e}{\rho}\mathbf{J}\wedge\mathbf{H}, \tag{2.18}$$

where $\mathbf{B}=\mu_e\mathbf{H}$.

The MHD energy equation for a viscous incompressible electrically conducting fluid with viscous dissipation, mass diffusion and *Joule* heating term in vector form is

$$\frac{\partial T}{\partial t}+(\mathbf{q}.\nabla)T=\frac{k}{\rho c_p}\nabla^2T+\frac{1}{\rho c_p}\phi+\frac{J^2}{\rho\sigma' c_p}+\frac{D_m k_T}{c_s c_p}\nabla^2C \tag{2.19}$$

where k is the thermal conductivity of the medium, ρ is the density of the fluid, c_p is the specific heat at constant pressure, D_m is the coefficient of mass diffusivity, k_T is the thermal diffusion ratio and c_s is the concentration susceptibility, T is the fluid temperature, $\frac{J^2}{\sigma'}$ is the *Joule* heating term, where $J^2 = \sigma'^2\mu_e^2(vH_z - wH_y)^2 + \sigma'^2\mu_e^2(wH_x - uH_z)^2 + \sigma'^2\mu_e^2(uH_y - vH_x)^2$, σ' is the electrical coductivity, C is the species concentration variable, ϕ denote the dissipation function involving the viscous stress and it represents the rate at which energy is being dissipated per unit volume through the action of viscosity. In fact the energy is dissipated in a viscous fluid in motion on account of internal friction and for an incompressible fluid

$$\phi = \mu\left[2\left\{\left(\frac{\partial u}{\partial x}\right)^2 + \left(\frac{\partial v}{\partial y}\right)^2 + \left(\frac{\partial w}{\partial z}\right)^2\right\} + \left(\frac{\partial v}{\partial x} + \frac{\partial u}{\partial y}\right)^2 + \left(\frac{\partial w}{\partial y} + \frac{\partial uv}{\partial z}\right)^2 + \left(\frac{\partial u}{\partial z} + \frac{\partial w}{\partial x}\right)^2\right] \tag{2.20}$$

which is always positive, since all the terms are quadratic, where μ is the coefficient of viscosity.

The MHD concentration equation for a viscous incompressible electrically conducting fluid with thermal diffusion in vector form is

$$\frac{\partial C}{\partial t} + (\mathbf{q}.\nabla)C = D_m\nabla^2 C + \frac{D_m k_T}{T_m}\nabla^2 T \tag{2.21}$$

where T_m is the mean fluid temperature.

The generalized Ohm's law in the absence of electric field (*Mayer,* 1958), is of the form

$$\mathbf{J} + \frac{\omega_e\tau_e}{H_0}\mathbf{J}\wedge\mathbf{H} = \sigma'\left(\mu_e\mathbf{q}\wedge\mathbf{H} + \frac{1}{en_e}\nabla P_e\right) \tag{2.22}$$

where ω_e is the cyclotron frequency, τ_e is the electron collision time, e is the electric charge, n_e is the number density of electron, P_e is the pressure of electron, $\mathbf{J}$ is the current density vector, $\mathbf{H}$ is the magnetic field intensity, H_0 is the applied constant magnetic field, μ_e is the magnetic permiablity, σ' is the electric conductivity, $\mathbf{q} = (u, v, w)$ is the velocity vector.

Neglecting the Hall-current, we have from equation (2.22)

$$\mathbf{J} = \sigma'(\mu_e\mathbf{q}\wedge\mathbf{H}) \ [\because \omega_e\tau_e = 0 \, and \, P_e = 0] \tag{2.23}$$

$$\text{Let } \mathbf{H} = (H_x, H_y, H_z), \tag{2.24}$$

where H_x, H_y, H_z be the components of magnetic field strength.

$$\text{Then } \mathbf{q}\wedge\mathbf{H}=\begin{vmatrix}\hat{i} & \hat{j} & \hat{k}\\ u & v & w\\ H_x & H_y & H_z\end{vmatrix}=\left(vH_z-wH_y\right)\ \hat{i}+\left(wH_x-uH_z\right)\ \hat{j}+\left(uH_y-vH_x\right)\ \hat{k} \tag{2.25}$$

Therefore the equation (2.23) becomes

$$\mathbf{J}=\sigma'\mu_e\left(vH_z-wH_y\right)\hat{i}+\sigma'\mu_e\left(wH_x-uH_z\right)\hat{j}+\sigma'\mu_e\left(uH_y-vH_x\right)\hat{k} \tag{2.26}$$

$$\text{Then } \mathbf{J}\wedge\mathbf{H}=\begin{vmatrix}\hat{i} & \hat{j} & \hat{k}\\ \sigma'\mu_e\left(vH_z-wH_y\right) & \sigma'\mu_e\left(wH_x-uH_z\right) & \sigma'\mu_e\left(uH_y-vH_x\right)\\ H_x & H_y & H_z\end{vmatrix}$$

$$=\sigma'\mu_e\left\{\left(wH_xH_z-uH_z^2\right)-\left(uH_y^2-vH_xH_y\right)\right\}\hat{i}+\sigma'\mu_e\left\{\left(uH_xH_y-vH_x^2\right)-\left(vH_z^2-wH_yH_z\right)\right\}\hat{j}$$

$$+\sigma'\mu_e\left\{\left(vH_yH_z-wH_y^2\right)-\left(wH_x^2-uH_xH_z\right)\right\}\hat{k}$$

$$=\left(\sigma'\mu_e wH_xH_z-\sigma'\mu_e uH_z^2-\sigma'\mu_e uH_y^2+\sigma'\mu_e vH_xH_y\right)\hat{i}$$

$$+\left(\sigma'\mu_e uH_xH_y-\sigma'\mu_e vH_x^2-\sigma'\mu_e vH_z^2+\sigma'\mu_e wH_yH_z\right)\hat{j}$$

$$+\left(\sigma'\mu_e vH_yH_z-\sigma'\mu_e wH_y^2-\sigma'\mu_e wH_x^2+\sigma'\mu_e uH_xH_z\right)\hat{k} \tag{2.27}$$

From equation (2.26)

$$J^2=\mathbf{J}\bullet\mathbf{J}=\left[\sigma'\mu_e\left(vH_z-wH_y\right)\hat{i}+\sigma'\mu_e\left(wH_x-uH_z\right)\hat{j}+\sigma'\mu_e\left(uH_y-vH_x\right)\hat{k}\right]$$

$$\bullet\left[\sigma'\mu_e\left(vH_z-wH_y\right)\hat{i}+\sigma'\mu_e\left(wH_x-uH_z\right)\hat{j}+\sigma'\mu_e\left(uH_y-vH_x\right)\hat{k}\right]$$

$$=\sigma'^2\mu_e^2(vH_z-wH_y)^2+\sigma'^2\mu_e^2(wH_x-uH_z)^2+\sigma'^2\mu_e^2(uH_y-vH_x)^2 \tag{2.28}$$

$$\text{Let } \boldsymbol{\Omega}=\left(\Omega_x,\Omega_y,\Omega_z\right) \text{ and } \mathbf{q}=(u,v,w). \tag{2.29}$$

$$\text{Then } \Omega\wedge\mathbf{q}=\begin{vmatrix}\hat{i} & \hat{j} & \hat{k}\\ \Omega_x & \Omega_y & \Omega_z\\ u & v & w\end{vmatrix}=\left(w\Omega_y-v\Omega_z\right)\hat{i}+\left(u\Omega_z-w\Omega_x\right)\hat{j}+\left(v\Omega_x-u\Omega_y\right)\hat{k} \tag{2.30}$$

$$\text{Let } \mathbf{F}=\left(F_x,F_y,F_z\right), \tag{2.31}$$

where F_x,F_y,F_z be the components of body force.

With the help of the equations (2.27), (2.29)- (2.31), the equation (2.18) becomes

$$\frac{\partial u}{\partial t}+u\frac{\partial u}{\partial x}+v\frac{\partial u}{\partial y}+w\frac{\partial u}{\partial z}=F_x-\frac{1}{\rho}\frac{\partial P}{\partial x}+\upsilon\left(\frac{\partial^2 u}{\partial x^2}+\frac{\partial^2 u}{\partial y^2}+\frac{\partial^2 u}{\partial z^2}\right)-2\left(w\Omega_y-v\Omega_z\right)-\frac{\upsilon}{K'}u$$

$$+\frac{\sigma'\mu_e{}^2}{\rho}\left\{wH_xH_z-uH_z^2-uH_y^2+vH_xH_y\right\} \tag{2.32}$$

$$\frac{\partial v}{\partial t}+u\frac{\partial v}{\partial x}+v\frac{\partial v}{\partial y}+w\frac{\partial v}{\partial z}=F_y-\frac{1}{\rho}\frac{\partial P}{\partial y}+\upsilon\left(\frac{\partial^2 v}{\partial x^2}+\frac{\partial^2 v}{\partial y^2}+\frac{\partial^2 v}{\partial z^2}\right)-2\left(u\Omega_z-w\Omega_x\right)-\frac{\upsilon}{K'}v$$

$$+\frac{\sigma'\mu_e^{\,2}}{\rho}\left\{uH_xH_y-vH_x^2-vH_z^2+wH_yH_z\right\} \tag{2.33}$$

$$\frac{\partial w}{\partial t}+u\frac{\partial w}{\partial x}+v\frac{\partial w}{\partial y}+w\frac{\partial w}{\partial z}=F_z-\frac{1}{\rho}\frac{\partial P}{\partial z}+\upsilon\left(\frac{\partial^2 w}{\partial x^2}+\frac{\partial^2 w}{\partial y^2}+\frac{\partial^2 w}{\partial z^2}\right)-2\left(v\Omega_x-u\Omega_y\right)-\frac{\upsilon}{K'}w$$

$$+\frac{\sigma'\mu_e^{\,2}}{\rho}\left\{vH_yH_z-wH_y^2-wH_x^2+uH_xH_z\right\} \tag{2.34}$$

In three-dimensional Cartesian coordinate system the equation (2.19) with the help of equation (2.20), (2.28) becomes

$$\frac{\partial T}{\partial t}+u\frac{\partial T}{\partial x}+v\frac{\partial T}{\partial y}+w\frac{\partial T}{\partial z}=\frac{k}{\rho c_p}\left(\frac{\partial^2 T}{\partial x^2}+\frac{\partial^2 T}{\partial y^2}+\frac{\partial^2 T}{\partial z^2}\right)+\frac{1}{\rho c_p}\phi+\frac{D_m k_T}{c_s c_p}\left(\frac{\partial^2 C}{\partial x^2}+\frac{\partial^2 C}{\partial y^2}+\frac{\partial^2 C}{\partial z^2}\right)$$

$$+\frac{\sigma'\mu_e^{2}}{\rho c_p}\left[(vH_z-wH_y)^2+(wH_x-uH_z)^2+(uH_y-vH_x)^2\right] \tag{2.35}$$

where ϕ is defined in equation (2.20).

In three-dimensional Cartesian coordinate system the equation (2.21) becomes

$$\frac{\partial C}{\partial t}+u\frac{\partial C}{\partial x}+v\frac{\partial C}{\partial y}+w\frac{\partial C}{\partial z}=D_m\left(\frac{\partial^2 C}{\partial x^2}+\frac{\partial^2 C}{\partial y^2}+\frac{\partial^2 C}{\partial z^2}\right)+\frac{D_m k_T}{T_m}\left(\frac{\partial^2 T}{\partial x^2}+\frac{\partial^2 T}{\partial y^2}+\frac{\partial^2 T}{\partial z^2}\right) \tag{2.36}$$

Thus in three-dimensional Cartesian coordinate system the continuity equation, the momentum equations, the energy equation and the concentration equations become

The continuity equation:

$$\frac{\partial u}{\partial x}+\frac{\partial v}{\partial y}+\frac{\partial w}{\partial z}=0 \tag{2.37}$$

The momentum equations:

$$\frac{\partial u}{\partial t}+u\frac{\partial u}{\partial x}+v\frac{\partial u}{\partial y}+w\frac{\partial u}{\partial z}=F_x-\frac{1}{\rho}\frac{\partial P}{\partial x}+\upsilon\left(\frac{\partial^2 u}{\partial x^2}+\frac{\partial^2 u}{\partial y^2}+\frac{\partial^2 u}{\partial z^2}\right)-2\left(w\Omega_y-v\Omega_z\right)-\frac{\upsilon}{K'}u$$

$$+\frac{\sigma'\mu_e^{\,2}}{\rho}\left\{wH_xH_z-uH_z^2-uH_y^2+vH_xH_y\right\} \tag{2.38}$$

$$\frac{\partial v}{\partial t}+u\frac{\partial v}{\partial x}+v\frac{\partial v}{\partial y}+w\frac{\partial v}{\partial z}=F_y-\frac{1}{\rho}\frac{\partial P}{\partial y}+\upsilon\left(\frac{\partial^2 v}{\partial x^2}+\frac{\partial^2 v}{\partial y^2}+\frac{\partial^2 v}{\partial z^2}\right)-2\left(u\Omega_z-w\Omega_x\right)-\frac{\upsilon}{K'}v$$

$$+\frac{\sigma'\mu_e^{\,2}}{\rho}\left\{uH_xH_y-vH_x^2-vH_z^2+wH_yH_z\right\} \tag{2.39}$$

$$\frac{\partial w}{\partial t}+u\frac{\partial w}{\partial x}+v\frac{\partial w}{\partial y}+w\frac{\partial w}{\partial z}=F_z-\frac{1}{\rho}\frac{\partial P}{\partial z}+\upsilon\left(\frac{\partial^2 w}{\partial x^2}+\frac{\partial^2 w}{\partial y^2}+\frac{\partial^2 w}{\partial z^2}\right)-2\left(v\Omega_x-u\Omega_y\right)-\frac{\upsilon}{K'}w$$

$$+\frac{\sigma'\mu_e^{\ 2}}{\rho}\left\{vH_yH_z - wH_y^2 - wH_x^2 + uH_xH_z\right\} \tag{2.40}$$

The energy equation:

$$\frac{\partial T}{\partial t}+u\frac{\partial T}{\partial x}+v\frac{\partial T}{\partial y}+w\frac{\partial T}{\partial z}=\frac{k}{\rho c_p}\left(\frac{\partial^2 T}{\partial x^2}+\frac{\partial^2 T}{\partial y^2}+\frac{\partial^2 T}{\partial z^2}\right)+\frac{D_m k_T}{c_s c_p}\left(\frac{\partial^2 C}{\partial x^2}+\frac{\partial^2 C}{\partial y^2}+\frac{\partial^2 C}{\partial z^2}\right)$$

$$+\frac{\upsilon}{c_p}\left[2\left\{\left(\frac{\partial u}{\partial x}\right)^2+\left(\frac{\partial v}{\partial y}\right)^2+\left(\frac{\partial w}{\partial z}\right)^2\right\}+\left(\frac{\partial v}{\partial x}+\frac{\partial u}{\partial y}\right)^2+\left(\frac{\partial w}{\partial y}+\frac{\partial v}{\partial z}\right)^2+\left(\frac{\partial u}{\partial z}+\frac{\partial w}{\partial x}\right)^2\right]$$

$$+\frac{\sigma'\mu_e^2}{\rho c_p}\left[(vH_z-wH_y)^2+(wH_x-uH_z)^2+(uH_y-vH_x)^2\right] \tag{2.41}$$

The concentration equation:

$$\frac{\partial C}{\partial t}+u\frac{\partial C}{\partial x}+v\frac{\partial C}{\partial y}+w\frac{\partial C}{\partial z}=D_m\left(\frac{\partial^2 C}{\partial x^2}+\frac{\partial^2 C}{\partial y^2}+\frac{\partial^2 C}{\partial z^2}\right)+\frac{D_m k_T}{T_m}\left(\frac{\partial^2 T}{\partial x^2}+\frac{\partial^2 T}{\partial y^2}+\frac{\partial^2 T}{\partial z^2}\right) \tag{2.42}$$

The next section thus deals the specific problems.

Case I

Let us consider an unsteady MHD free convection and mass transfer flow of an electrically conducting viscous fluid through a porous medium along an infinite vertical porous plate $y=0$ with viscous dissipation and *Joule* heating in a rotating system. The flow is also assumed to be in the x-direction which is taken along the plate in the upward direction and y-axis is normal to it. Initially the plate is at rest, after that the whole system is allowed to rotate with a constant angular velocity Ω about the y-axis. Since the system rotates about $y-$axis, so we can take $\mathbf{\Omega}=(0,-\Omega,0)$. The temperature and the species concentration at the plate are instantly raised from T_w and C_w to T_∞ and C_∞ respectively, which are thereafter maintained constant, where T_∞ and C_∞ are the temperature and species concentration of the uniform flow respectively. A uniform magnetic field of magnitude B_0 is imposed to the plate $y=0$, to be acting along the $y-$axis which is assumed to be electrically non-conducting. We assumed that the magnetic *Reynolds* number of the flow is taken to be small enough so that the induced magnetic field is negligible in comparison with applied one (*Pai*, 1962), therefore the magnetic field is of the form $\mathbf{B}=(0,B_0,0)$ and the magnetic lines of force are fixed relative to the fluid. The equation of conservation of charge $\nabla.\mathbf{J}=0$ gives $J_y=$constant, where the current density $\mathbf{J}=(J_x,J_y,J_z)$. The direction of propagation is considered only along the $y-$axis and does not have any variation along the $y-$axis and the derivative of J_y with respect to y namely $\frac{\partial J_y}{\partial y}=0$. Thus

J_y = constant and since the plate is electrically non-conducting, this constant is zero and hence $J_y = 0$ at the plate and hence zero everywhere.

The $x-$component momentum equation reduces to the boundary layer equation if the only contribution to the body force is made by gravity, the body force per unit mass is $F_x = -\rho g$ where g is the local acceleration due to gravitity, further no body force exists in the direction of y, i.e. $\left(\frac{\partial P}{\partial y} = 0, F_y = 0\right)$. Hence $x-$component of pressure gradient at any point in the boundary layer must equal to the pressure gradient in the quiescent region outside the boundary layer. However in this region $u = v = 0$. Therefore $x-$component of the momentum equation become $\frac{\partial P}{\partial x} = -\rho_\infty g$, where ρ_∞ is the density of the surrounding fluid at temperature T_∞. For small difference in density, $(\rho - \rho_\infty)$ is related to the temperature and mass differences $(T - T_\infty)$ and $(C - C_\infty)$ respectively through the thermal volume expansion coefficient β and mass volume expansion coefficient β^* by the relation $\frac{\rho - \rho_\infty}{\rho} = -\beta(T - T_\infty) - \beta^*(C - C_\infty)$.

Therefore $F_x - \frac{1}{\rho}\frac{\partial P}{\partial x} = g\beta(T - T_\infty) + g\beta^*(C - C_\infty)$ (2.1.1)

With reference to the above assumptions, the continuity equation (2.37), the momentum equations (2.38)-(2.40), the energy equation (2.41) and the concentration equation (2.42) can be written as follows:

The continuity equation:

$$\frac{\partial u}{\partial x} + \frac{\partial v}{\partial y} + \frac{\partial w}{\partial z} = 0 \tag{2.1.2}$$

The momentum equations:

$$\frac{\partial u}{\partial t} + u\frac{\partial u}{\partial x} + v\frac{\partial u}{\partial y} + w\frac{\partial u}{\partial z} = \upsilon\left(\frac{\partial^2 u}{\partial x^2} + \frac{\partial^2 u}{\partial y^2} + \frac{\partial^2 u}{\partial z^2}\right) + g\beta(T - T_\infty) + g\beta^*(C - C_\infty)$$

$$+ 2\Omega w - \frac{\upsilon}{K'}u - \frac{\sigma' {B_0}^2 u}{\rho} \tag{2.1.3}$$

$$\frac{\partial v}{\partial t} + u\frac{\partial v}{\partial x} + v\frac{\partial v}{\partial y} + w\frac{\partial v}{\partial z} = \upsilon\left(\frac{\partial^2 v}{\partial x^2} + \frac{\partial^2 v}{\partial y^2} + \frac{\partial^2 v}{\partial z^2}\right) - \frac{\upsilon}{K'}v \tag{2.1.4}$$

$$\frac{\partial w}{\partial t} + u\frac{\partial w}{\partial x} + v\frac{\partial w}{\partial y} + w\frac{\partial w}{\partial z} = \upsilon\left(\frac{\partial^2 w}{\partial x^2} + \frac{\partial^2 w}{\partial y^2} + \frac{\partial^2 w}{\partial z^2}\right) - 2\Omega u - \frac{\upsilon}{K'}w - \frac{\sigma' {B_0}^2 w}{\rho} \tag{2.1.5}$$

The energy equation:

$$\frac{\partial T}{\partial t}+u\frac{\partial T}{\partial x}+v\frac{\partial T}{\partial y}+w\frac{\partial T}{\partial z}=\frac{k}{\rho c_p}\left(\frac{\partial^2 T}{\partial x^2}+\frac{\partial^2 T}{\partial y^2}+\frac{\partial^2 T}{\partial z^2}\right)+\frac{D_m k_T}{c_s c_p}\left(\frac{\partial^2 C}{\partial x^2}+\frac{\partial^2 C}{\partial y^2}+\frac{\partial^2 C}{\partial z^2}\right)$$

$$+\frac{\upsilon}{c_p}\left[2\left\{\left(\frac{\partial u}{\partial x}\right)^2+\left(\frac{\partial v}{\partial y}\right)^2+\left(\frac{\partial w}{\partial z}\right)^2\right\}+\left(\frac{\partial v}{\partial x}+\frac{\partial u}{\partial y}\right)^2+\left(\frac{\partial w}{\partial y}+\frac{\partial v}{\partial z}\right)^2+\left(\frac{\partial u}{\partial z}+\frac{\partial w}{\partial x}\right)^2\right]$$

$$+\frac{\sigma' B_0^2}{\rho c_p}\left[u^2+w^2\right] \qquad (2.1.6)$$

The concentration equation:

$$\frac{\partial C}{\partial t}+u\frac{\partial C}{\partial x}+v\frac{\partial C}{\partial y}+w\frac{\partial C}{\partial z}=D_m\left(\frac{\partial^2 C}{\partial x^2}+\frac{\partial^2 C}{\partial y^2}+\frac{\partial^2 C}{\partial z^2}\right)+\frac{D_m k_T}{T_m}\left(\frac{\partial^2 T}{\partial x^2}+\frac{\partial^2 T}{\partial y^2}+\frac{\partial^2 T}{\partial z^2}\right) \qquad (2.1.7)$$

Since the plate occupying the plane $y=0$ is of infinite extent and the fluid motion is unsteady, **all physical quantities will depend only upon y and t.** Thus mathematically the problem reduces to a one dimensional problem. Then the equations (2.1.2)-(2.1.7) become

$$\frac{\partial v}{\partial y}=0 \qquad (2.1.8)$$

$$\frac{\partial u}{\partial t}+v\frac{\partial u}{\partial y}=g\beta\left(T-T_\infty\right)+g\beta^*\left(C-C_\infty\right)+\upsilon\frac{\partial^2 u}{\partial y^2}+2\Omega w-\frac{\upsilon}{K'}u-\frac{\sigma' {B_0}^2 u}{\rho} \qquad (2.1.9)$$

$$\frac{\partial v}{\partial t}+v\frac{\partial v}{\partial y}=\upsilon\frac{\partial^2 v}{\partial y^2}-\frac{\upsilon}{K'}v \qquad (2.1.10)$$

$$\frac{\partial w}{\partial t}+v\frac{\partial w}{\partial y}=\upsilon\frac{\partial^2 w}{\partial y^2}-2\Omega u-\frac{\upsilon}{K'}w-\frac{\sigma' {B_0}^2 w}{\rho} \qquad (2.1.11)$$

$$\frac{\partial T}{\partial t}+v\frac{\partial T}{\partial y}=\frac{k}{\rho c_p}\frac{\partial^2 T}{\partial y^2}+\frac{D_m k_T}{c_s c_p}\frac{\partial^2 C}{\partial y^2}+\frac{\sigma' B_0^2}{\rho c_p}\left[u^2+w^2\right]+\frac{\upsilon}{c_p}\left[2\left(\frac{\partial v}{\partial y}\right)^2+\left(\frac{\partial u}{\partial y}\right)^2+\left(\frac{\partial w}{\partial y}\right)^2\right] \qquad (2.1.12)$$

$$\frac{\partial C}{\partial t}+v\frac{\partial C}{\partial y}=D_m\frac{\partial^2 C}{\partial y^2}+\frac{D_m k_T}{T_m}\frac{\partial^2 T}{\partial y^2} \qquad (2.1.13)$$

Let the viscosity of the fluid be small and δ be the small thickness of the boundary layer. Let $\varepsilon << 1$ be the order of magnitude of δ, i.e., $O(\delta)=\varepsilon$. Let the order of magnitude of u, w are one, i.e. $O(u)=1$, $O(w)=1$. Then the order of magnitude of v and y are ε and the order of magnitude of t is one, i.e., $O(v)=\varepsilon$, $O(y)=\varepsilon$ and $O(t)=1$.

Hence $O\left(\frac{\partial u}{\partial t}\right)=1$, $O\left(\frac{\partial u}{\partial y}\right)=\frac{1}{\varepsilon}$, $O\left(\frac{\partial^2 u}{\partial y^2}\right)=\frac{1}{\varepsilon^2}$ and $O\left(\frac{\partial v}{\partial t}\right)=\varepsilon$, $O\left(\frac{\partial v}{\partial y}\right)=1$, $O\left(\frac{\partial^2 v}{\partial y^2}\right)=\frac{1}{\varepsilon}$ within the boundary layer.

On considering the above mentioned order the equations (2.1.8)-(2.1.11) become;

$$\frac{\partial v}{\partial y}=0 \tag{2.1.14}$$

1

$$\frac{\partial u}{\partial t}+v\frac{\partial u}{\partial y}=g\beta\left(T-T_{\infty}\right)+g\beta^{*}\left(C-C_{\infty}\right)+\upsilon\frac{\partial^{2}u}{\partial y^{2}}+2\Omega w-\frac{\upsilon}{K'}u-\frac{\sigma'{B_0}^{2}u}{\rho} \tag{2.1.15}$$

1 ε $\frac{1}{\varepsilon}$ $\frac{1}{\varepsilon^{2}}$ 1 1 1

$$\frac{\partial v}{\partial t}+v\frac{\partial v}{\partial y}=\upsilon\frac{\partial^{2}v}{\partial y^{2}}-\frac{\upsilon}{K'}v \tag{2.1.16}$$

ε ε 1 $\frac{1}{\varepsilon}$ ε

$$\frac{\partial w}{\partial t}+v\frac{\partial w}{\partial y}=\upsilon\frac{\partial^{2}w}{\partial y^{2}}-2\Omega u-\frac{\upsilon}{K'}w-\frac{\sigma'{B_0}^{2}w}{\rho} \tag{2.1.17}$$

1 ε $\frac{1}{\varepsilon}$ $\frac{1}{\varepsilon^{2}}$ 1 1 1

Since the viscous boundary layer and thermal boundary layer are both small in this case, so let δ be the thermal boundary layer thickness and let $\varepsilon<<1$ be the order of magnitude of δ, i.e., $O(\delta)=\varepsilon$. Let the order of magnitude of T and C be one, i.e., $O(T)=1$ and $O(C)=1$.

Hence $O\left(\frac{\partial T}{\partial t}\right)=1, O\left(\frac{\partial T}{\partial y}\right)=\frac{1}{\varepsilon}$, $O\left(\frac{\partial^{2}T}{\partial y^{2}}\right)=\frac{1}{\varepsilon^{2}}$ and $O\left(\frac{\partial C}{\partial t}\right)=1, O\left(\frac{\partial C}{\partial y}\right)=\frac{1}{\varepsilon}$,

$O\left(\frac{\partial^{2}C}{\partial y^{2}}\right)=\frac{1}{\varepsilon^{2}}$ within the boundary layer.

Then the equations (2.1.12) and (2.1.13) with order become

$$\frac{\partial T}{\partial t}+v\frac{\partial T}{\partial y}=\frac{k}{\rho c_{p}}\frac{\partial^{2}T}{\partial y^{2}}+\frac{D_{m}k_{T}}{c_{s}c_{p}}\frac{\partial^{2}C}{\partial y^{2}}+\frac{\sigma'B_{0}^{2}}{\rho c_{p}}\left[u^{2}+w^{2}\right]+\frac{\upsilon}{c_{p}}\left[2\left(\frac{\partial v}{\partial y}\right)^{2}+\left(\frac{\partial u}{\partial y}\right)^{2}+\left(\frac{\partial w}{\partial y}\right)^{2}\right] \tag{2.1.18}$$

1 ε $\frac{1}{\varepsilon}$ $\frac{1}{\varepsilon^{2}}$ $\frac{1}{\varepsilon^{2}}$ 1 1 1 $\frac{1}{\varepsilon^{2}}$ $\frac{1}{\varepsilon^{2}}$

$$\frac{\partial C}{\partial t}+v\frac{\partial C}{\partial y}=D_{m}\frac{\partial^{2}C}{\partial y^{2}}+\frac{D_{m}k_{T}}{T_{m}}\frac{\partial^{2}T}{\partial y^{2}} \tag{2.1.19}$$

1 ε $\frac{1}{\varepsilon}$ $\frac{1}{\varepsilon^{2}}$ $\frac{1}{\varepsilon^{2}}$

Equations (2.1.14)-(2.1.19) require that $O\left(g\beta\left(T-T_{\infty}\right)\right)=1, O\left(g\beta^{*}\left(C-C_{\infty}\right)\right)=1$, $O(2\Omega)=1$, $O\left(\frac{\upsilon}{K'}\right)=1$, $O\left(\frac{\sigma'{B_0}^{2}}{\rho}\right)=1$, $O\left(\frac{k}{\rho c_{p}}\right)=\varepsilon^{2}$, $O\left(\frac{D_{m}k_{T}}{c_{s}c_{p}}\right)=\varepsilon^{2}$, $O(D_{m})=\varepsilon^{2}$, $O\left(\frac{D_{m}k_{T}}{T_{m}}\right)=\varepsilon^{2}$ and

$$O\left(\frac{\upsilon}{c_p}\right)=\varepsilon^2.$$

Since the viscosity is very small, so neglecting the small order terms, then quations (2.1.14)-(2.1.19) become

$$\frac{\partial v}{\partial y}=0 \tag{2.1.20}$$

$$\frac{\partial u}{\partial t}+v\frac{\partial u}{\partial y}=\upsilon\frac{\partial^2 u}{\partial y^2}+g\beta\left(T-T_\infty\right)+g\beta^*\left(C-C_\infty\right)+2\Omega w-\frac{\upsilon}{K'}u-\frac{\sigma' {B_0}^2 u}{\rho} \tag{2.1.21}$$

$$\frac{\partial w}{\partial t}+v\frac{\partial w}{\partial y}=\upsilon\frac{\partial^2 w}{\partial y^2}-2\Omega u-\frac{\upsilon}{K'}w-\frac{\sigma' {B_0}^2 w}{\rho} \tag{2.1.22}$$

$$\frac{\partial T}{\partial t}+v\frac{\partial T}{\partial y}=\frac{k}{\rho c_p}\frac{\partial^2 T}{\partial y^2}+\frac{D_m k_T}{c_s c_p}\frac{\partial^2 C}{\partial y^2}+\frac{\sigma' B_0^2}{\rho c_p}\left[u^2+w^2\right]+\frac{\upsilon}{c_p}\left[\left(\frac{\partial u}{\partial y}\right)^2+\left(\frac{\partial w}{\partial y}\right)^2\right] \tag{2.1.23}$$

$$\frac{\partial C}{\partial t}+v\frac{\partial C}{\partial y}=D_m\frac{\partial^2 C}{\partial y^2}+\frac{D_m k_T}{T_m}\frac{\partial^2 T}{\partial y^2} \tag{2.1.24}$$

The boundary conditions for the problem are

$$\left.\begin{array}{l} t\le 0, u=0, v=0, w=0, T=T_\infty, C=C_\infty \text{ for all values of y} \\ t>0,\ u=0, v=v_0(t), w=0, T=T_w, C=C_w \quad \text{at} \quad y=0 \\ t>0,\ u\to U_0, \qquad w\to 0, T\to T_\infty, C\to C_\infty \quad \text{at} \quad y\to\infty \end{array}\right\} \tag{2.1.25}$$

The fluid is assumed to be moving in the upward direction with a velocity U_0 and then equations (2.1.21)-(2.1.24) become

$$\frac{\partial v}{\partial y}=0 \tag{2.1.20a}$$

$$\frac{\partial u}{\partial t}+v\frac{\partial u}{\partial y}=\upsilon\frac{\partial^2 u}{\partial y^2}+g\beta\left(T-T_\infty\right)+g\beta^*\left(C-C_\infty\right)+2\Omega w-\frac{\upsilon}{K'}\left(U_0-u\right)-\frac{\sigma' {B_0}^2}{\rho}\left(U_0-u\right) \tag{2.1.21a}$$

$$\frac{\partial w}{\partial t}+v\frac{\partial w}{\partial y}=\upsilon\frac{\partial^2 w}{\partial y^2}-2\Omega(U_0-u)-\frac{\upsilon}{K'}w-\frac{\sigma' {B_0}^2 w}{\rho} \tag{2.1.22a}$$

$$\frac{\partial T}{\partial t}+v\frac{\partial T}{\partial y}=\frac{k}{\rho c_p}\frac{\partial^2 T}{\partial y^2}+\frac{D_m k_T}{c_s c_p}\frac{\partial^2 C}{\partial y^2}+\frac{\upsilon}{c_p}\left[\left(\frac{\partial u}{\partial y}\right)^2+\left(\frac{\partial w}{\partial y}\right)^2\right]+\frac{\sigma' B_0^2}{\rho c_p}\left[\left(U_0-u\right)^2+w^2\right] \tag{2.1.23a}$$

$$\frac{\partial C}{\partial t}+v\frac{\partial C}{\partial y}=D_m\frac{\partial^2 C}{\partial y^2}+\frac{D_m k_T}{T_m}\frac{\partial^2 T}{\partial y^2} \tag{2.1.24a}$$

and the boundary conditions for the problems are

$$\left.\begin{array}{l} t>0,\ u=0,\ v=v_0(t), w=0,\ T=T_w,\ C=C_w \quad \text{at} \quad y=0 \\ t>0,\ u\to U_0, \qquad w\to 0,\ T\to T_\infty, C\to C_\infty \quad \text{as} \quad y\to\infty \end{array}\right\} \tag{2.1.25a}$$

where u, v are the velocity components in the x, y directions respectively, υ is the kinematic viscosity, g is the acceleration due to gravity, ρ is the density, β is the thermal volumetric coefficient expanssion, β^* is the volumetric coefficient of expanssion for concentration, T, T_w, T_∞ are the temperature of the fluid inside the thermal boundary layer, the plate temperature and the fluid temperature in the free stream respectivly while C, C_w, C_∞ are the coressponding concentrations, K' is the permiability of the porous medium, k is the thermal conductivity of the medium, k_T is the thermal difusion rato, c_p is the specific heat at constant pressure, D_m is the coefficient of mass diffusivity, T_m is the mean fluid temperature, c_s is the concentration susceptibility, σ' is the electric conductivity.

Case II

Let us consider a steady MHD free convection and mass transfer flow of an electrically conducting viscous incompressible fluid through a porous medium along a semi-infinite vertical porous plate $y = 0$ in a rotating system. The detailed descriptions of the present problem are similar to those of ***case-I,*** and thus are not repeated here for brevity.

The continuity equation is:

$$\frac{\partial u}{\partial x}+\frac{\partial v}{\partial y}+\frac{\partial w}{\partial z}=0 \tag{2.2.1}$$

The momentum equations are:

$$u\frac{\partial u}{\partial x}+v\frac{\partial u}{\partial y}+w\frac{\partial u}{\partial z}=\upsilon\left(\frac{\partial^2 u}{\partial x^2}+\frac{\partial^2 u}{\partial y^2}+\frac{\partial^2 u}{\partial z^2}\right)+g\beta\left(T-T_\infty\right)+g\beta^*\left(C-C_\infty\right)$$

$$+2\Omega w-\frac{\upsilon}{K'}u-\frac{\sigma' {B_0}^2 u}{\rho} \tag{2.2.2}$$

$$u\frac{\partial v}{\partial x}+v\frac{\partial v}{\partial y}+w\frac{\partial v}{\partial z}=\upsilon\left(\frac{\partial^2 v}{\partial x^2}+\frac{\partial^2 v}{\partial y^2}+\frac{\partial^2 v}{\partial z^2}\right)-\frac{\upsilon}{K'}v \tag{2.2.3}$$

$$u\frac{\partial w}{\partial x}+v\frac{\partial w}{\partial y}+w\frac{\partial w}{\partial z}=\upsilon\left(\frac{\partial^2 w}{\partial x^2}+\frac{\partial^2 w}{\partial y^2}+\frac{\partial^2 w}{\partial z^2}\right)-2\Omega u-\frac{\upsilon}{K'}w-\frac{\sigma' {B_0}^2 w}{\rho} \tag{2.2.4}$$

The energy equation is

$$u\frac{\partial T}{\partial x}+v\frac{\partial T}{\partial y}+w\frac{\partial T}{\partial z}=\frac{k}{\rho c_p}\left(\frac{\partial^2 T}{\partial x^2}+\frac{\partial^2 T}{\partial y^2}+\frac{\partial^2 T}{\partial z^2}\right)+\frac{D_m k_T}{c_s c_p}\left(\frac{\partial^2 C}{\partial x^2}+\frac{\partial^2 C}{\partial y^2}+\frac{\partial^2 C}{\partial z^2}\right)$$

$$+\frac{\upsilon}{c_p}\left[2\left\{\left(\frac{\partial u}{\partial x}\right)^2+\left(\frac{\partial v}{\partial y}\right)^2+\left(\frac{\partial w}{\partial z}\right)^2\right\}+\left(\frac{\partial v}{\partial x}+\frac{\partial u}{\partial y}\right)^2+\left(\frac{\partial w}{\partial y}+\frac{\partial v}{\partial z}\right)^2+\left(\frac{\partial u}{\partial z}+\frac{\partial w}{\partial x}\right)^2\right]$$

$$+\frac{\sigma' B_0^2}{\rho c_p}\left[u^2+w^2\right] \tag{2.2.5}$$

The concentration equation is

$$u\frac{\partial C}{\partial x}+v\frac{\partial C}{\partial y}+w\frac{\partial C}{\partial z}=D_m\left(\frac{\partial^2 C}{\partial x^2}+\frac{\partial^2 C}{\partial y^2}+\frac{\partial^2 C}{\partial z^2}\right)+\frac{D_m k_T}{T_m}\left(\frac{\partial^2 T}{\partial x^2}+\frac{\partial^2 T}{\partial y^2}+\frac{\partial^2 T}{\partial z^2}\right) \tag{2.2.6}$$

Since the plate occupying the plane $y=0$ is of semi-infinite extent and the motion is steady, **all physical quantities will depend only upon** x **and** y. Thus mathematically the problem reduces to a two dimensional problem.

Then the equations (2.2.1)-(2.2.6) become

$$\frac{\partial u}{\partial x}+\frac{\partial v}{\partial y}=0 \tag{2.2.7}$$

$$u\frac{\partial u}{\partial x}+v\frac{\partial u}{\partial y}=\upsilon\left(\frac{\partial^2 u}{\partial x^2}+\frac{\partial^2 u}{\partial y^2}\right)+g\beta\left(T-T_\infty\right)+g\beta^*\left(C-C_\infty\right)+2\Omega w-\frac{\upsilon}{K'}u-\frac{\sigma' {B_0}^2 u}{\rho} \tag{2.2.8}$$

$$u\frac{\partial v}{\partial x}+v\frac{\partial v}{\partial y}=\upsilon\left(\frac{\partial^2 v}{\partial x^2}+\frac{\partial^2 v}{\partial y^2}\right)-\frac{\upsilon}{K'}v \tag{2.2.9}$$

$$u\frac{\partial w}{\partial x}+v\frac{\partial w}{\partial y}=\upsilon\left(\frac{\partial^2 w}{\partial x^2}+\frac{\partial^2 w}{\partial y^2}\right)-2\Omega u-\frac{\upsilon}{K'}w-\frac{\sigma' {B_0}^2 w}{\rho} \tag{2.2.10}$$

$$\begin{aligned}u\frac{\partial T}{\partial x}+v\frac{\partial T}{\partial y}=&\frac{k}{\rho c_p}\left(\frac{\partial^2 T}{\partial x^2}+\frac{\partial^2 T}{\partial y^2}\right)+\frac{D_m k_T}{c_s c_p}\left(\frac{\partial^2 C}{\partial x^2}+\frac{\partial^2 C}{\partial y^2}\right)+\frac{\sigma' B_0^2}{\rho c_p}\left[u^2+w^2\right]\\&+\frac{\upsilon}{c_p}\left[2\left\{\left(\frac{\partial u}{\partial x}\right)^2+\left(\frac{\partial v}{\partial y}\right)^2\right\}+\left(\frac{\partial v}{\partial x}+\frac{\partial u}{\partial y}\right)^2+\left(\frac{\partial w}{\partial y}\right)^2+\left(\frac{\partial w}{\partial x}\right)^2\right]\end{aligned} \tag{2.2.11}$$

$$u\frac{\partial C}{\partial x}+v\frac{\partial C}{\partial y}=D_m\left(\frac{\partial^2 C}{\partial x^2}+\frac{\partial^2 C}{\partial y^2}\right)+\frac{D_m k_T}{T_m}\left(\frac{\partial^2 T}{\partial x^2}+\frac{\partial^2 T}{\partial y^2}\right) \tag{2.2.12}$$

Let the viscosity of the fluid be small and δ be small thickness of the boundary layer. Let $\varepsilon<<1$ be the order of magnitude of δ, i.e., $O(\delta)=\varepsilon$. Let the order of magnitude of u, w and x are one, i.e. $O(u)=1$, $O(w)=1$ and $O(x)=1$. Then the order of magnitude of v and y are ε, i.e., $O(v)=\varepsilon$ and $O(y)=\varepsilon$.

Hence $O\left(\frac{\partial u}{\partial x}\right)=1$, $O\left(\frac{\partial^2 u}{\partial x^2}\right)=1$, $O\left(\frac{\partial u}{\partial y}\right)=\frac{1}{\varepsilon}$, $O\left(\frac{\partial^2 u}{\partial y^2}\right)=\frac{1}{\varepsilon^2}$ and $O\left(\frac{\partial v}{\partial x}\right)=\varepsilon$, $O\left(\frac{\partial^2 v}{\partial x^2}\right)=\varepsilon$, $O\left(\frac{\partial v}{\partial y}\right)=1$, $O\left(\frac{\partial^2 v}{\partial y^2}\right)=\frac{1}{\varepsilon}$ within the boundary layer.

Then the equation (2.2.7)-(2.2.10) become

$$\frac{\partial u}{\partial x}+\frac{\partial v}{\partial y}=0 \tag{2.2.13}$$

1 1

$$u\frac{\partial u}{\partial x}+v\frac{\partial u}{\partial y}=\upsilon\left(\frac{\partial^2 u}{\partial x^2}+\frac{\partial^2 u}{\partial y^2}\right)+g\beta\left(T-T_\infty\right)+g\beta^*\left(C-C_\infty\right)+2\Omega w-\frac{\upsilon}{K'}u-\frac{\sigma' {B_0}^2 u}{\rho} \tag{2.2.14}$$

1 1 ε $\frac{1}{\varepsilon}$ 1 $\frac{1}{\varepsilon^2}$ 1 1 1

$$u\frac{\partial v}{\partial x}+v\frac{\partial v}{\partial y}=\upsilon\left(\frac{\partial^2 v}{\partial x^2}+\frac{\partial^2 v}{\partial y^2}\right)-\frac{\upsilon}{K'}v \tag{2.2.15}$$

1 ε ε 1 ε $\frac{1}{\varepsilon}$ ε

$$u\frac{\partial w}{\partial x}+v\frac{\partial w}{\partial y}=\upsilon\left(\frac{\partial^2 w}{\partial x^2}+\frac{\partial^2 w}{\partial y^2}\right)-2\Omega u-\frac{\upsilon}{K'}w-\frac{\sigma' {B_0}^2 w}{\rho} \tag{2.2.16}$$

1 1 ε $\frac{1}{\varepsilon}$ 1 $\frac{1}{\varepsilon^2}$ 1 1 1

Since the viscous boundary layer and the thermal boundary layer thickness are same in this case, so let δ be the thermal boundary layer thickness and let $\varepsilon << 1$ be the order of magnitude of δ, i.e., $O(\delta)=\varepsilon$. Let the order of magnitude of T and C be one, i.e. $O(T)=1$ and $O(C)=1$.

Hence $O\left(\frac{\partial T}{\partial x}\right)=1$, $O\left(\frac{\partial^2 T}{\partial x^2}\right)=1$, $O\left(\frac{\partial T}{\partial y}\right)=\frac{1}{\varepsilon}$, $O\left(\frac{\partial^2 T}{\partial y^2}\right)=\frac{1}{\varepsilon^2}$ and $O\left(\frac{\partial C}{\partial x}\right)=1$, $O\left(\frac{\partial^2 C}{\partial x^2}\right)=1$, $O\left(\frac{\partial C}{\partial y}\right)=\frac{1}{\varepsilon}$, $O\left(\frac{\partial^2 C}{\partial y^2}\right)=\frac{1}{\varepsilon^2}$ within the boundary layer.

Then the equations (2.2.11) and (2.2.12) become

$$u\frac{\partial T}{\partial x}+v\frac{\partial T}{\partial y}=\frac{k}{\rho c_p}\left(\frac{\partial^2 T}{\partial x^2}+\frac{\partial^2 T}{\partial y^2}\right)+\frac{D_m k_T}{c_s c_p}\left(\frac{\partial^2 C}{\partial x^2}+\frac{\partial^2 C}{\partial y^2}\right)+\frac{\sigma' B_0^2}{\rho c_p}\left[u^2+w^2\right]$$

1 1 ε $\frac{1}{\varepsilon}$ 1 $\frac{1}{\varepsilon^2}$ 1 $\frac{1}{\varepsilon^2}$ 1 1

$$+\frac{\upsilon}{c_p}\left[2\left\{\left(\frac{\partial u}{\partial x}\right)^2+\left(\frac{\partial v}{\partial y}\right)^2\right\}+\left(\frac{\partial v}{\partial x}+\frac{\partial u}{\partial y}\right)^2+\left(\frac{\partial w}{\partial y}\right)^2+\left(\frac{\partial w}{\partial x}\right)^2\right] \tag{2.2.17}$$

1 1 ε^2 $\frac{1}{\varepsilon^2}$ $\frac{1}{\varepsilon^2}$ 1

$$u\frac{\partial C}{\partial x}+v\frac{\partial C}{\partial y}=D_m\left(\frac{\partial^2 C}{\partial x^2}+\frac{\partial^2 C}{\partial y^2}\right)+\frac{D_m k_T}{T_m}\left(\frac{\partial^2 T}{\partial x^2}+\frac{\partial^2 T}{\partial y^2}\right) \tag{2.2.18}$$

1 1 $\varepsilon \frac{1}{\varepsilon}$ 1 $\frac{1}{\varepsilon^2}$ 1 $\frac{1}{\varepsilon^2}$

Equations (2.2.14)-(2.2.18) requires that $O(g\beta(T-T_\infty))=1$, $O(g\beta^*(C-C_\infty))=1$, $O(2\Omega)=1$,

$O\left(\frac{\upsilon}{K'}\right)=1$, $O\left(\frac{\sigma' B_0^{\,2}}{\rho}\right)=1$, $O\left(\frac{k}{\rho c_p}\right)=\varepsilon^2$, $O\left(\frac{D_m k_T}{c_s c_p}\right)=\varepsilon^2$, $O(D_m)=\varepsilon^2$,

$O\left(\frac{D_m k_T}{T_m}\right)=\varepsilon^2, O\left(\frac{\upsilon}{c_p}\right)=\varepsilon^2$.

Since the viscosity is very small, so neglecting the small order terms, we have from equations (2.2.13)-(2.2.18)

$$\frac{\partial u}{\partial x}+\frac{\partial v}{\partial y}=0 \tag{2.2.19}$$

$$u\frac{\partial u}{\partial x}+v\frac{\partial u}{\partial y}=\upsilon\frac{\partial^2 u}{\partial y^2}+g\beta\left(T-T_\infty\right)+g\beta^*\left(C-C_\infty\right)+2\Omega w-\frac{\upsilon}{K'}u-\frac{\sigma' B_0^{\,2}u}{\rho} \tag{2.2.20}$$

$$u\frac{\partial w}{\partial x}+v\frac{\partial w}{\partial y}=\upsilon\frac{\partial^2 w}{\partial y^2}-2\Omega u-\frac{\upsilon}{K'}w-\frac{\sigma' B_0^{\,2}w}{\rho} \tag{2.2.21}$$

$$u\frac{\partial T}{\partial x}+v\frac{\partial T}{\partial y}=\frac{k}{\rho c_p}\frac{\partial^2 T}{\partial y^2}+\frac{D_m k_T}{c_s c_p}\frac{\partial^2 C}{\partial y^2}+\frac{\sigma' B_0^2}{\rho c_p}\left[u^2+w^2\right]+\frac{\upsilon}{c_p}\left\{\left(\frac{\partial u}{\partial y}\right)^2+\left(\frac{\partial w}{\partial y}\right)^2\right\} \tag{2.2.22}$$

$$u\frac{\partial C}{\partial x}+v\frac{\partial C}{\partial y}=D_m\frac{\partial^2 C}{\partial y^2}+\frac{D_m k_T}{T_m}\frac{\partial^2 T}{\partial y^2} \tag{2.2.23}$$

The boundary conditions for the problem are

$$\left.\begin{array}{l} u=0, v=v_0(x), w=0, \quad T=T_w, \quad C=C_w \quad \text{at} \quad y=0 \\ u\to U_0, \qquad\quad w\to 0, \; T\to T_\infty, \; C\to C_\infty \quad \text{at} \quad y\to\infty \end{array}\right\} \tag{2.2.25}$$

The fluid is assumed to be moving in the upward direction with a velocity U_0 and then equations (2.2.20)-(2.2.22) become

$$\frac{\partial u}{\partial x}+\frac{\partial v}{\partial y}=0 \tag{2.2.19a}$$

$$u\frac{\partial u}{\partial x}+v\frac{\partial u}{\partial y}=\upsilon\frac{\partial^2 u}{\partial y^2}+g\beta\left(T-T_\infty\right)+g\beta^*\left(C-C_\infty\right)+2\Omega w+\frac{\upsilon}{K}\left(U_0-u\right)+\frac{\sigma' B_0^{\,2}}{\rho}\left(U_0-u\right) \tag{2.2.20a}$$

$$u\frac{\partial w}{\partial x}+v\frac{\partial w}{\partial y}=\upsilon\frac{\partial^2 w}{\partial y^2}+2\Omega\left(U_0-u\right)-\frac{\upsilon}{K}w-\frac{\sigma' B_0^{\,2}w}{\rho} \tag{2.2.21a}$$

$$u\frac{\partial T}{\partial x}+v\frac{\partial T}{\partial y}=\frac{k}{\rho c_p}\frac{\partial^2 T}{\partial y^2}+\frac{D_m k_T}{c_s c_p}\frac{\partial^2 C}{\partial y^2}+\frac{\upsilon}{c_p}\left[\left(\frac{\partial u}{\partial y}\right)^2+\left(\frac{\partial w}{\partial y}\right)^2\right]+\frac{\sigma' B_0^2}{\rho c_p}\left[\left(U_0-u\right)^2+w^2\right] \tag{2.2.22a}$$

$$u\frac{\partial C}{\partial x}+v\frac{\partial C}{\partial y}=D_m\frac{\partial^2 C}{\partial y^2}+\frac{D_m k_T}{T_m}\frac{\partial^2 T}{\partial y^2} \tag{2.2.23a}$$

The boundary conditions for the problem are

$$\left.\begin{array}{l} u=0,\ v=v_0(x),\ w=0,\ T=T_w,\ C=C_w \quad \text{at } y=0 \\ u\to U_0, \qquad\qquad w\to 0,\ T\to T_\infty,\ C\to C_\infty \ \text{ at } y\to\infty \end{array}\right\} \tag{2.2.24a}$$

The symboles were discussed as earlier.

Chapter 3

The Calculation Technique

3.1. The Shooting Method

To solve the boundary layer equations by using Shooting method technique, there are two asymptotic boundary condition and hence two unknown conditions $f''(0)$ and $\theta'(0)$ are to be assumed. Within the context of initial value method and *Nachtsheim-Swigert* iteration technique the outer boundary conditions may be functionally represented as

$$f'(\eta_{\max}) = f'(f''(0), \theta'(0)) = \delta_1 \tag{3.1}$$

$$\theta(\eta_{\max}) = \theta(f''(0), \theta'(0)) = \delta_2 . \tag{3.2}$$

With asymptotic convergence criteria given by

$$f''(\eta_{\max}) = f''(f''(0), \theta'(0)) = \delta_3 \tag{3.3}$$

$$\theta'(\eta_{\max}) = \theta'(f''(0), \theta'(0)) = \delta_4 . \tag{3.4}$$

Let us choose $f''(0) = g_1$, $\theta'(0) = g_2$.

Retaining only the first order terms from the Taylor's expansion from equations (3.1)-(3.4) we get

$$f'(\eta_{\max}) = f_c'(\eta_{\max}) + \frac{\partial f'}{\partial g_1}\Delta g_1 + \frac{\partial f'}{\partial g_2}\Delta g_2 = \delta_1 \tag{3.5}$$

$$\theta(\eta_{\max}) = \theta_c(\eta_{\max}) + \frac{\partial \theta}{\partial g_1}\Delta g_1 + \frac{\partial \theta}{\partial g_2}\Delta g_2 = \delta_2 \tag{3.6}$$

$$f''(\eta_{\max}) = f_c''(\eta_{\max}) + \frac{\partial f''}{\partial g_1}\Delta g_1 + \frac{\partial f''}{\partial g_2}\Delta g_2 = \delta_3 \tag{3.7}$$

$$\theta'(\eta_{\max}) = \theta_c'(\eta_{\max}) + \frac{\partial \theta'}{\partial g_1}\Delta g_1 + \frac{\partial \theta'}{\partial g_2}\Delta g_2 = \delta_4 \tag{3.8}$$

where the subscript 'c' indicates the value of the function at $\eta_{\max}$ determine from the trial integration. Solution of these equations in a least squares sense requires determining the minimum value of

$$E = \delta_1^{\,2} + \delta_2^{\,2} + \delta_3^{\,2} + \delta_4^{\,2} \longrightarrow \text{Error} \tag{3.9}$$

with respect to g_1 and g_2.

Now diferentiating E with respect to g_1 and g_2 we get

$$\delta_1 \frac{\partial \delta_1}{\partial g_1} + \delta_2 \frac{\partial \delta_2}{\partial g_1} + \delta_3 \frac{\partial \delta_3}{\partial g_1} + \delta_4 \frac{\partial \delta_4}{\partial g_1} = 0 \tag{3.10}$$

$$\delta_1 \frac{\partial \delta_1}{\partial g_2} + \delta_2 \frac{\partial \delta_2}{\partial g_2} + \delta_3 \frac{\partial \delta_3}{\partial g_2} + \delta_4 \frac{\partial \delta_4}{\partial g_2} = 0. \tag{3.11}$$

Applying equations (3. 5)-(3. 8) in equation (3. 10), we obtain

$$\left[\left(\frac{\partial f'}{\partial g_1}\right)^2 + \left(\frac{\partial \theta}{\partial g_1}\right)^2 + \left(\frac{\partial f''}{\partial g_1}\right)^2 + \left(\frac{\partial \theta'}{\partial g_1}\right)^2\right]\Delta g_1 + \left(\frac{\partial f'}{\partial g_2}\frac{\partial f'}{\partial g_1} + \frac{\partial \theta}{\partial g_2}\frac{\partial \theta}{\partial g_1} + \frac{\partial f''}{\partial g_2}\frac{\partial f''}{\partial g_1} + \frac{\partial \theta'}{\partial g_2}\frac{\partial \theta'}{\partial g_1}\right)\Delta g_2$$

$$= -\left[f_c' \frac{\partial f'}{\partial g_1} + \theta_c \frac{\partial \theta}{\partial g_1} + f_c'' \frac{\partial f''}{\partial g_1} + \theta_c' \frac{\partial \theta'}{\partial g_1}\right]. \tag{3.12}$$

Similarly applying equations (3. 5)-(3.8) in equation (3.11), we obtain

$$\left[\left(\frac{\partial f'}{\partial g_2}\right)^2 + \left(\frac{\partial \theta}{\partial g_2}\right)^2 + \left(\frac{\partial f''}{\partial g_2}\right)^2 + \left(\frac{\partial \theta'}{\partial g_2}\right)^2\right]\Delta g_2 + \left(\frac{\partial f'}{\partial g_1}\frac{\partial f'}{\partial g_2} + \frac{\partial \theta}{\partial g_1}\frac{\partial \theta}{\partial g_2} + \frac{\partial f''}{\partial g_1}\frac{\partial f''}{\partial g_2} + \frac{\partial \theta'}{\partial g_1}\frac{\partial \theta'}{\partial g_2}\right)\Delta g_1$$

$$= -\left[f_c' \frac{\partial f'}{\partial g_2} + \theta_c \frac{\partial \theta}{\partial g_2} + f_c'' \frac{\partial f''}{\partial g_2} + \theta_c' \frac{\partial \theta'}{\partial g_2}\right]. \tag{3.13}$$

The equations (3. 12) and (3. 13), can be written as

$$a_{11}\Delta g_1 + a_{12}\Delta g_2 = b_1 \tag{3.14}$$

$$a_{21}\Delta g_1 + a_{22}\Delta g_2 = b_2, \tag{3.15}$$

where

$$a_{11} = \left(\frac{\partial f'}{\partial g_1}\right)^2 + \left(\frac{\partial \theta}{\partial g_1}\right)^2 + \left(\frac{\partial f''}{\partial g_1}\right)^2 + \left(\frac{\partial \theta'}{\partial g_1}\right)^2 \tag{3.16}$$

$$a_{12} = \frac{\partial f'}{\partial g_2}\frac{\partial f'}{\partial g_1} + \frac{\partial \theta}{\partial g_2}\frac{\partial \theta}{\partial g_1} + \frac{\partial f''}{\partial g_2}\frac{\partial f''}{\partial g_1} + \frac{\partial \theta'}{\partial g_2}\frac{\partial \theta'}{\partial g_1} \tag{3.17}$$

$$a_{21} = \frac{\partial f'}{\partial g_1}\frac{\partial f'}{\partial g_2} + \frac{\partial \theta}{\partial g_1}\frac{\partial \theta}{\partial g_2} + \frac{\partial f''}{\partial g_1}\frac{\partial f''}{\partial g_2} + \frac{\partial \theta'}{\partial g_1}\frac{\partial \theta'}{\partial g_2} \tag{3.18}$$

$$a_{22} = \left[\left(\frac{\partial f'}{\partial g_2}\right)^2 + \left(\frac{\partial \theta}{\partial g_2}\right)^2 + \left(\frac{\partial f''}{\partial g_2}\right)^2 + \left(\frac{\partial \theta'}{\partial g_2}\right)^2\right] \tag{3.19}$$

$$b_1 = -\left[f_c' \frac{\partial f'}{\partial g_1} + \theta_c \frac{\partial \theta}{\partial g_1} + f_c'' \frac{\partial f''}{\partial g_1} + \theta_c' \frac{\partial \theta'}{\partial g_1}\right] \tag{3.20}$$

$$b_2 = -\left[f_c' \frac{\partial f'}{\partial g_2} + \theta_c \frac{\partial \theta}{\partial g_2} + f_c'' \frac{\partial f''}{\partial g_2} + \theta_c' \frac{\partial \theta'}{\partial g_2}\right]. \tag{3.21}$$

In matrix form, equations (3.14) and (3.15) can be writen as

$$\begin{pmatrix} a_{11} & a_{12} \\ a_{21} & a_{22} \end{pmatrix} \begin{pmatrix} \Delta g_1 \\ \Delta g_2 \end{pmatrix} = \begin{pmatrix} b_1 \\ b_2 \end{pmatrix}. \tag{3.22}$$

Now we will solve the system of linear equations (3.22) by Cramers rule and thus we have

$$\Delta g_1 = \frac{\det A_1}{\det A}, \ \Delta g_2 = \frac{\det A_2}{\det A}, \tag{3.23}$$

where

$$\det A = \begin{vmatrix} a_{11} & a_{12} \\ a_{21} & a_{22} \end{vmatrix} = (a_{11}a_{22} - a_{12}a_{21}) \tag{3.24}$$

$$\det A_1 = \begin{vmatrix} b_1 & a_{12} \\ b_2 & a_{22} \end{vmatrix} = (b_1 a_{22} - b_2 a_{12}) \tag{3.25}$$

$$\det A_2 = \begin{vmatrix} a_{11} & b_1 \\ a_{21} & b_2 \end{vmatrix} = (b_2 a_{11} - b_1 a_{21}). \tag{3.26}$$

Then we obtain the (unspecified) missing values g_1 and g_2 as

$$g_1 \equiv g_1 + \Delta g_1 \tag{3.27}$$

$$g_2 \equiv g_2 + \Delta g_2 . \tag{3.28}$$

Thus adopting **this type of numerical technique** described above, a computer program will be setup for the solution of the basic nonlinear differential equations of our problem where the integration technique will be adopted as the six order *Runge-Kutta* method of integration. Based on the integrations done with the above numerical technique, the obtained results will be presented in the appropriate section.

Chapter 4

Viscous dissipation and Joule heating effects on unsteady MHD combined heat and mass transfer flow through a porous medium in a rotating system

4.1. Introduction

In a rotating system, the Coriolis force is very significant as compared to viscous and inertia forces occurring in the basic fluid equations. In stellar studies it is generally admitted that the Coriolis force due to Earth's rotation has a strong effect on the hydromagnetic flow in the Earth's liquid core. Considering this aspect of the rotational flows, model studies were carried out on MHD free convection and mass transfer flows in a rotating system by many investigators of whom the names *Debnath*(1975), *Debnath et al.(1979), Raptis and Perdikis(1982)* are worth mentioning.

In the above mentioned work, the *Soret* and *Dufour* effects were neglegted on the basis that they are of a smaller order of magnitude than the effects described by *Fourier's* and *Fick's* laws. However, exceptions are observed therein. The thermal diffusion (*Soret*) effect, for instance, has been utlized for isotope separation and in mixture between gases with very light molecular weight (H_2, H_e) and of medium molecular weight (N_2, air), the diffusion-thermo (*Dufour*) effect was found to be of order of considerable magnetude such that it cannot be ignored (*Eckert and Drake, 1972).* In veiw of the importance of above mentioned effects, *Kafoussias and Williams (1995)* studied *Soret* and *Dufour* effects on mixed free-forced convection and mass transfer boundary layer flow with temperature dependent viscosity. *Anghel et al. (2000)* investigated the *Dufour* and *Soret* effects on free-convection boundary layer flow over a vertical surface embedded in a porous medium. Recently, *Postelnicu (2004)* studied numerically the influence of a magnetic field on heat and mass transfer by natural convection from vertical in porous media consedering *Soret* and *Dufour* effects. Quite recently, *Alam and Rahman (2006)* investigated the *Dufour* and *Soret* effects on mixed convection flow past a vertical porous flat plate with variable sucction. The effect of *Joule* heating on MHD combined heat and mass transfer flow of an electrically conducting viscous incompressible fluid past an

infinite plate was, however considered by *Hossain (1990).*

Hence, our objective is to investigate the unsteady MHD combined heat and mass transfer flow through a porous mediüm past an infinite vertical porous plate with viscous dissipation and *Joule* heating effects in a rotating system.

4.2. The Governing Equations

Let us consider an unsteady MHD combined heat and mass transfer flow of an electrically conducting viscous fluid through a porous medium along an infinite vertical porous plate $y = 0$ in a rotating system. The flow is also assumed to be moving in the x-direction with a uniform velocity U_0 which is taken along the plate in the upward direction and y-axis is normal to it. Initially the plate is at rest, after that the whole system is allowed to rotate with a constant angular velocity Ω about the y-axis. Since the system rotates about $y-$axis, so we can take $\mathbf{\Omega} = (0,-\Omega,0)$. The temperature and the species concentration at the plate are instantly raised from T_w and C_w to T_∞ and C_∞ respectively, which are thereafter maintained as constant, where T_∞ and C_∞ are the temperature and species concentration of the uniform flow respectively. A uniform magnetic field $\mathbf{B}$ is taken to be acting along the $y-$axis which is assumed to be electrically non-conducting. Following *Pai (1962)*, it is assumed that the magnetic *Reynolds* number of the flow be small enough so that the induced magnetic field is negligible in comparison with applied one, so that the magnetic lines of force are fixed relative to the fluid. The equation of conservation of charge $\nabla.\mathbf{J} = 0$ gives J_y = constant, where thecurrent density $\mathbf{J} = (J_x, J_y, J_z)$. Since the plate is electrically non-conducting, this constant is zero and hence $J_y = 0$ at the plate and hence zero everywhere. The physical configaration considered here is shown in Fig. 4.1. With reference to the generalized equations described in ***case-I* of Chapter 2**, the one dimensional problem for MHD combined heat and mass transfer flow under the above assumptions can be put as:

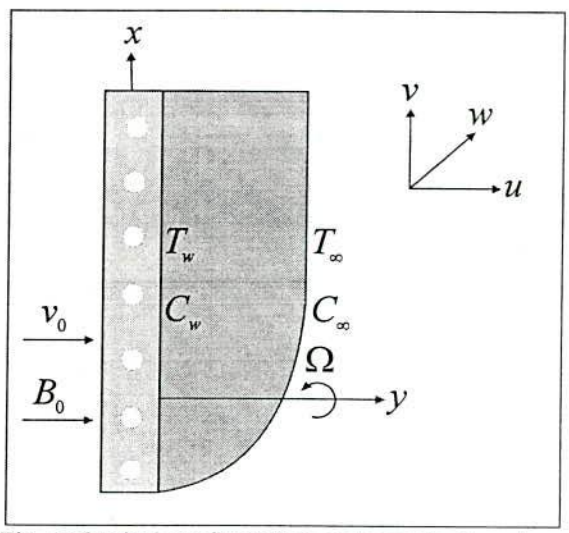

Fig. 1 Physical configuration and coordinate system

$$\frac{\partial v}{\partial y} = 0 \tag{4.1}$$

$$\frac{\partial u}{\partial t}+v\frac{\partial u}{\partial y}=\upsilon\frac{\partial^2 u}{\partial y^2}+g\beta\left(T-T_\infty\right)+g\beta^*\left(C-C_\infty\right)+2\Omega w+\frac{\upsilon}{K'}\left(U_0-u\right)+\frac{\sigma' {B_0}^2}{\rho}\left(U_0-u\right) \tag{4.2}$$

$$\frac{\partial w}{\partial t}+v\frac{\partial w}{\partial y}=\upsilon\frac{\partial^2 w}{\partial y^2}+2\Omega(U_0-u)-\frac{\upsilon}{K'}w-\frac{\sigma' {B_0}^2 w}{\rho} \tag{4.3}$$

$$\frac{\partial T}{\partial t}+v\frac{\partial T}{\partial y}=\frac{k}{\rho c_p}\frac{\partial^2 T}{\partial y^2}+\frac{D_m k_T}{c_s c_p}\frac{\partial^2 C}{\partial y^2}+\frac{\upsilon}{c_p}\left[\left(\frac{\partial u}{\partial y}\right)^2+\left(\frac{\partial w}{\partial y}\right)^2\right]+\frac{\sigma' B_0^2}{\rho c_p}\left[\left(U_0-u\right)^2+w^2\right] \tag{4.4}$$

$$\frac{\partial C}{\partial t}+v\frac{\partial C}{\partial y}=D_m\frac{\partial^2 C}{\partial y^2}+\frac{D_m k_T}{T_m}\frac{\partial^2 T}{\partial y^2} \tag{4.5}$$

and the boundary conditions for the problem are

$$\left.\begin{array}{l} t>0,\ u=0,\ v=v_0(t), w=0,\ T=T_w,\ C=C_w \quad \text{at}\ \ y=0 \\ t>0,\ u=U_0, \qquad\qquad w=0,\ T\to T_\infty, C\to C_\infty \ \text{ as }\ y\to\infty \end{array}\right\} \tag{4.6}$$

Following the work of Sattar (1993), a transformation is now made as;

$U_0-u=u_1\ \ \therefore u=U_0-u_1$

So the equations (4.2)-(4.5) and boundary condition (4.6) respectively transform to

$$\frac{\partial u_1}{\partial t}+v\frac{\partial u_1}{\partial y}=\upsilon\frac{\partial^2 u_1}{\partial y^2}-g\beta\left(T-T_\infty\right)-g\beta^*\left(C-C_\infty\right)-2\Omega w-\frac{\upsilon}{K'}u_1-\frac{\sigma' {B_0}^2}{\rho}u_1 \tag{4.7}$$

$$\frac{\partial w}{\partial t}+v\frac{\partial w}{\partial y}=\upsilon\frac{\partial^2 w}{\partial y^2}+2\Omega u_1-\frac{\upsilon}{K'}w-\frac{\sigma' {B_0}^2 w}{\rho} \tag{4.8}$$

$$\frac{\partial T}{\partial t}+v\frac{\partial T}{\partial y}=\frac{k}{\rho c_p}\frac{\partial^2 T}{\partial y^2}+\frac{D_m k_T}{c_s c_p}\frac{\partial^2 C}{\partial y^2}+\frac{\upsilon}{c_p}\left[\left(\frac{\partial u_1}{\partial y}\right)^2+\left(\frac{\partial w}{\partial y}\right)^2\right]+\frac{\sigma' B_0^2}{\rho c_p}\left[{u_1}^2+w^2\right] \tag{4.9}$$

$$\frac{\partial C}{\partial t}+v\frac{\partial C}{\partial y}=D_m\frac{\partial^2 C}{\partial y^2}+\frac{D_m k_T}{T_m}\frac{\partial^2 T}{\partial y^2} \tag{4.10}$$

$$\left.\begin{array}{l} t>0,\ u_1=U_0, v=v_0(t), w=0,\ T=T_w,\ C=C_w \quad \text{at}\ \ y=0 \\ t>0,\ u_1=0, \qquad\qquad w=0,\ T\to T_\infty,\ C\to C_\infty \ \text{as}\ \ y\to\infty \end{array}\right\} \tag{4.11}$$

where u, v are the velocity components in the x, y directions respectively, υ is the kinematic viscosity, g is the acceleration due to gravity, ρ is the density, β is the thermal volumetric coefficient expanssion, β^* is the volumetric coefficient of expanssion for concentration, T, T_w, T_∞ are the temperature of the fluid inside the thermal boundary layer, the plate temperature and the fluid temperature in the free stream respectivly while C, C_w, C_∞ are the coressponding concentrations, K' is the permiability of the porous medium, k is the thermal conductivity of the medium, k_T is the thermal difusion rato, c_p is the specific heat at constant pressure, D_m is the coefficient of mass diffusivity, T_m is the mean fluid temperature, c_s is the concentration

susceptibility, σ' is the electric conductivity.

4.3. Mathematical Formulations

In order to obtain similar solutions we introduce a similarity parameter σ as

$$\sigma = \sigma(t) \tag{4.12}$$

such that σ is the time dependent length scale. In terms of this length scale, a convenient solution of equation (4.1) is considered to be

$$v = -v_0 \frac{\upsilon}{\sigma(t)} \tag{4.13}$$

Here the constant v_0 represents a dimensionless normal velocity at the plate which is positive for suction and negative for blowing.

We now introduce the following dimensionless variables

$$\eta = \frac{y}{\sigma} \tag{4.14}$$

$$f(\eta) = \frac{u_1}{U_0} \tag{4.15}$$

$$\therefore \frac{u}{U_0} = 1 - f(\eta)$$

$$g_0(\eta) = \frac{w}{U_0} \tag{4.16}$$

$$\theta(\eta) = \frac{T - T_\infty}{T_w - T_\infty} \tag{4.17}$$

$$\phi(\eta) = \frac{C - C_\infty}{C_w - C_\infty} \tag{4.18}$$

From the equation (4.15), we have

$$u_1 = U_0 f(\eta) \tag{4.19}$$

From the equation (4.19), we have the following derivatives

$$\frac{\partial u_1}{\partial t} = -\frac{U_0}{\sigma} \eta f'(\eta) \frac{\partial \sigma}{\partial t} \tag{4.20}$$

$$\frac{\partial u_1}{\partial y} = \frac{U_0}{\sigma} f'(\eta) \tag{4.21}$$

$$\frac{\partial^2 u_1}{\partial y^2} = \frac{U_0}{\sigma^2} f''(\eta) \tag{4.22}$$

Again from the equation (4.17), we have

$$(T - T_\infty) = (T_w - T_\infty)\theta(\eta) \tag{4.23}$$

Also from the equation (4.18), we have

$$(C-C_\infty)=(C_w-C_\infty)\phi(\eta) \tag{4.24}$$

Substituting the equations (4.13), (4.16) and (4.19)-(4.24) into the equation (4.7), we get

$$f''+\left(\frac{\sigma}{\upsilon}\frac{\partial\sigma}{\partial t}\eta+v_0\right)f'-G_r\theta-G_m\phi-2Rg_0-(K+M)f=0 \tag{4.25}$$

where $G_r=\frac{g\beta(T_w-T_\infty)\sigma^2}{U_0\upsilon}$ is the local *Grashof* number, $G_m=\frac{g\beta^*(C_w-C_\infty)\sigma^2}{U_0\upsilon}$ is the local modified *Grashof* number, $K=\frac{\sigma^2}{K'}$ is the permeability parameter, $M=\frac{\sigma' B_0{}^2\sigma^2}{\rho\upsilon}$ is the Magnetic parameter and $R=\frac{\Omega\sigma^2}{\upsilon}$ is the rotational parameter.

Again, from the equation (4.16), we have

$$w=U_0g_0(\eta) \tag{4.26}$$

From the equation (4.26), we have the following derivatives

$$\frac{\partial w}{\partial t}=-\frac{U_0}{\sigma}\frac{\partial\sigma}{\partial t}\eta g_0'(\eta) \tag{4.27}$$

$$\frac{\partial w}{\partial y}=\frac{U_0}{\sigma}g_0'(\eta) \tag{4.28}$$

$$\frac{\partial^2 w}{\partial y^2}=\frac{U_0}{\sigma^2}g_0''(\eta) \tag{4.29}$$

Substituting the equations (4.13), (4.19), (4.26)-(4.29) into the equation (4.8), we get

$$g_0''+\left(\frac{\sigma}{\upsilon}\frac{\partial\sigma}{\partial t}\eta+v_0\right)g_0'+2Rf-(K+M)g_0=0 \tag{4.30}$$

Again, from the equation (4.17), we have

$$T=T_\infty+(T_w-T_\infty)\theta(\eta) \tag{4.31}$$

From the equation (4.31), we have the following derivatives

$$\frac{\partial T}{\partial t}=-\frac{(T_w-T_\infty)}{\sigma}\frac{\partial\sigma}{\partial t}\eta\theta'(\eta) \tag{4.32}$$

$$\frac{\partial T}{\partial y}=\frac{(\mathrm{T_w}-T_\infty)}{\sigma}\theta'(\eta) \tag{4.33}$$

$$\frac{\partial^2 T}{\partial y^2}=\frac{(\mathrm{T_w}-T_\infty)}{\sigma^2}\theta''(\eta) \tag{4.34}$$

Further, from the equation (4.18), we have

$$C=C_\infty+(C_w-C_\infty)\phi(\eta) \tag{4.35}$$

From the equation (4.35), we have the following derivatives

$$\frac{\partial C}{\partial t} = -\frac{(C_w - C_\infty)}{\sigma}\frac{\partial \sigma}{\partial t}\eta\phi'(\eta) \tag{4.36}$$

$$\frac{\partial C}{\partial y} = \frac{(C_w - C_\infty)}{\sigma}\phi'(\eta) \tag{4.37}$$

$$\frac{\partial^2 C}{\partial y^2} = \frac{(C_w - C_\infty)}{\sigma^2}\phi''(\eta) \tag{4.38}$$

Substituting the equations (4.13), (4.19), (4.21), (4.26),(4.28), (4.32)-(4.34) and (4.38) into the equation (4.9), we have

$$\theta''(\eta) + \left(\frac{\sigma}{\upsilon}\frac{\partial \sigma}{\partial t}\eta + v_0\right)P_r\theta'(\eta) + D_f\phi''(\eta) + P_r E_c\left\{(f')^2 + (g_0')^2\right\} + P_r E_c M\left\{(f)^2 + (g_0)^2\right\} = 0 \tag{4.39}$$

where $P_r = \frac{\rho \upsilon c_p}{k}$ is the *Prandlt* number and $D_f = \frac{D_m k_T \rho}{c_s K'}\frac{(C_w - C_\infty)}{(T_w - T_\infty)}$ is the *Dufour* number,

$E_c = \frac{U_0^2}{c_p(T_w - T_\infty)}$ is the *Eckert* number.

Again substituting the equations (4.13), (4.34), (4.36)-(4.38) into the equation (4.10), we get

$$\phi''(\eta) + \left(\frac{\sigma}{\upsilon}\frac{\partial \sigma}{\partial t}\eta + v_0\right)S_c\phi'(\eta) + S_0\theta''(\eta) = 0 \tag{4.40}$$

where $S_c = \frac{\upsilon}{D_m}$ is the *Schmidt* number and $S_0 = \frac{k_T}{T_m}\frac{(T_w - T_\infty)}{(C_w - C_\infty)}$ is the *Soret* number.

The corresponding boundary conditions for the above mentioned problem are

$$\left.\begin{array}{l} f = 1,\ g_0 = 0,\ \theta = 1,\ \phi = 1 \ \text{ at } \ \eta = 0 \\ f = 0,\ g_0 = 0,\ \theta = 0,\ \phi = 0 \ \text{ as } \ \eta \to \infty \end{array}\right\} \tag{4.41}$$

The equations (4.25), (4.30), (4.39) and (4.40) are similar except for the term $\frac{\sigma}{\upsilon}\frac{\partial \sigma}{\partial t}$ where time (t) appears explicitly. Thus the similarity condition requires that $\frac{\sigma}{\upsilon}\frac{\partial \sigma}{\partial t}$ in the equations (4.25), (4.30), (4.39) and (4.40) must be a constant quantity. Hence following works of *Sattar and Alam (1994)* one can try a class of solution of the equations (4.25), (4.30), (4.39) and (4.40) by assuming that

$$\frac{\sigma}{\upsilon}\frac{\partial \sigma}{\partial t} = c \ \text{(a constant)} \tag{4.42}$$

Now integrating (4.42) one obtains

$$\sigma = \sqrt{2c\upsilon t} \tag{4.43}$$

where the constant of integration is determined through the condition that $\sigma = 0$ when $t = 0$. It

thus appears from (4.43) that, by making a realistic choice of 'c' to be equal to '2' in (4.43) the length scale σ becomes equal to $\sigma = 2\sqrt{\upsilon t}$ which exactly corresponds to the usual scaling factor considered for various unsteady boundary layer flows (*Schlichting,1968)*. Since σ is a scaling factor as well as a similarity parameter, any value of 'c' in (4.43) would not change the nature of the solution except that the scale would be different. Finally, introducing (4.43) with $c = 2$ in equations (4.25), (4.30), (4.39) and (4.40) we respectively have the following dimensionless ordinary coupled non-linear differential equations

$$f'' + 2\xi f' - G_r\theta - G_m\phi - Kf - Mf - 2Rg_0 = 0 \tag{4.44}$$

$$g_0'' + 2\xi g_0' - Kg_0 - Mg_0 + 2Rf = 0 \tag{4.45}$$

$$\theta''(\eta) + 2P_r\xi\theta'(\eta) + D_f\phi''(\eta) + P_rE_c\left\{(f')^2 + (g_0')^2\right\} + P_rE_cM\left\{(f)^2 + (g_0)^2\right\} = 0 \tag{4.46}$$

$$\phi'' + 2\xi S_c\phi' + S_0\theta'' = 0 \tag{4.47}$$

where $\xi = \eta + \frac{v_0}{2}$.

The corresponding boundary conditions are

$$\left.\begin{array}{l} f = 1,\ g_0 = 0,\ \theta = 1,\ \phi = 1 \quad \text{at} \quad \eta = 0 \\ f = 0,\ g_0 = 0,\ \theta = 0,\ \phi = 0 \quad \text{as} \quad \eta \to \infty \end{array}\right\} \tag{4.48}$$

In all the above equations primes denote the differentiation with respect to η.

The next section deals the Skin-friction, the *Nusselt* number and the *Sherwood* number of the problem.

4.4. Skin-friction coefficients, Nusselt number and Sherwood number

The quantities of chief physical interest are the skin friction coefficients, the *Nusselt* number and the *Sherwood* number. The equation defining the components of wall skin frictions are

$\tau_x = \mu\left(\frac{\partial u}{\partial y}\right)_{y=0}$ and $\tau_z = \mu\left(\frac{\partial w}{\partial y}\right)_{y=0}$; which are proportional to $\left(\frac{\partial f}{\partial \eta}\right)_{\eta=0}$ and $\left(\frac{\partial g_0}{\partial \eta}\right)_{\eta=0}$.

The *Nusselt* number is denoted by $N_u = -\frac{1}{\Delta t}\left(\frac{\partial T}{\partial y}\right)_{y=0}$; which is proportional to $-\left(\frac{\partial \theta}{\partial \eta}\right)_{\eta=0}$,

hence we have $N_u \propto \theta'(0)$.

The *Sherwood* number is denoted by $S_h = -\frac{1}{\Delta t}\left(\frac{\partial C}{\partial y}\right)_{y=0}$ which is proportional to $-\left(\frac{\partial \phi}{\partial \eta}\right)_{\eta=0}$,

hence we have $S_h \propto \phi'(0)$

The numerical values proportional to the skin-friction coefficients, the *Nusselt* number and

the *Sherwood* number are sorted in Tables 4.1-4.5.

4.5. Numerical Solutions and Calculation Procedure

Equations (4.44)-(4.47) with boundary conditions (4.48) are solved numerically by a standard initial value solver, i.e., the shooting method. For this purpose, we have applied the *Nacthsheim-Swigert* iteration technique.

In shooting method, the missing (unspecified) initial condition at the initial point of the interval is assumed and the differential equation is integrated numerically as an initial value problem to the terminal point. The accuracy of the assumed missing initial condition is then checked by comparing the calculated value of the dependent variable at the terminal point with its given value there. If a difference exists, another value of the missing initial condition must be assumed and the process is repeated. This process is continued until the agreement between the calculated and the given condition at the terminal point is within the specified degree of accuracy. For this type of iterative approach, one naturally inquires whether or not there is a systematic way of finding each succeeding (assumed) value of the missing initial condition.

The boundary conditions (4.48) associated with the ordinary nonlinear differential equations (4.44)-(4.47) of the boundary layer type is of the two-point asymptotic class. Two-point boundary conditions have values of the dependent variable specified at two different values of the independent variable. Specification of an asymptotic boundary condition implies the value of velocity approaches to unity and the value of temperature approaches to zero as the outer specified value of the independent variable is approached. The method of numerical integration of two-point asymptotic boundary value problem of the boundary layer type, the initial value method, requires that the problem is to be recast as an initial value problem. Thus it is necessary to set up as many boundary conditions at the surface as there are at infinity. The governing differential equations are then integrated with these assumed surface boundary conditions. If the required outer boundary condition is satisfied, a solution has been achieved. However, this is not generally the case. Hence a method must be devised to logically estimate the new surface boundary conditions for the next trial integration. Asymptotic boundary value problems such as those governing the boundary layer equations are further complicated by the fact that the outer boundary condition is specified at infinity. In the trial integration infinity is numerically approximated by some large value of the independent variable. There is no a priori general method of estimating this value. Selection of too small a maximum value for the independent variable may not allow the solution to asymptotically converge to the required accuracy. Selecting a large value may result in divergence of the trial integration or in slow convergence of surface boundary conditions required satisfying the asymptotic outer boundary condition. Selecting too large a value of the independent variable is expensive in terms of computer time.

Nachtsheim-Swigert developed an iteration method, which overcomes these difficulties. Extension of the Nachtsheim-Swigert iteration shell to above equation system of differential equations (4.44)-(4.47) is straightforward. In equation (4.48) there are four asymptotic boundary conditions and hence four unknown surface conditions $f'(0), g_0'(0), \theta'(0)$ and $\phi'(0)$ is required.

4.6. Results and Discussion

In this thesis viscous dissipation and *Joule* heating effect on unsteady MHD combined heat and mass transfer flow through a porous medium in a rotating system have been investigated using the *Nachtsheim-Swigert* shooting iteration techneque. To study the physical situation of this problem, we have computed the numerical values of the velocity, temperature and concentration within the boundary layer and also find the skin friction coefficients, *Nusselt and Sherwood* numbers at the plate. It can be seen that the solutions are affected by the non dimensional parameters and numbers namely suction parameter v_0, local *Grashof* number G_r, local modified *Grashof* number G_m, permiability parametr K, Magnetic parameter M, *Prandtl* number P_r, *Eckert* number E_c, *Dufour* number D_f, *Schmidt* number S_c, *Soret* number S_0 and rotation parameter R. The value of G_r and G_m are taken to be large, since these values correspond to a cooling problem that is generally encountered in nuclear engineering in connection with the cooling of reactors. For *Prandtl* number P_r six values 0.2, 0.5, 0.71, 1.0, 2.0 and 5.0 are considered $(0.2, 0.5$ and 0.71 for air at 20^0C and $1, 2, 5$ for water$)$. The values 0.1, 0.5, 0.6, 0.95, 5.0 and 10.0 are also considered for the *Schmidt* number S_c which represents specific conditions of the flow $(0.95$ for CO_2 and $0.1, 0.5, 0.6, 5$ and 10 for water$)$. In particular, $S_c = 0.6$ corresponds to water vapor that represents a diffusive chemical species of most common interest in air. The values of other parameters are however chosen arbitrarily. With the above mentioned parameters, the primary (u/U_0) and the secondary (g_0) velocity profiles are presented in Figs. 4.2-4.19, the temperature fields are presented in Figs. 4.20-4.28 and the concentration fields are presented in Figs. 4.29-4.37.

Fig. 4.2 shows the primary velocity fields for different values of Suction parameter v_0. It is observed from this figure that the velocity decreases with the increase of suction parameter v_0. For both $v_0 > 0$ and $v_0 < 0$ indicating the usual fact that the suction stabilizes the boundary layer growth. The free convection effect is also apparent in this figure. For $\eta = 1.2$, the velocity profile is found to increase and reaches maximum value in a region close to the leading edge of the plate, then gradually decrease to one. Fig. 4.3 shows the primary velocity field for different

values of Magnetic parameter M. We see from Fig. 4.3 that the velocity field decreases with the increase of Magnetic parameter M. These effects are much more stronger near the surface of the plate. In Fig. 4.4, the effects of rotation parameter R on the primary velocity is shown. It is observed from this figure that rotation parameter has a negligible minor decreasing effect on the primary velocity with the increase of R. In Figs. 4.5- 4.7, the effects of *Soret* number S_0, *Dufour* number D_f and *Eckert* number E_c on the primary velocity are shown respectively. It is observed from Fig. 4.5 that the primary velocity increases with the increase of *Soret* number S_0. Fig. 4.6 shows that the velocity field increases with the increase of *Dufour* number D_f and maintain uniform increasing behaviour. Fig. 4.7 shows that the primary velocity field increases with the increase of *Eckert* number E_c. To increase the fluid motion we need to consider viscous dissipation. From viscous dissipation term we obtained dimensionless parameter E_c. This prameter is called the fluid motion controling parameter. Fig. 4.8 shows the primary velocity field for different values of *Prandtl* number P_r. It is seen from this figure that magnitude of the primary velocity has a overshoot behaviour for small *Prandtl* number P_r. But for larger values of $P_r\left(P_r=5\right)$, the primary velocity is found to decerease monotonically and hence there appears a thin boundary layer indicating the decerease of the free convection. In Figs. 4.9 and 4.10 the effect of *Schmidt* number S_c and permeability parameter K on the primary velocity are shown respectively. Fig. 4.9 shows that the primary velocity field decreases with the increase of *Schmidt* number S_c. The same is the case for permeability parameter K as dipicted in Fig. 4.10. The effects of various parameters on the secondary velocities are shown in Figs. 4.11-4.19. The effect of the Suction parameter v_0 on the secondary velocity is shown in Figs. 4.11. It is observed from this figure that the secondary velocity increases with the increase of Suction parameter v_0 for both $v_0>0$ and $v_0<0$, indicating the usual fact that suction stabilizes the boundary layer growth. The free convection effect is also apparent in this figure. For $\eta=1$, the velocity profile is found to increase from $-0.1$and reaches maximum value in a region close to the leading edge of the plate, then gradually increase to zero. Fig. 4.12 shows the secondary velocity field for different values of Magnetic parameter M. We see from this figure that the secondary velocity field increases with the increase of Magnetic parameter M. These effects are much more stronger near the surface of the plate. Fig. 4.13 shows the secondary velocity for different values of Rotation parameter R. It is observed from this figure that rotation parameter has a larger decreasing effect on the secondary velocity with the increase of R. In Figs. 4.14- 4.16, the effects of *Soret* number S_0, *Dufour* number D_f and *Eckert* number E_c on

the secondary velocity are shown respectively. It is observed from Fig. 4.14 that the secondary velocity decreases with the increase of *Soret* number S_0 while for large values of S_0, the secondary velocity decrease much more. Fig. 4.15 shows that the velocity increases with the increase of *Dufour* number D_f and maintain uniform decreasing behaviour. Fig. 4.16 shows that the secondary velocity increases with the increase of *Eckert* number E_c. Fig. 4.17 shows the secondary velocity for different values of *Prandtl* number P_r. We see from this figure (Fig. 4.17) that magnitude of the velocity has a overshoot behaviour for small *Prandtl* number P_r. But for larger values of $P_r\left(P_r=5\right)$, the velocity is found to inecerease monotonically and hence there appears a thin boundary layer indicating the incerease of the free convection. In Figs. 4.18 and 4.19 the effect of *Schmidt* number S_c and Permeaability parameter K on the secondary velocity are shown respectively. Fig. 4.18 shows that the secondary velocity increases with the increase of *Schmidt* number S_c. Fig. 4.19 shows that the secondary velocity field increases with the increase of permeability parameter K and maintain a uniform increasing behaviour.

The effect of Suction parameter (v_0) on the temperature field is shown in Fig. 4.20. It is observed from this figure that the temperature field decreases with the increase of suction parameter v_0. The effects of Magnetic parameter M and rotation parameter R on the temperature field are shown in Figs. 4.21 and 4.22 respectively. We see from the Fig. 4.21 that there is a minor increasing effect on the temperature field for the increase of Magnetic parameter M and where as there is minor decreasing effect on the temperature field for increase of rotation parameter R. Fig. 4.23 shows the temperature field for different values of *Soret* number S_o. It is seen from this figure that the temperature field decreases with the increase of *Soret* number S_o. Figs. 4.24 and 4.25 show the temperature field for different values of *Dufour number* D_f and *Eckert* number E_c. We see from these figures (Figs. 4.24-4.25) that the temperature field to increase with the increase of D_f, E_c and D_f maintain a uniform increasing behaviour. Fig. 4.26 shows the temperature field for different values of *Prandtl* number P_r. We see from this figure that the temperature field has a large decreasing effect with the increase of *Prandtl* number P_r. Fig. 4.27 shows the temperature field for different values of *Schmidt* number S_c. We see from Fig. 4.27 that the temperature field has inecreasing effect with the increase of *Schmidt* number S_c. Fig. 4.28 shows the temperatue field for different values of permeability parameter K. We see from Fig. 4.28 that temperatue field has a minor decreasing effect with the increase of permeability parameter K.

The effects of various parameters on the concentration field are shown in Figs. 4.29-4.37. Fig. 4.29 shows the concentration field for different values of suction parameter v_0. We see from Fig. 4.29 that the concentration field decreases with the increase of suction parameter v_0 and maintain a uniform decreasing behaviour. Figs. 4.30 and 4.31 show the concentration field for different values of Magnecting parameter M and Rotation parameter R. We see from these figures that there are negligible increasing efffct in concentration field for increase in both of the Magnectic parameter M and rotation parameter R. Figs. 4.32 and 4.33 show the concentration field for different values of *Soret* number S_o and *Dufour* number D_f. It is observed from these figures that the *Soret* number S_o has a large increasing effect while the *Dufour* number D_f has a minor decreasing effect on concentration. Fig. 4.34 shows the concentration field for different values of *Eckert* number E_c. Fig. 4.34 shows that there is negligible decreasing effect in concentration field with the increase of *Eckert* number E_c. Fig. 4.35 shows the concentration field for different values of *Prandtl* number P_r. Fig. 4.35 shows that there is an increasing effect on concentration field with the increase of Prandtl number P_r. Fig. 4.36 shows the concentration field for different values of *Schmidt* number S_c. It is observed from this figure that the concentration field has a large decreasing effect with the increase of *Schmidt* number S_c. Fig. 4.37 shows the concentration field for different values of permiability parameter K. We see from this figure that there is a negligible increasing effect on the concentration field with the increase of permiability parameter K.

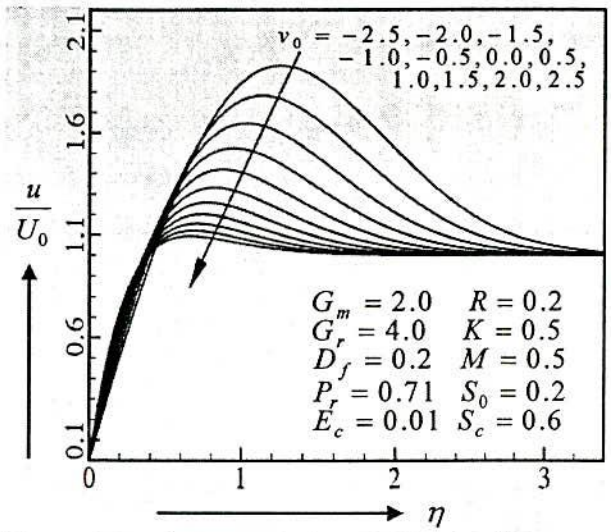

Figure 4.2. Primary velocity profiles for different values of v_0

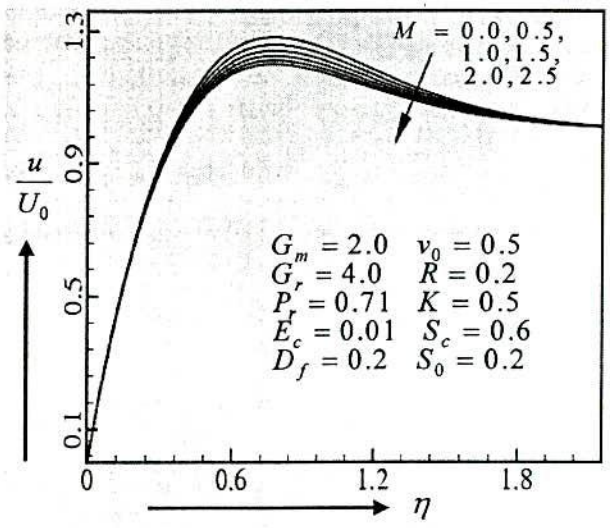

Figure 4.3. Primary velocity profiles for different values of M

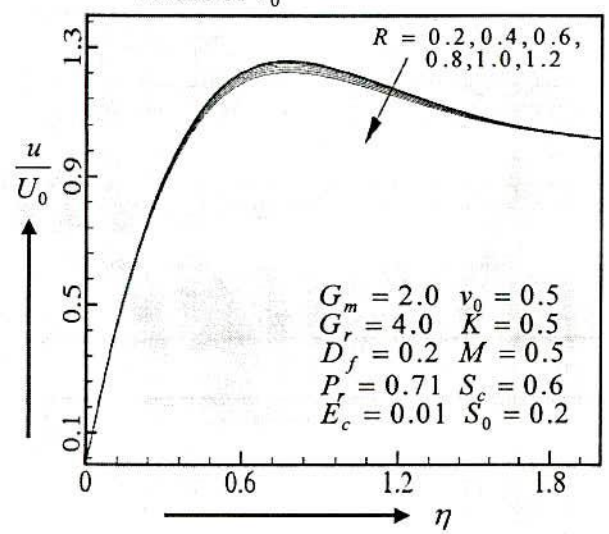

Figure 4.4. Primary velocity profiles for different values of R

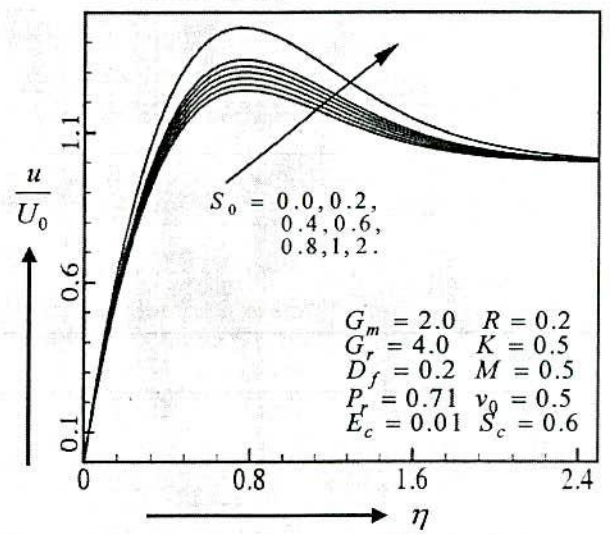

Figure 4.5. Primary velocity profiles for different values of S_0

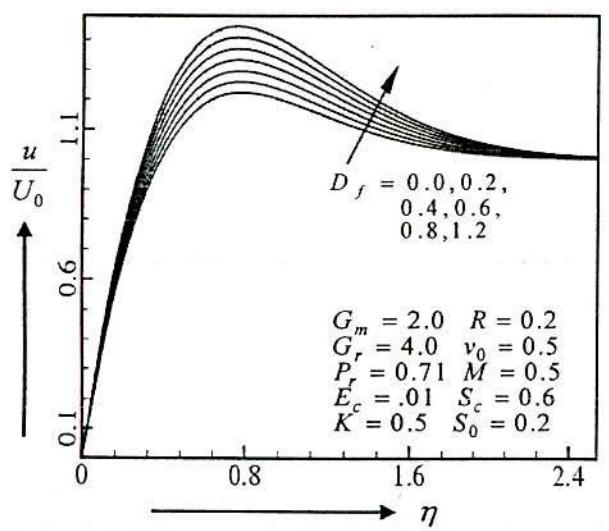

Figure 4.6. Primary velocity profiles for different values of D_f

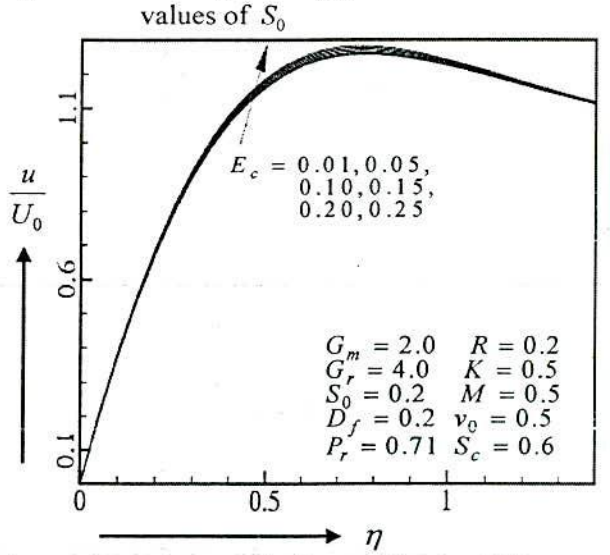

Figure 4.7. Primary velocity profiles for different values of E_c

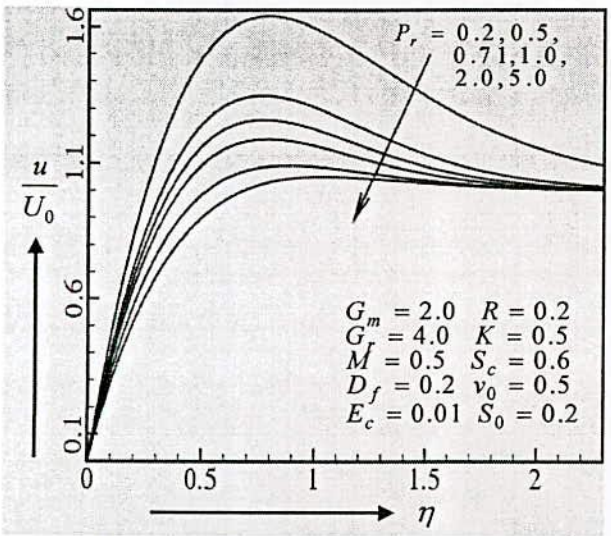

Figure 4.8. Primary velocity profiles for different values of P_r

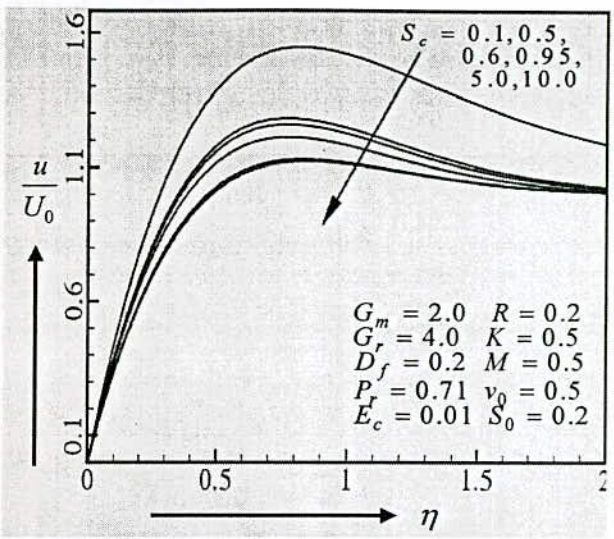

Figure4.9. Primary velocity profiles for different values of S_c

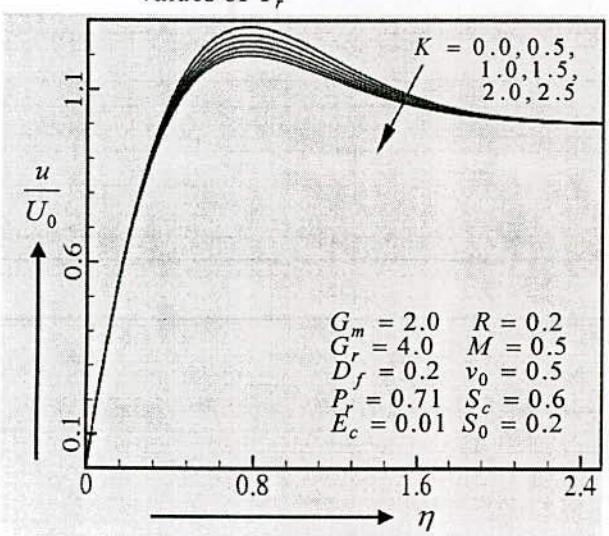

Figure 4.10. Primary velocity profiles for different values of K

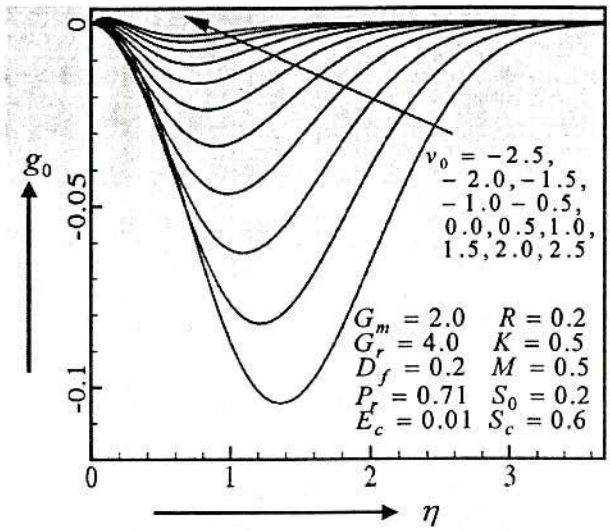

Figure 4.11. Secondary velocity profiles for different values of v_0

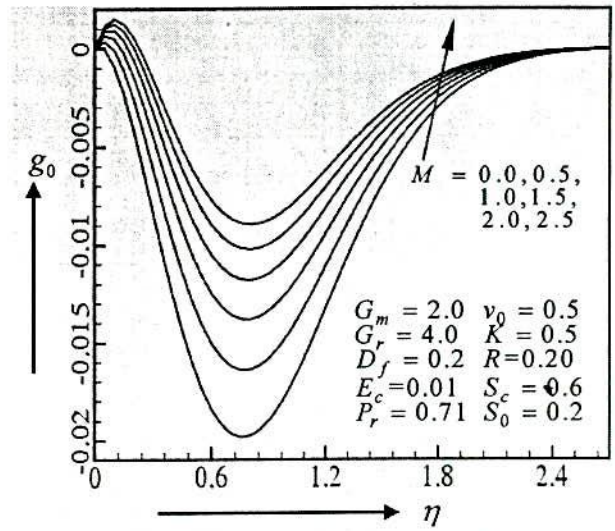

Figure 4.12. Secondary velocity profiles for different values of M

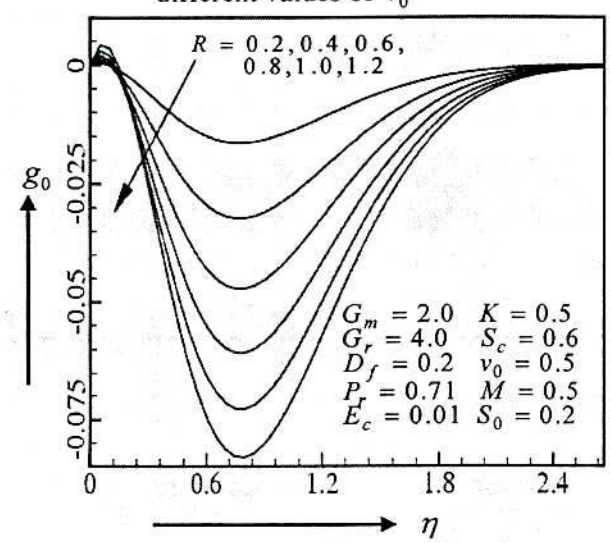

Figure 4.13. Secondary velocity profiles for different values of R

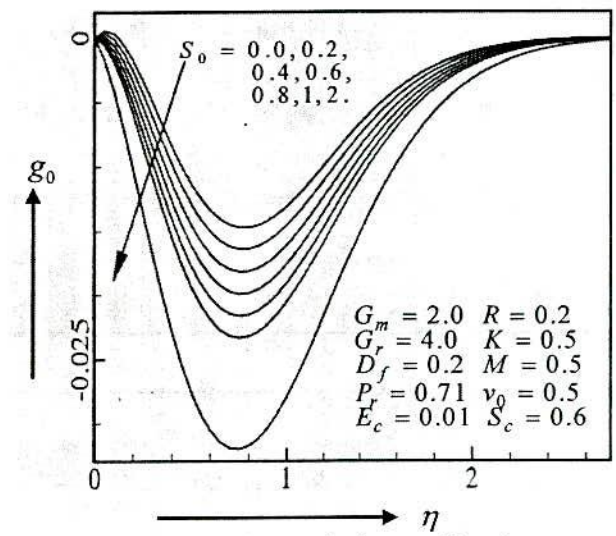

Figure 4.14. Secondary velocity profiles for different values of S_0

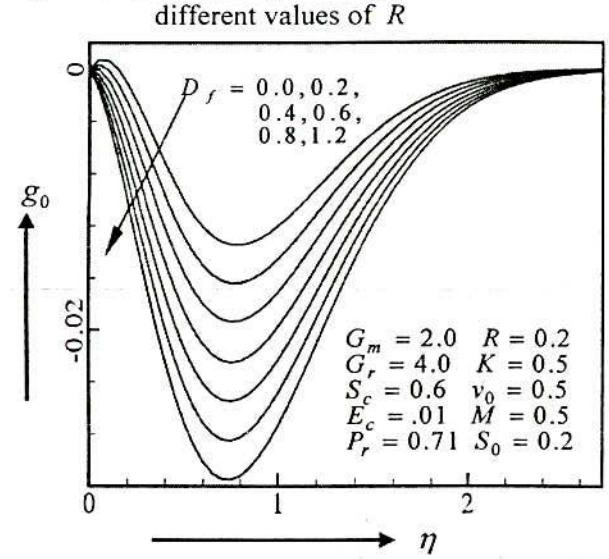

Figure 4.15. Secondary velocity profiles for different values of D_f

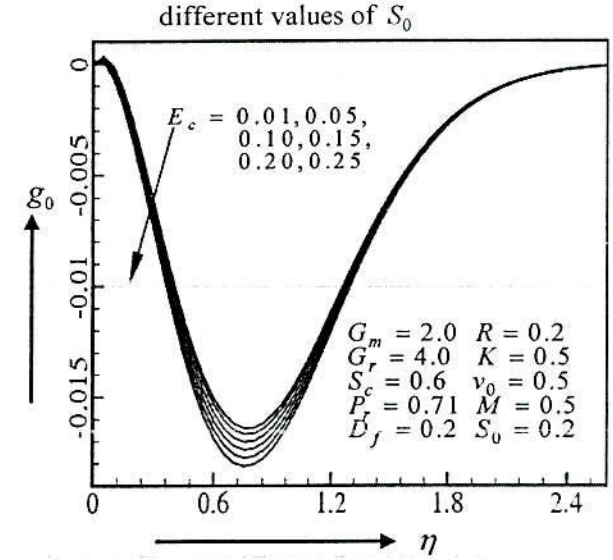

Figure 4.16. Secondary velocity profiles for different values of E_c

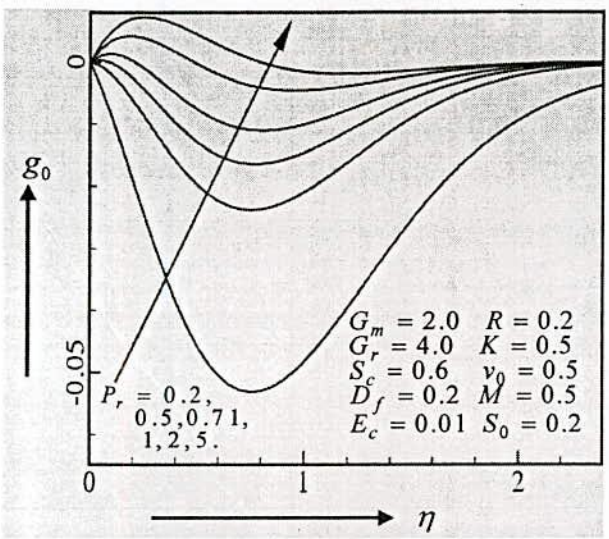

Figure 4.17. Secondary velocity profiles for different values of P_r

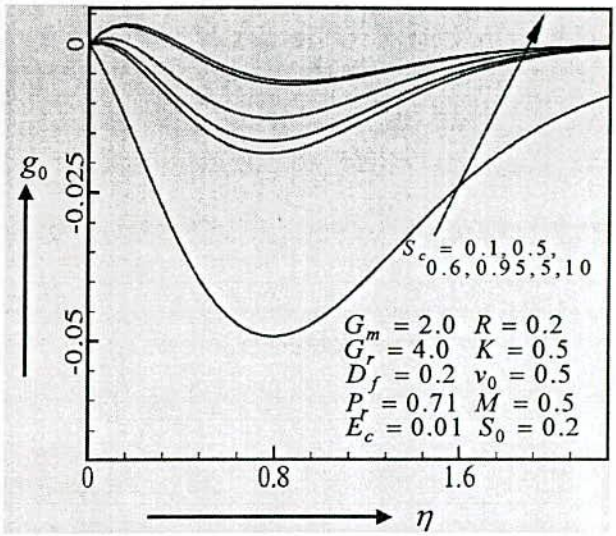

Figure 4.18. Secondary velocity profiles for different values of S_c

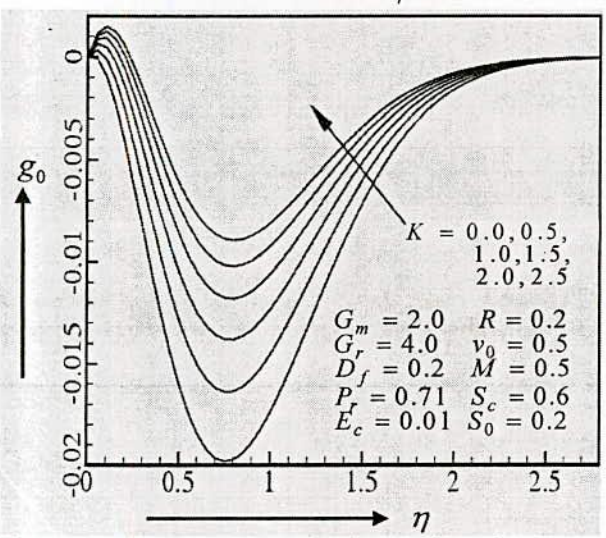

Figure 4.19. Secondary velocity profiles for different values of K

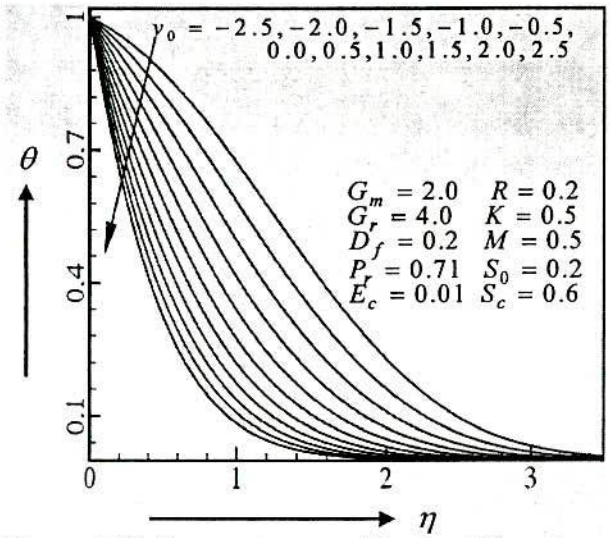

Figure 4.20. Temperature profiles for different values of v_0

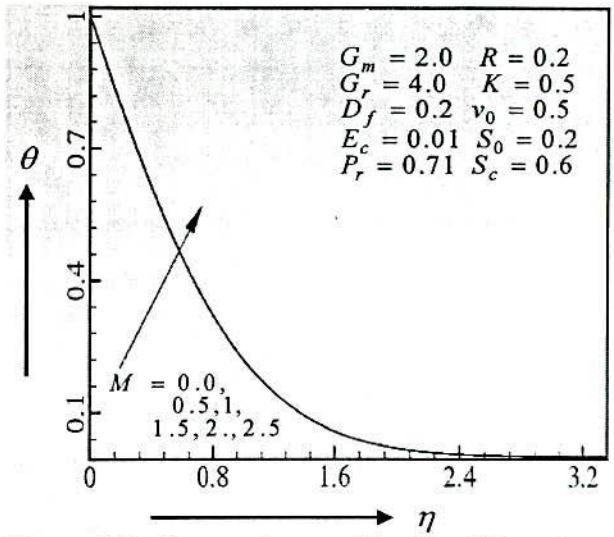

Figure 4.21. Temperature profiles for different values of M

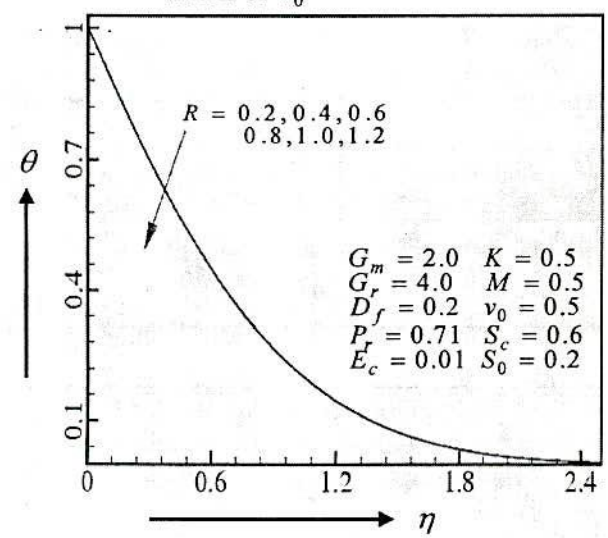

Figure 4.22. Temperature profiles for different values of R

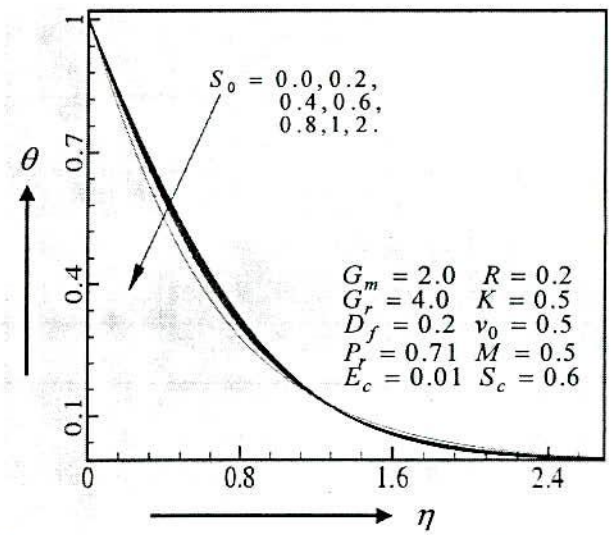

Figure 4.23. Temperature profiles for different values of S_0

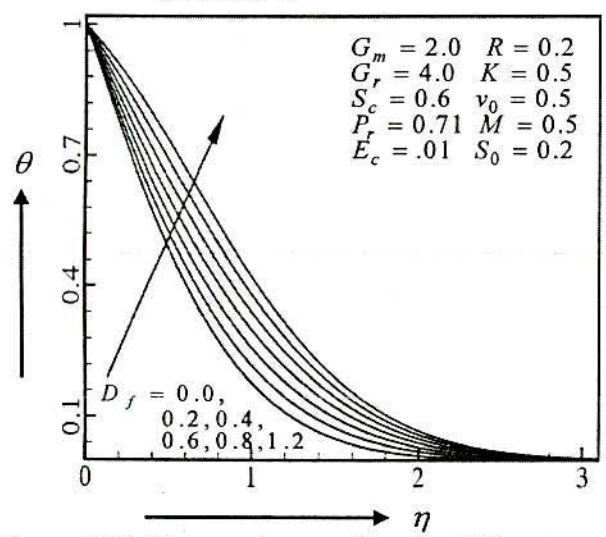

Figure 4.24. Temperature profiles for different values of D_f

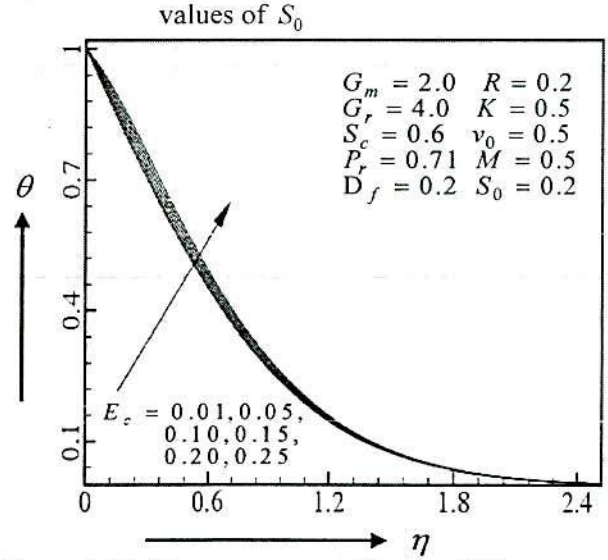

Figure 4.25. Temperature profiles for different values of E_c

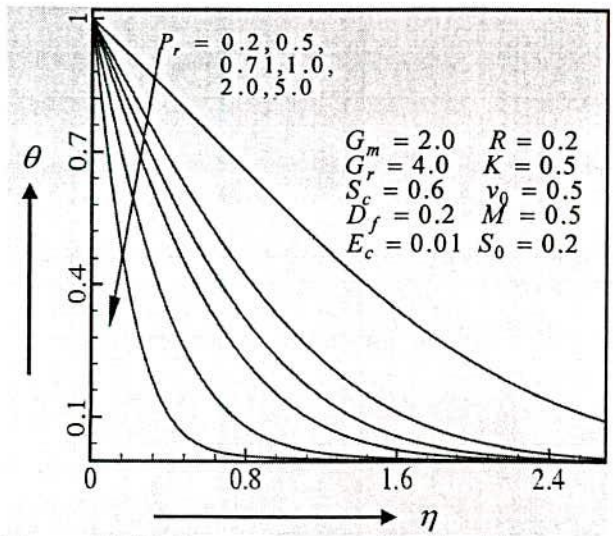

Figure 45.26. Temperature profiles for different values of P_r

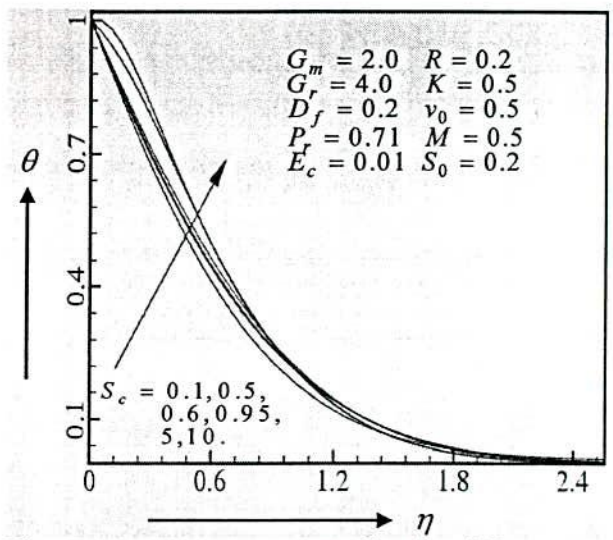

Figure 4.27. Temperature profiles for different values of S_c

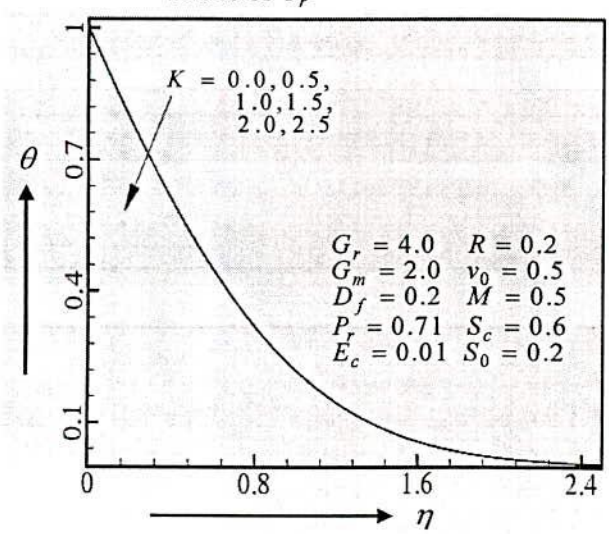

Figure 4.28. Temperature profiles for different values of K

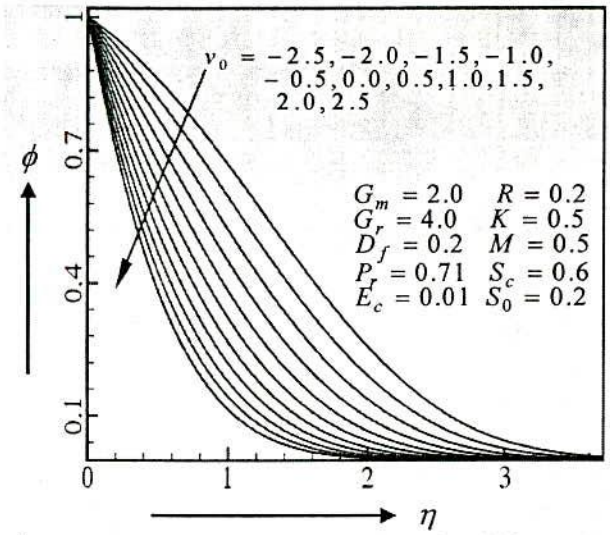

Figure 4.29. Concentration profiles for different values of v_0

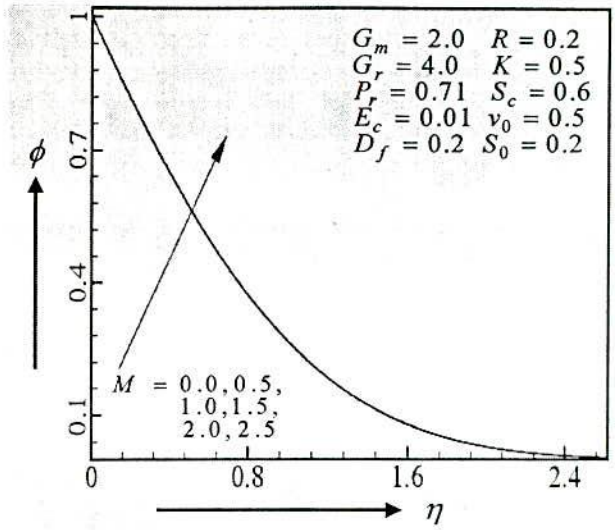

Figure 4.30. Concentration profiles for different values of M

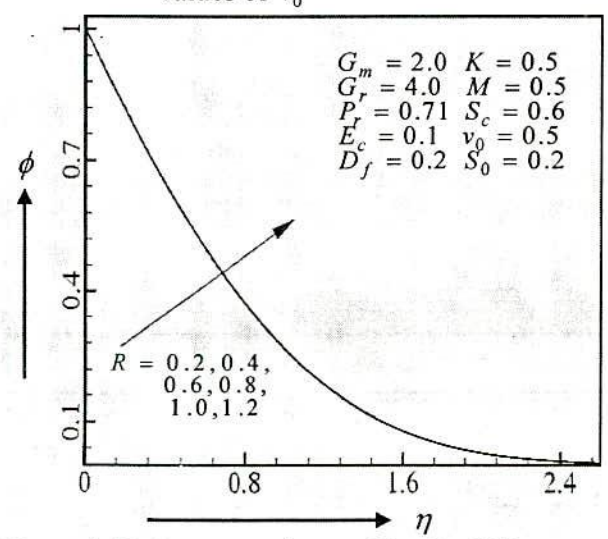

Figure 4.31. Concentration profiles for different values of R

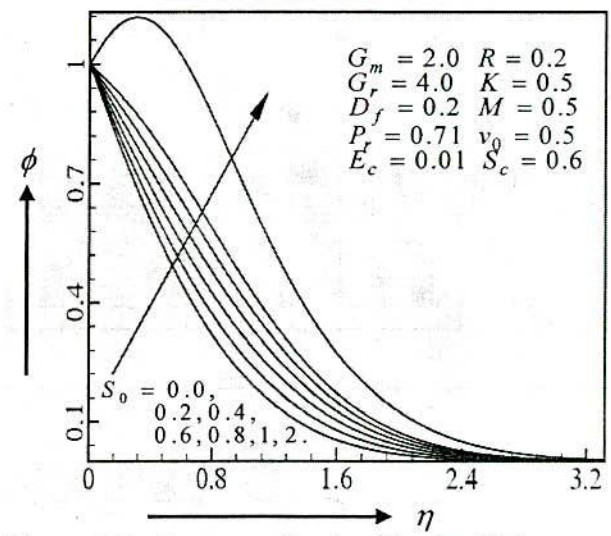

Figure 4.32. Concentration profiles for different values of S_0

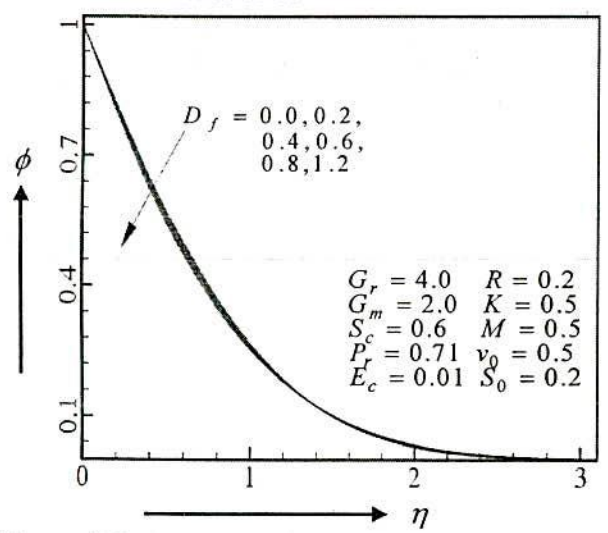

Figure 4.33. Concentration profiles for different values of D_f

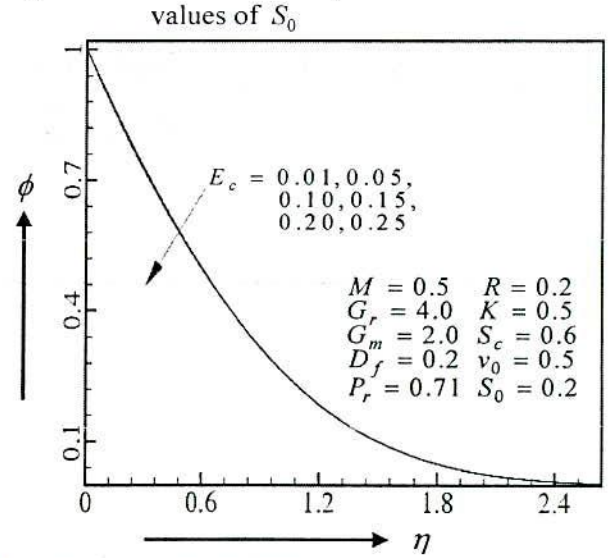

Figure 4.34. Concentration profiles for different values of E_c

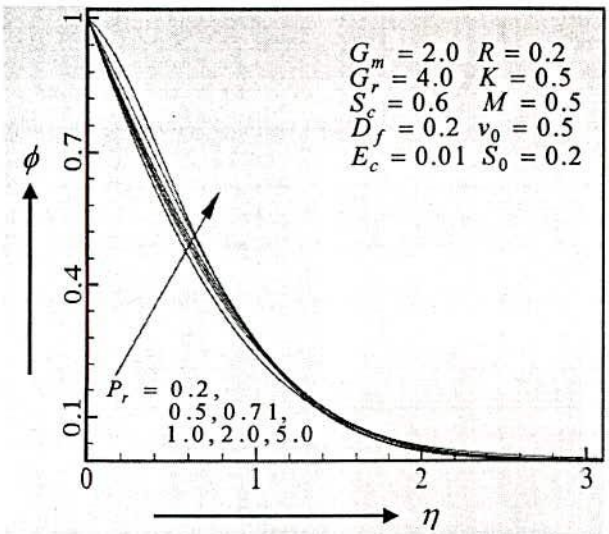

Figure 4.35. Concentration profiles for different values of P_r

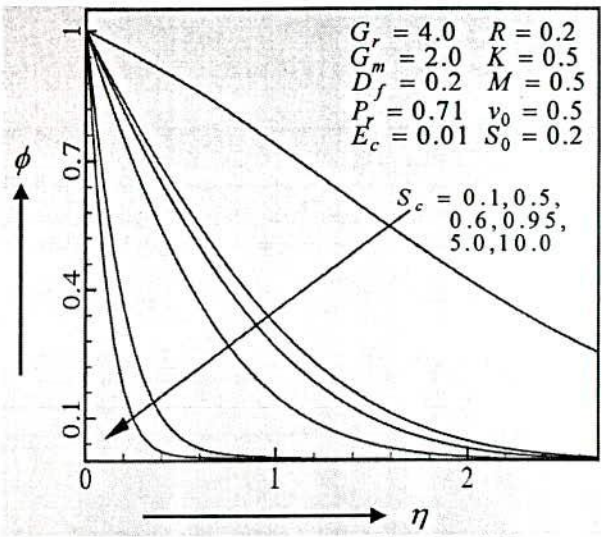

Figure 4.36. Concentration profiles for different different values of S_c

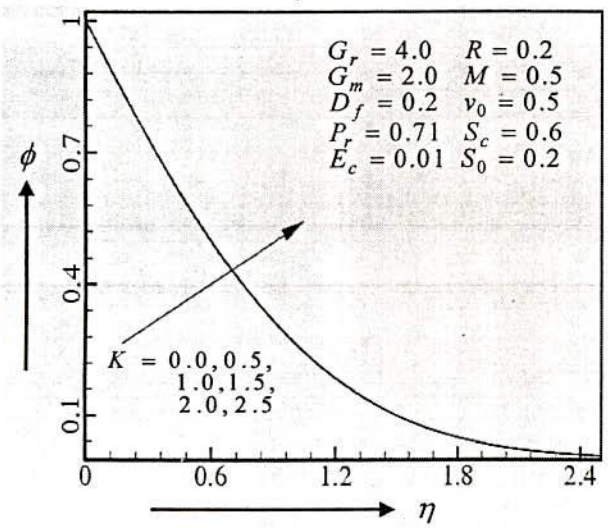

Figure 4.37. Concentration profiles for different values of K

Finally, to identify the effects of various parameters on the components of skin friction τ_x and τ_z, the *Nusselt* number N_u and the *Sherwood* number S_h, numerical values proportional to these quantites are tabuleted in n Tables 4.1-4.5.

From Table 4.1 we observe that the skin friction component τ_x decreases while the skin friction component τ_z, the *Nusselt* number N_u and the *Sherwood* number S_h increase with the increase of the suction parameter v_0. From table 4.2 we observe that the skin friction component τ_x and the *Nusselt* number N_u decrease while the skin friction component τ_z and the *Sherwood* number S_h increase with the increase of Magnetic parameter M. It is also seen from this table that the skin friction components τ_x, τ_z and the *Nusselt* number N_u increase while the *Sherwood* number S_h decreases with the increase of rotation parameter R. From table 4.3 we observe that the skin friction components τ_x, τ_z and the *Sherwood* number S_h decrease while the *Nusselt* number N_u increases with the increase of *Soret* number S_o. It is also seen from this table that the skin friction components τ_x, τ_z and the *Nusselt* number N_u decrease while the *Sherwood* number S_h increases with the increase of *Dufour* number D_f. From table 4.4 we see that the skin friction components τ_x, τ_z and the *Nusselt* number N_u decrease while the *Sherwood* number S_h increases with the increase of *Eckert* number E_c. It is also seen from this table that the skin friction components τ_x, τ_z and the *Nusselt* number N_u increase while the *Sherwood* number S_h decreases with the increase of *Prandtl* number P_r. From table 4.5 we see that the skin friction components τ_x, τ_z and the *Sherwood* number S_h increase while the *Nusselt* number N_u decreases with the increase of *Schmidt* number S_c. It is also seen from this table that the skin friction component τ_x and the Sherwood number S_h decrease while the *Nusselt* number N_u and the skin friction component τ_z increase with the increase of permeability parameter K.

Table 4.1. Numerical values proportional to τ_x, τ_z, N_u and S_h taking $S_0 = 0.2$, $P_r = 0.71$, $G_r = 4.0, M = 0.5, G_m = 2.0$ $R = 0.2, S_c = 0.6, D_f = 0.2$, and $K = 0.5$ with v_0 to vary.

v_0	τ_x	τ_z	N_u	S_h
-2.5	-2.6032464	.0014727	.1673914	.2104289
-2.0	-2.8947463	.0021206	.2555351	.2944314
-1.5	-3.1834914	.0024919	.3695305	.3953901
-1.0	-3.4635933	.0026889	.5090191	.5122146
-0.5	-3.7319032	.0052704	.6729678	.6443044
0.0	-3.9932877	.0101798	.8583514	.7897933
0.5	-4.2507479	.0164058	1.0629937	.9479664
1.0	-4.5132391	.0224362	1.2831548	1.1165286
1.5	-4.7820944	.0280299	1.5172842	1.2951847
2.0	-5.0656228	.0323564	1.7616756	1.4812378
2.5	-5.3630997	.0356604	2.0152589	1.6743904

Table 4.2. Numerical values proportional to τ_x, τ_z, N_u and S_h taking $v_0 = 0.5, P_r = 0.71$, $G_r = 4, G_m = 2, E_c = 0.01$, $S_0 = 0.2$, $S_c = 0.6$, $D_f = 0.2$, and $K = 0.5$ with M and R to vary.

M	R	τ_x	τ_z	N_u	S_h
0.0	0.2	-4.2344149	.0081242	1.0629978	.9479650
0.5	,,	-4.2507479	.0164058	1.0629737	.9479664
1.0	,,	-4.2756963	.0224165	1.0629457	.9479731
1.5	,,	-4.3069663	.0268456	1.0628202	.9479950
2.0	,,	-4.3429325	.0301456	1.0626362	.9480284
2.5	,,	-4.3824178	.0326225	1.0624076	.9480706
0.5	0.2	-4.2507479	.0164058	1.0629937	.9479664
,,	0.4	-4.2424756	.0342374	1.0630951	.9479461
,,	0.6	-4.2293755	.0547700	1.0632559	.9479139
,,	0.8	-4.2123720	.0790073	1.0634654	.9478719
,,	1.0	-4.1925757	.1076129	1.0637104	.9478227
,,	1.2	-4.1711530	.1408961	1.0639772	.9477690

Table 4.3. Numerical values proportional to τ_x, τ_z, N_u and S_h taking $G_r = 4, G_m = 2, R = 0.2$, $P_r = 0.71$, $M = 0.5$, $E_c = 0.01, D_f = 0.2$ and $K = 0.5$ with S_o and D_f to vary.

S_o	D_f	τ_x	τ_z	N_u	S_h
0.0	0.2	-4.2025309	.0208051	1.0428578	1.0737806
0.2	,,	-4.2507479	.0164058	1.0629937	.9479664
0.4	,,	-4.3014694	.0117596	1.0841053	.8138759
0.6	,,	-4.3518490	.0072496	1.1071507	.6714501
0.8		-4.4031363	.0027171	1.1320007	.5192737
1.0	,,	-4.4553906	-.0018386	1.1588972	.3560743
2.0	,,	-4.7357468	-.0252839	1.3364527	-.6919651
0.2	0.0	-4.1591154	.0243176	1.1677855	.9303618
,,	0.2	-4.2507479	.0164058	1.0629937	.9479664
,,	0.4	-4.3440604	.0084581	.9514506	.9668413
,,	0.6	-4.4417967	.0001190	.8315179	.9866385
,,	0.8	-4.5396087	-.0080151	.7036162	1.0084741
,,	1.0	-4.6395221	-.0161977	.5660337	1.0321457
,,	1.2	-4.7416906	-.0244308	.4174119	1.0579172

Table 4.4. Numerical values proportional to τ_x, τ_z, N_u and S_h taking $v_0 = 0.5, G_r = 4$, $G_m = 2.0, D_f = 0.2, R = 0.2$, $M = 0.5, S_0 = 0.2, K = 0.5$ and $S_c = 0.6$ with E_c and P_r to vary.

E_c	P_r	τ_x	τ_z	N_u	S_h
0.01	0.71	-4.2507479	.0164058	1.0629937	.9479664
0.05	,,	-4.2673767	.0155146	.9737796	.9650861
0.10	,,	-4.2885688	.0143770	.8602184	.9868772
0.15	,,	-4.3102339	.0132118	.7442928	1.0091210
0.20	,,	-4.3323969	.0120176	.6258948	1.0318381
0.25	,,	-4.3550848	.0107925	.5049080	1.0550507
0.01	0.2	-5.0958795	-.0736414	.4131745	1.0478780
,,	0.5	-4.4695450	-.0030727	.8289705	.9862668
,,	0.71	-4.2507479	.0164058	1.0629937	.9479664
,,	1.0	-4.0524785	.0317635	1.3501521	.8982374
,,	2.0	-3.6983730	.0540075	2.1914565	.7447885
,,	5.0	-3.3345954	.0699603	4.2541584	.3487130

Table 4.5. Numerical values propirtional to τ_x, τ_z, N_u and S_h taking $v_0 = 0.5, G_r = 4$, $G_m = 2$, $D_f = 0.2, R = 0.2, M = 0.5$, $S_0 = 0.2$, $E_c = 0.01$, and $S_c = 0.6$ with S_c and K to vary.

S_c	K	τ_x	τ_z	N_u	S_h
0.1	0.5	-4.8288756	-.0586941	1.1579655	.2091358
0.5	,,	-4.3030211	.0112868	1.0808105	.8306082
0.6	,,	-4.2507479	.0164058	1.0629937	.9479664
0.95	,,	-4.1317398	.0267169	1.0026651	1.3134241
5.0	,,	-3.8196615	.0455131	.4351708	4.3254822
10.0	,,	-3.7436779	.0480643	-.1818954	7.3924571
0.6	0.0	-4.2345562	.0081132	1.0625083	.9480607
,,	0.5	-4.2507479	.0164058	1.0629937	.9479664
,,	1.0	-4.2756023	.0224224	1.0633463	.9478972
,,	1.5	-4.3068075	.0268546	1.0636004	.9478465
,,	2.0	-4.3427274	.0301562	1.0637800	.9478101
,,	2.5	-4.3821786	.0326339	1.0639021	.9477847

Chapter 5

Viscous dissipation and Joule heating effects on Steady MHD combined heat and mass transfer flow through a porous medium in a rotating system

5.1. Introduction

The steady and unsteady thermal boundary layer of an incompressible fluid have been investigated as basic boundary layers problems in a rotating fluid which generally appear in Oceanic, Atmospheric and Cosmic fluid dynamics and in Solar Physics or Geophysics. *Soundalgekar and Pop (1979)* studied the free convective effects in a rotating viscous fluid past an infinite vertical porous plate. *Raptis and Perdikis(1982)* studied the effect of mass transfer on a free convective flow past an infinite porous plate in a rotating fluid.

The *Soret* and *Dufour* effect have been discussed clearly in **(Chapter 2)** and we are not repeating that again. In view of the importance of *Soret* and *Dufour* effects, *Kafoussias and Williams (1995)* studied thermal-diffusion and diffusion-thermo effects on mixed convective mass transfer boundary layer flow with temperature dependent viscosity. *Anghel et al.(2000)* investigated the *Dufour* and *Soret* effects on free convection boundary layer flow over a vertical surface embedded in a porous medium. Recently, *Postelnicu (2004)* studied numerically the influence of a magnetic field on heat and mass transfer flow considering *Soret* and *Dufour* effects. Quite recently, *Alam and Rahman (2006)* investigated the *Dufour* and *Soret* effects on mixed convection flow past a vertical porous flat plate with variable suction. The effect of of *Joule* heating on MHD free convection flow of an electrically conducting semi-infinite vertical plate was however, considered by *Hossain (1990)*. Hence, our objective is to investigate the steady MHD combined heat and mass transfer flow through a porous medium past a semi-infinite vertical porous plate in a rotating system with *Soret*, *Dufour* and permeability effects along with viscous dissipation and *Joule* heating.

5.2. The Governing Equations

Let us consider an steady MHD combined heat and mass transfer flow of an electrically conducting viscous fluid through a porous medium along a semi-infinite vertical porous plate $y = 0$ in a rotating system. The fluid is also assumed to be moving with a uniform velocity U_o in the x-direction which is taken along the plate in the upward direction and y-axis is normal to it. Initially the plate is at rest, after that the whole system is allowed to rotate with a instantly angular velocity Ω about the y-axis. Since the system rotates about $y-$axis, so we can take $\mathbf{\Omega} = (0,-\Omega,0)$. The temperature and the species concentration at the plate are instantly raised from T_w and C_w to T_∞ and C_∞ respectively, which are thereafter maintained as constant, where T_∞ and C_∞ are the temperature and species concentration of the uniform flow respectively. A uniform magnetic field $\mathbf{B}$ is taken to be acting along the $y-$axis which is assumed to be electrically non-conducting. We assumed following *Pai (1962)* that the magnetic Reynolds number of the flow be small enough so that the induced magnetic field is negligible in comparison with applied one and the magnetic lines of force are fixed relative to the fluid. The equation of conservation of charge $\nabla.\mathbf{J} = 0$ gives $J_y = $ constant, where the current density $\mathbf{J} = (J_x, J_y, J_z)$. Since the plate is electrically non-conducting, this constant is zero and hence $J_y = 0$ at the plate and also zero everywhere. The physical configuration considered here is shown in Fig. 5.1. With reference to the generalized equations described **in *case-II* of Chapter 2**, the two dimensional problem for combined heat and mass transfer under the above assumptions can be put as

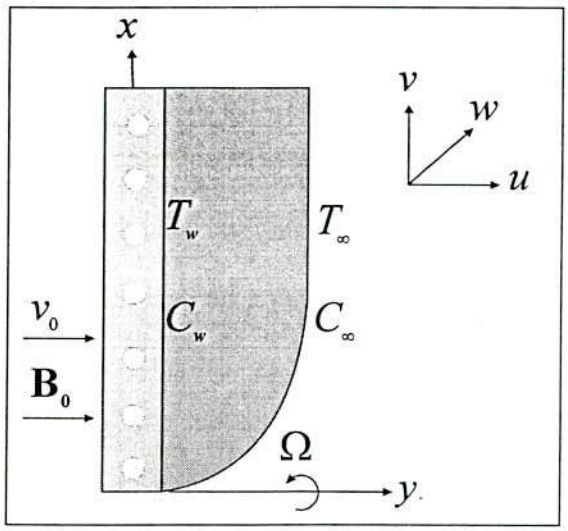

Fig. 1. Physical configuration and coordinate sysrem

$$\frac{\partial u}{\partial x}+\frac{\partial v}{\partial y}=0 \tag{5.1}$$

$$u\frac{\partial u}{\partial x}+v\frac{\partial u}{\partial y}=\upsilon\frac{\partial^2 u}{\partial y^2}+g\beta(T-T_\infty)\ +g\beta^*(C-C_\infty)+2\Omega w+\frac{\upsilon}{K'}(U_0-u)+\frac{\sigma' B_0{}^2}{\rho}(U_0-u) \tag{5.2}$$

$$u\frac{\partial w}{\partial x}+v\frac{\partial w}{\partial y}=\upsilon\frac{\partial^2 w}{\partial y^2}+2\Omega(U_0-u)-\frac{\upsilon}{K'}w-\frac{\sigma' B_0{}^2 w}{\rho} \tag{5..3}$$

$$u\frac{\partial T}{\partial x}+v\frac{\partial T}{\partial y}=\frac{\kappa}{\rho c_p}\frac{\partial^2 T}{\partial y^2}+\frac{D_m k_T}{c_s c_p}\frac{\partial^2 C}{\partial y^2}+\frac{\upsilon}{c_p}\left[\left(\frac{\partial u}{\partial y}\right)^2+\left(\frac{\partial w}{\partial y}\right)^2\right]+\frac{\sigma' B_0^2}{\rho c_p}\left[(U_0-u)^2+w^2\right] \tag{5.4}$$

$$u\frac{\partial C}{\partial x}+v\frac{\partial C}{\partial y}=D_m\frac{\partial^2 C}{\partial y^2}+\frac{D_m k_T}{T_m}\frac{\partial^2 T}{\partial y^2} \tag{5.5}$$

The boundary conditions for the problem are

$$\left.\begin{aligned} &u=0, v=v_0(x),\ w=0, T=T_w,\ C=C_w \quad at\ y=0\\ &u=U_0, \qquad\qquad w=0, T\to T_\infty, C\to C_\infty \ as\ y\to\infty \end{aligned}\right\} \tag{5.6}$$

Following the work of Sattar (1993), a transformation is now made as;

$U_0-u=u_1 \ \therefore u=U_0-u_1$

So the equations (5.1)-(5.5) and the boundary conditions (5.6), respectively transform to,

$$-\frac{\partial u_1}{\partial x}+\frac{\partial v}{\partial y}=0 \tag{5.7}$$

$$(U_0-u_1)\frac{\partial u_1}{\partial x}+v\frac{\partial u_1}{\partial y}=\upsilon\frac{\partial^2 u_1}{\partial y^2}-g\beta(T-T_\infty)\ -g\beta^*(C-C_\infty)-2\Omega w-\frac{\upsilon}{K'}u_1-\frac{\sigma' B_0{}^2}{\rho}u_1 \tag{5.8}$$

$$(U_0-u_1)\frac{\partial w}{\partial x}+v\frac{\partial w}{\partial y}=\upsilon\frac{\partial^2 w}{\partial y^2}+2\Omega u_1-\frac{\upsilon}{K'}w-\frac{\sigma' B_0{}^2 w}{\rho} \tag{5.9}$$

$$(U_0-u_1)\frac{\partial T}{\partial x}+v\frac{\partial T}{\partial y}=\frac{k}{\rho c_p}\frac{\partial^2 T}{\partial y^2}+\frac{D_m k_T}{c_s c_p}\frac{\partial^2 C}{\partial y^2}+\frac{\upsilon}{c_p}\left[\left(\frac{\partial u_1}{\partial y}\right)^2+\left(\frac{\partial w}{\partial y}\right)^2\right]+\frac{\sigma' B_0^2}{\rho c_p}\left[u_1^2+w^2\right] \tag{5.10}$$

$$(U_0-u_1)\frac{\partial C}{\partial x}+v\frac{\partial C}{\partial y}=D_m\frac{\partial^2 C}{\partial y^2}+\frac{D_m k_T}{T_m}\frac{\partial^2 T}{\partial y^2} \tag{5.11}$$

$$\left.\begin{aligned} &u_1=U_0, v=v_0(x), w=0, T=T_w, C=C_w \quad at\ \ y=0\\ &u_1=0, \qquad\qquad w=0, T\to T_\infty, C\to C_\infty \ as\ \ y\to\infty \end{aligned}\right\} \tag{5.12}$$

where u,v are the velocity components in the x,y directions respectively, υ is the kinematic viscosity, g is the acceleration due to gravity, ρ is the density, β is the thermal volumetric coefficient expanssion, β^* is the volumetric coefficient of expanssion for concentration, T, T_w, T_∞ are the temperature of the fluid inside the thermal boundary layer, the plate temperature and the fluid temperature in the free stream respectivly while C, C_w, C_∞ are the coressponding concentrations, K' is the permiability of the porous medium, k is the thermal conductivity of the medium, k_T is the thermal difusion rato, c_p is the specific heat at constant pressure, D_m is the coefficient of mass diffusivity, T_m is the mean fluid temperature, c_s is the concentration susceptibility, σ' is the electric conductivity.

5.3. Mathematical Formulations

In order to solve the above system of equations (5.8)-(5.11) with the boundary conditions (5.12), we adopt the well defined similarity analysis to attain similarity solutions.For this purpose, the

following similarity transformation are now introduced;

$$\eta = y\sqrt{\frac{U_0}{2\upsilon x}} \tag{5.13}$$

$$g_0(\eta) = \frac{w}{U_0} \tag{5.14}$$

$$\theta(\eta) = \frac{T - T_\infty}{T_w - T_\infty} \tag{5.15}$$

$$\phi(\eta) = \frac{C - C_\infty}{\bar{x}(C_0 - C_\infty)} \tag{5.16}$$

$$\psi = \sqrt{2\upsilon x U_0} f(\eta) \tag{5.17}$$

$$u_1 = \frac{\partial \psi}{\partial y} = U_0 f'(\eta) \tag{5.18}$$

$$\therefore \frac{u}{U_0} = 1 - f'(\eta)$$

Now for reasons of similarity, the plate concentration is assumed to be

$$C_w(x) = C_\infty + \bar{x}(C_0 - C_\infty), \tag{5.19}$$

where C_0 is considered to be mean concentration and $\bar{x} = \frac{xU_0}{\upsilon}$.

The continuity equation (5.7) then yields

$$v = \frac{\partial \psi}{\partial x} = -\sqrt{\frac{\upsilon U_0}{2x}} \left[\eta f'(\eta) - f(\eta)\right] \tag{5.20}$$

From the equation (5.18), we have the following derivatives

$$\frac{\partial u_1}{\partial x} = -\frac{\eta}{2x} U_0 f''(\eta) \tag{5.21}$$

$$\frac{\partial u_1}{\partial y} = U_0 \sqrt{\frac{U_0}{2\upsilon x}} f''(\eta) \tag{5.22}$$

$$\frac{\partial^2 u_1}{\partial y^2} = \frac{{U_0}^2}{2\upsilon x} f'''(\eta) \tag{5.23}$$

Again from the equation (5.15) we have

$$(T - T_\infty) = (T_w - T_\infty)\theta(\eta) \tag{5.24}$$

Also from the equation (5.16), we have

$$(C - C_\infty) = \frac{U_0}{\upsilon}(C_0 - C_\infty) x \phi(\eta) \tag{5.25}$$

Thus, on introducing equations (5.14), (5.18), (5.20)-(5.25) in equation (5.8), we obtain

$$f''' + (\eta - 1) f'' - G_r \theta - G_m \phi - R g_0 - (K + M) f' = 0 \tag{5.26}$$

where $G_r = \frac{g\beta(T_w - T_\infty)2x^3}{\upsilon^2}$ is the local *Grashof* number, $G_m = \frac{g\beta^*(C_w - C_\infty)2x^3}{\upsilon^2}$ is the local modified *Grashof* number, $K = \frac{2\upsilon x}{K' U_0}$ is the permeability parameter, $M = \frac{2x\sigma' B_0^{\,2}}{\rho U_0}$ is the Magnetic parameter and $R = \frac{4\Omega x}{U_0}$ is the rotational parameter, $f_w = v_0 \sqrt{\frac{2x}{U_0 \upsilon}}$ is the Suction parameter. Here f_w is the dimensionless velocity. $f_w > 0$ indicates the suction and $f_w < 0$ the injection.

Again from the equation (5.14), we have

$$w = U_0 g_0(\eta) \tag{5.27}$$

From the equation (5.27), we have the following derivatives

$$\frac{\partial w}{\partial x} = -\frac{\eta}{2x} U_0 g_0'(\eta) \tag{5.28}$$

$$\frac{\partial w}{\partial y} = U_0 \sqrt{\frac{U_0}{2\upsilon x}} g_0'(\eta) \tag{5.29}$$

$$\frac{\partial^2 w}{\partial y^2} = \frac{U_0^{\,2}}{2\upsilon x} g_0''(\eta) \tag{5.30}$$

Substituting the equations (5.18), (5.20), (5.27) - (5.30) into the equation (5.9), we get

$$g_0'' + (\eta - f) g_0' + R f' - (K + M) g_0 = 0 \tag{5.31}$$

Now from the equation (5.15), we have

$$T = T_\infty + (T_w - T_\infty)\theta(\eta) \tag{5.32}$$

From the equation (5.32), we have the following derivatives

$$\frac{\partial T}{\partial x} = -\frac{\eta}{2x} (\mathrm{T_w} - T_\infty)\theta'(\eta) \tag{5.33}$$

$$\frac{\partial T}{\partial y} = \sqrt{\frac{U_0}{2\upsilon x}} (\mathrm{T_w} - T_\infty)\theta'(\eta) \tag{5.34}$$

$$\frac{\partial^2 T}{\partial y^2} = \frac{U_0}{2\upsilon x} (\mathrm{T_w} - T_\infty)\theta''(\eta) \tag{5.35}$$

Again from the equation (5.16), we have

$$C = C_\infty + \frac{U_0}{\upsilon} (C_0 - C_\infty) x \phi(\eta) \tag{5.36}$$

From the equation (5.36), we have the following derivatives

$$\frac{\partial C}{\partial x} = -\frac{U_0}{\upsilon}(C_0 - C_\infty)\left(\frac{\eta}{2}\phi' - \phi\right) \tag{5.37}$$

$$\frac{\partial C}{\partial y} = \frac{U_0}{\upsilon}\sqrt{\frac{U_0}{2\upsilon x}}(C_0 - C_\infty)x\phi'(\eta) \tag{5.38}$$

$$\frac{\partial^2 C}{\partial y^2} = \frac{U^2{}_0}{2\upsilon^2}(C_0 - C_\infty)\phi''(\eta) \tag{5.39}$$

Substituting the equations (5.18), (5.20), (5.22), (5.27), (5.29), (5.33)-(5.35) and (5.39) into the equation (5.10), we get

$$\theta'' + P_r(\eta - f)\theta' + D_f\phi'' + P_rE_c\left\{(f'')^2 + (g_0')^2\right\} + P_rE_cM\left\{(f')^2 + (g_0)^2\right\} = 0 \tag{5.40}$$

where $P_r = \frac{\rho\upsilon c_p}{\kappa}$ is the *Prandtl* number, $D_f = \frac{D_m k_T \rho}{c_s K'}\frac{(C_w - C_\infty)}{(T_w - T_\infty)}$ is the *Dafour* number,

$E_c = \frac{U_0^2}{c_p(T_w - T_\infty)}$ is the *Eckert* number, $M = \frac{2x\sigma' B_0^2}{\upsilon U_0}$ is the Magnetic parameter,

$\bar{x} = \frac{xU_0}{\tau}$, $\bar{x}(C_0 - C_\infty) = C_w - C_\infty$

Again substituting the equations (5.18), (5.20), (5.35), (5.37)-(5.39) into the equation (5.11) we get

$$\phi'' + S_c(\eta - f)\phi' + 2S_c(f' - 1)\phi + S_0\theta'' = 0 \tag{5.41}$$

where $S_c = \frac{\upsilon}{D_m}$ is the *Schmidt* number and $S_0 = \frac{k_T}{T_m}\frac{(T_w - T_\infty)}{(C_w - C_\infty)}$ is the *Soret* number.

Thus the equation (5.8)-(5.11), reduces to the following dimensionless ordinary nonlinear coupled differential equations:

$$f''' + (\eta - 1)f'' - G_r\theta - G_m\phi - Rg_0 - (K + M)f' = 0 \tag{5.42}$$

$$g_0'' + (\eta - f)g_0' + Rf' - (K + M)g_0 = 0 \tag{5.43}$$

$$\theta'' + P_r(\eta - f)\theta' + D_f\phi'' + P_rE_c\left\{(f'')^2 + (g_0')^2\right\} + P_rE_cM\left\{(f')^2 + (g_0)^2\right\} = 0 \tag{5.44}$$

$$\phi'' + S_c(\eta - f)\phi' + 2S_c(f' - 1)\phi + S_0\theta'' = 0 \tag{5.45}$$

The corresponding boundary conditions are

$$\left.\begin{array}{l} f = f_w,\ f' = 1,\ g_0 = 0,\ \theta = 1,\ \phi = 1 \quad \text{at } \eta = 0 \\ f' = 0, \qquad g_0 = 0,\ \theta = 0,\ \phi = 0 \quad \text{at } \eta \to \infty \end{array}\right\} \tag{5.46}$$

The next section deals with the skin-friction coefficents, the *Nusselt* number and the *Sherwood* number of the problem.

5.4. Skin-friction coefficients, Nusselt number and Sherwood number

The quantities of chief physical interest are the skin friction coefficients, the *Nusselt* number and the *Sherwood* number. The equation defining the wall skin frictions are

$\tau_x = \mu\left(\frac{\partial u}{\partial y}\right)_{y=0}$, $\tau_z = \mu\left(\frac{\partial w}{\partial y}\right)_{y=0}$ which are proportional to $\left(\frac{\partial^2 f}{\partial \eta^2}\right)_{\eta=0}$ and $\left(\frac{\partial g_0}{\partial \eta}\right)_{\eta=0}$.

The Nusselt number is denoted by $N_u = -\frac{1}{\Delta t}\left(\frac{\partial T}{\partial y}\right)_{y=0}$; which is proportional to $-\left(\frac{\partial \theta}{\partial \eta}\right)_{\eta=0}$,

hence we have $N_u \propto \theta'(0)$.

The *Sherwood* number is denoted by $S_h = -\frac{1}{\Delta t}\left(\frac{\partial C}{\partial y}\right)_{y=0}$; which is proportional to $-\left(\frac{\partial \phi}{\partial \eta}\right)_{\eta=0}$,

hence we have $S_h \propto \phi'(0)$.

The numerical values proportional to the skin-friction coefficients, the *Nusselt* number and the *Sherwood* number are sorted in Tables 5.1-5.5.

5.5. Numerical Solution

Equations (5.42)-(5.45) with boundary conditions (5.46) are solved numerically by a standard initial value solver, i.e., the shooting method. For the purpose, we have applied the *Nacthsheim-Swigert* iteration technique. The same is discussed in the earlier case and we are not going to discuss that here again.

5.6. Results and Discussion

In this thesis, the effects of viscous dissipation and joule heating on steady MHD combined heat and mass transfer flow through a porous medium in a rotating system have been investigated using *Nachtsheim-Swigerts* shooting iteration technique. To study the physical situation of this problem, we have computed the numerical values of the velocities, temperature, concenteration, within the boundary layer and also find the skin friction coefficients, *Nussel and Sherwood* number at the plate. It can be seen that the solutions are affected by the nondimensional parameters and numbers, namely suction parameter f_w, local *Grashof* number G_r, local modified *Grashof* number G_m, permiability parameter K, Magnetic parameter M, *Prandtl* number P_r, *Eckert* number E_c, *Dufour* number D_f, *Schmidt* number S_c, *Soret* number S_o, rotation parameter R.

The values of G_r, G_m are taken to be large, since these values corresponds to a cooling

problem, that is generally encountered in nuclear engineering in connection with the cooling of reactors.

The result of numerical calculations are presented in the form of parimary $\left(\frac{u}{U_0}\right)$ and secondary (g_0) velocities in Figs. (5.2)-(5.19) for different values of f_w, M, R, S_0, D_f, E_c, P_r, S_c and K. The values $0.2, 0.5, 0.71, 1, 2$ and 5 are considered for *Prandtl* number P_r ($0.2, 0.5, 0.71$ for air and $1.0, 2.0, 5.0$ for water). The values $0.1, 0.5, 0.6, 0.95, 5$ and 10 are also considered for *Schmidt* number S_c, which represent specific conditions of the flow (0.95 for CO_2 and $0.1, 0.5, 0.6, 5$ and 10 for water). The values of other parameters are chosen arbitrarily. The effects of various parameters on the primary velocity are shown in Figs. 5.2-5.10. From Fig. 5.2, it can be seen that the primary velocity field increases with the increase of suction parameter f_w, for both $f_w > 0$ and $f_w < 0$, indicating the usual fact that suction stabilizes the boundary layer growth. The free convection effect is also apparent in this figure. For $\eta = 1.5$, the velocity field is found to increase and reaches a maximum value in a region close to the leading edge of the plate, then gradually decreases to one. Fig. 5.3 shows the primary velocity for different values of Magnetic parameter M and has a decreasing effect with increase of M. The magnetic field can therefore be used to control the flow characteristics. The variation of the primary velocity for different values of rotation parameter R is shown in Fig. 5.4. It is seen that the Rotation parameter R has a minor decreasing effect on the primary velocity. In Figs. 5.5-5.7 the variations of the primary velocity for different values of *Soret* number S_o, *Dufour* number D_f and the *Eckert* number E_c are shown respectivly. From these figures it is observed that the primary velocity uniformly increases with the increase of *Soret* number S_o, *Dufour* number D_f and the *Eckert* number E_c. In Figs. 5.8-5.10, the variations of the primary velocities for different values of *Prandtl* number P_r, *Schmidt* number S_c, Permeability parameter K are shown respectively. Fig.5.8 and 5.9 show that the magnitude of the primary velocities have a overshoot behaviour for small *Prandtl* number P_r and *Schimdt* number S_c. But for larger values of $P_r\,(P_r = 0.5)$ and S_c the velocities are found to decrease monotonically and hence there appears a thin boundary layer indicating the decrease of the free convection. Also the parimary velocity decreases with the increase of Permeability parameter K.

The effects of various parameters on the secondary velocity (g_0) are shown in Figs. 5.11-5.19. From Fig. 5.11, it can be seen that the secondary velocity field decreases with the increase of

suction parameter f_w, for both $f_w > 0$ and $f_w < 0$, indicating the usual fact that suction stabilizes the boundary layer growth. The free convection effect is also apparent in this figure. For $\eta = 1.8$, the velocity field is found to decrease and reaches a minimum value in a region close to the lading edge of the plate, then gradually inecreases to zero. Fig. 5.12 shows the secondary velocity for different values of Magnetic parameter M and shows a large increasing effect with increase of M. In Figs. 5.13-5.16 the variations of the secondary velocity for different values of rotation parameter R, *Soret* number S_o, *Dufour* number D_f and the *Eckert* number E_c, are shown respectivly. From these figures it is observed that the secondary velocity decreases with the increase of rotation parameter R, *Soret* number S_o, *Dufour* number D_f and the *Eckert* number E_c. In Figs. 5.17-5.19, the variations of the secondary velocities for different values of *Prandtl* number P_r, *Schmidt* number S_c and Permeability parameter K are shown respectively. It is observed from these figures that the large increasing effects are occurred on the secondary velocity with the increase of *Prandtl* number P_r, *Schmidt* number S_c and Permeability parameter K.

The effects of various parameters on non-dimensional temperature are shown in Figs. 5.20-5.28. In Figs. 5.20 and 5.21, the temperature profiles for different values of the Suction parameter f_w, Magnetic parameter M are shown respectively. It is observed from these figures that the temperature increases uniformly with the increase of Suction parameter f_w and minor increasing effect is found with the increase of Magnetic parameter M. In Figs. 5.22 and 5.23, the temperature field for different values of rotation parameter R and *Soret* number S_o are shown respectively. It is observed from these figures that the Rotation parameter R has a negligible minor decreasing effect on the temperature while *Soret* number S_o has a minor decreasing effect on the temperature. In Figs. 5.24 and 5.25, the temperature fields for different values of *Dufour* number D_f and *Eckert* number E_c are shown respectively. It is observed from these figures that the temperature field increases uniformly with the increase of *Dufour* number D_f and *Eckert* number E_c. The temperature field is shown in Fig. 5.26, for different values of Prandtl number P_r. It is observed from Fig. 5.26 that the *Prandtl* number P_r has a large decreasing effect on temperature. In Figs. 5.27 and 5.28, the temperature profiles for different values of *Schmidt* number S_c and both Permeability parameter K are shown respectively. It is observed from these figures that both the *Schmidt* number S_c and Permeability parameter K have increasing effect on temperature though the effect of permeability parameter K is minor.

The effects of various parameters on the concentration field are shown in Figs. 5.29 - 5.37. In Figs. 5.29 and 5.30, the concentration profiles for different values of Suction parameter f_w and Magnetic parameter M are shown respectively. It is observed from these figures that the concentration increases uniformly as the suction parameter f_w increases while Magnetic parameter M has a minor increasing effect on the concentration with the increase of M . In Figs. 5.31 and 5.32, the concentration profiles for different values of Rotation parameter R and *Soret* number S_o are shown respectively. It is observed from these figures that the Rotation parameter R has a minor increasing effect on the concentration while Soret number S_o has decreasing effect on the concentration. Figs. 5.33 and 5.34 represents the concentration profiles for different values of *Dufour* number D_f and *Eckert* number E_c respectively. It is observed from these figures that the concentration decreases as the *Dufour* number D_f increases while the concentration decreases as the *Eckert* number E_c increases. In Figs. 5.35-37, the concentration profiles for different values of *Prandtl* number P_r, *Schmidt* number S_c and Permeability parameter K are shown respectively. It is seen from these figures that the *Prandtl* number P_r has increasing effect on the concentration as the *Prandtl* number P_r increases while the concenteration field rapidly decreases with the increase of *Schmidt* number S_c. It is also seen from Fig. 5.37 that the permeability parameter K has a minor increasing effect on the concentration field.

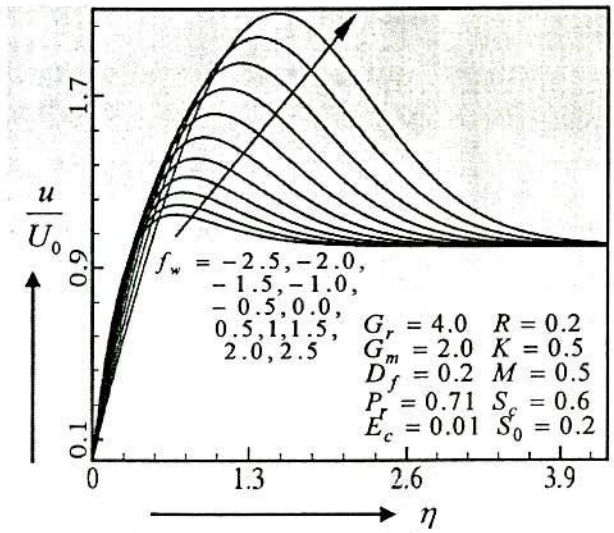

Figure 5.2. Primary velocity profiles for different values of f_w

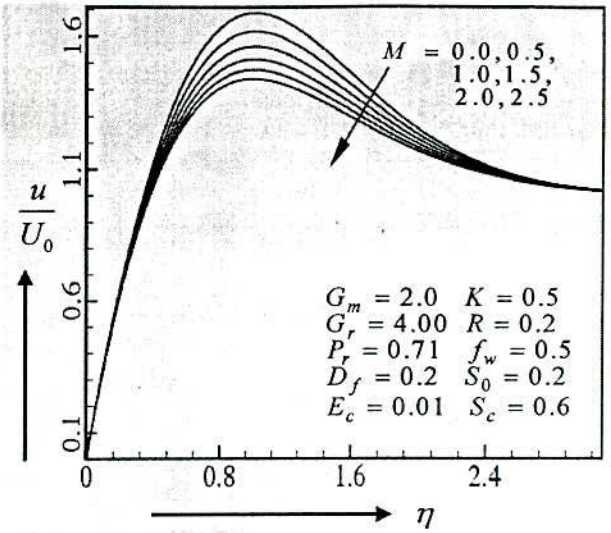

Figure 5.3. Primary velocity profiles for different values of M

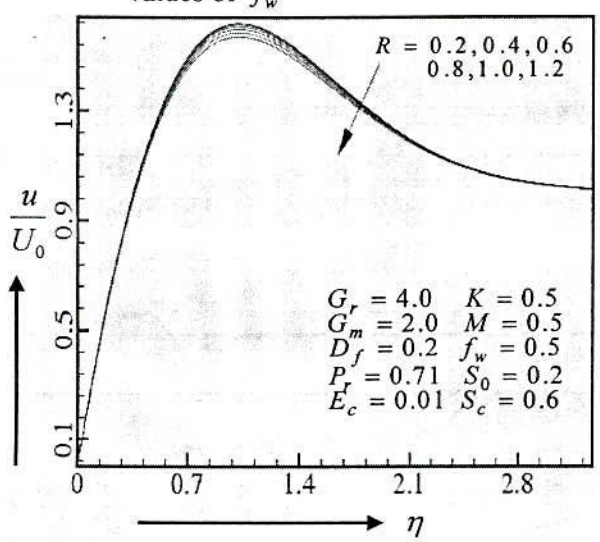

Figure 5.4. Primary velocity profiles for different values of R

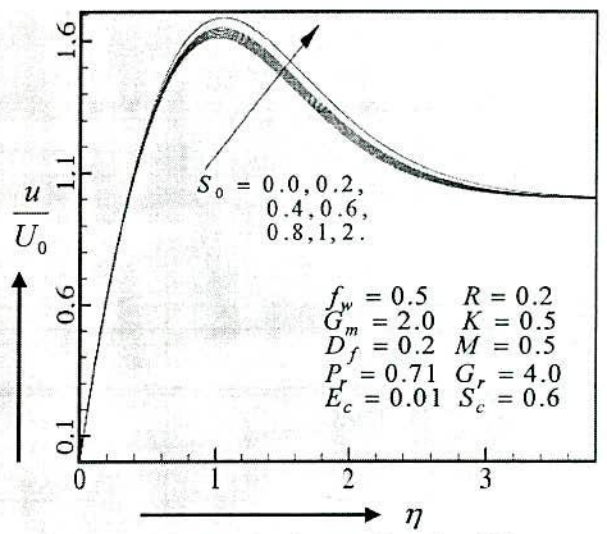

Figure 5.5.Primary velocity profiles for different values of S_0

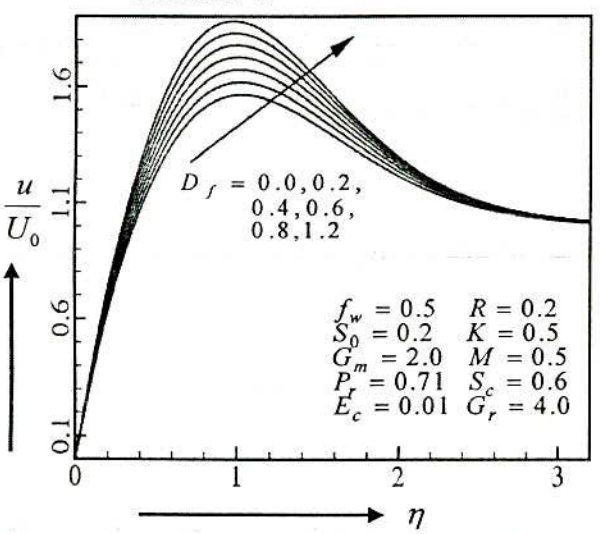

Figure 5.6. Primary velocity profiles for different values of D_f

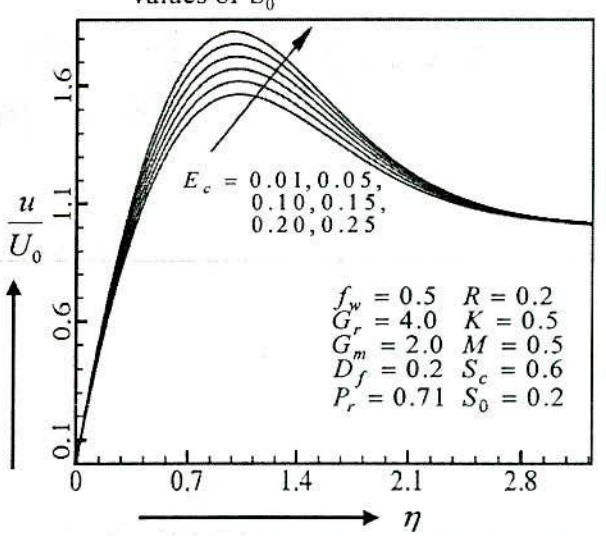

Figure 5.7. Primary velocity profiles for different values of E_c

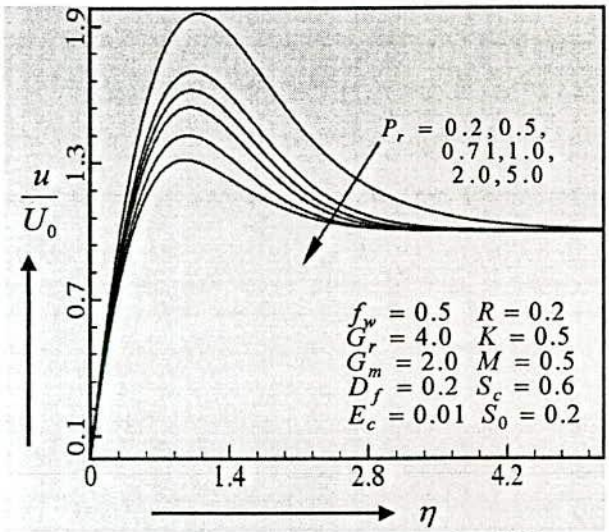

Figure 5.8. Primary velocity profiles for different values of P_r

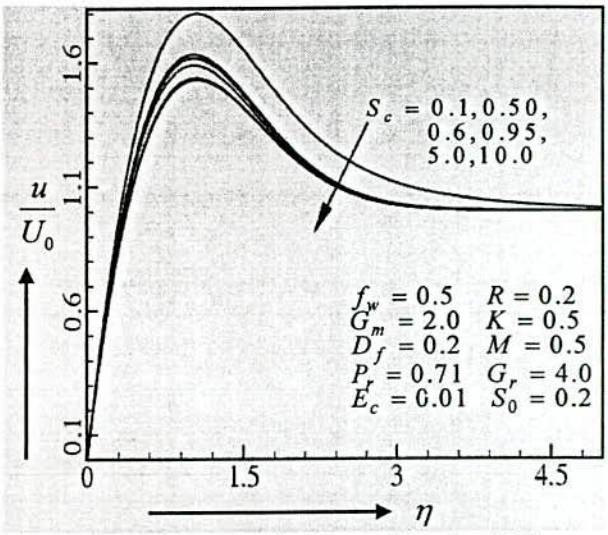

Figure 5.9. Primary velocity profiles for different values of S_c

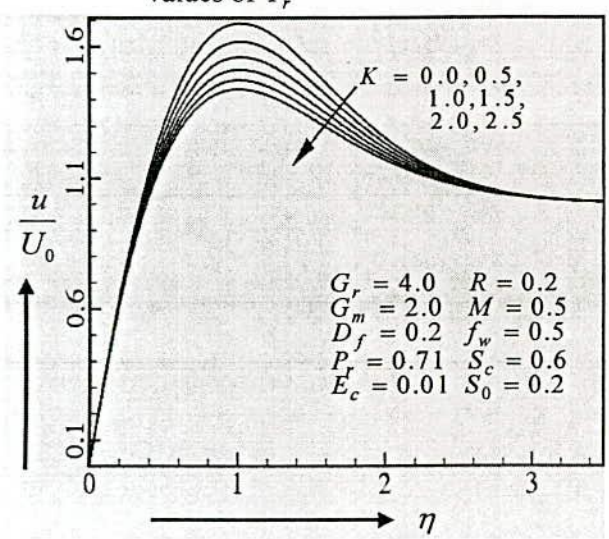

Figure 5.10. Primary velocity profiles for different values of K

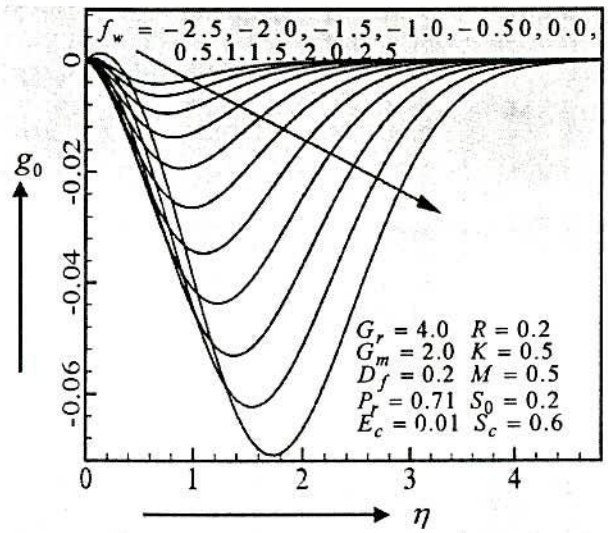

Figure 5.11. Secondary velocity profiles for different values of f_w

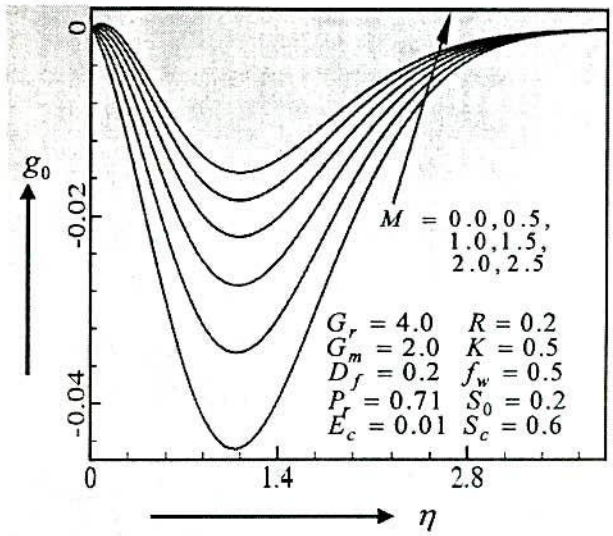

Figure 5.12. Secondary velocity profiles for different values of M

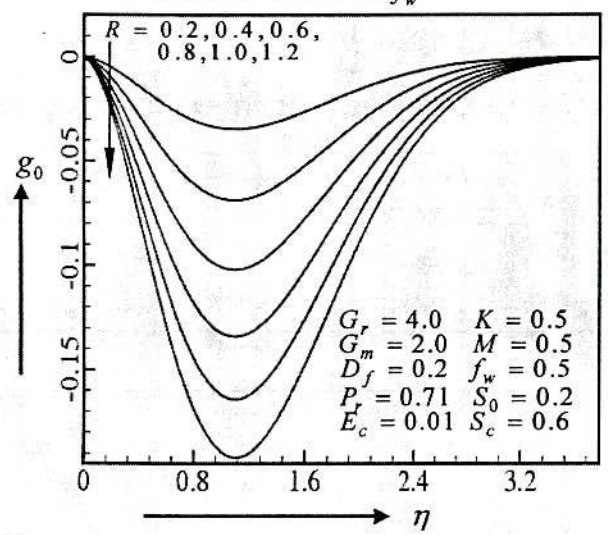

Figure 5.13. Secondary velocity profiles for different values of R

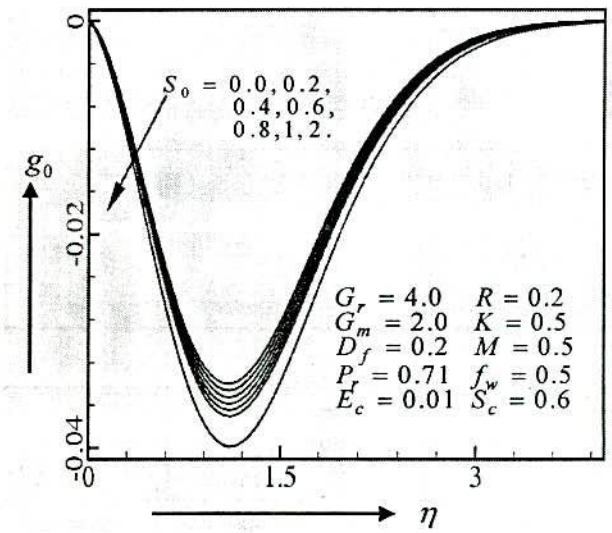

Figure 5.14. Secondary velocity profiles for different values of S_0

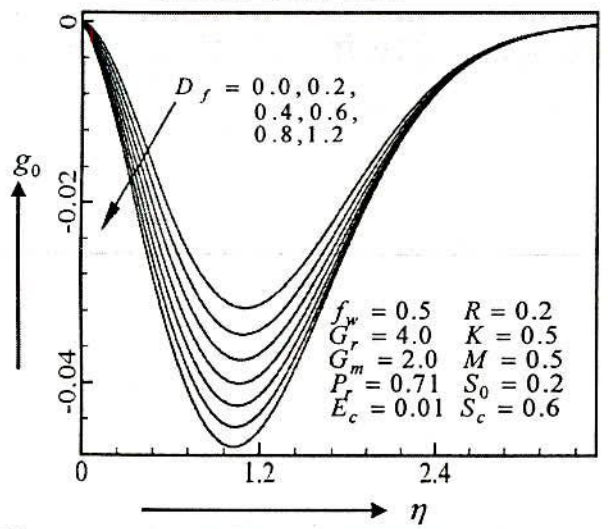

Figure 5.15: Secondary velocity profiles for different values of D_f

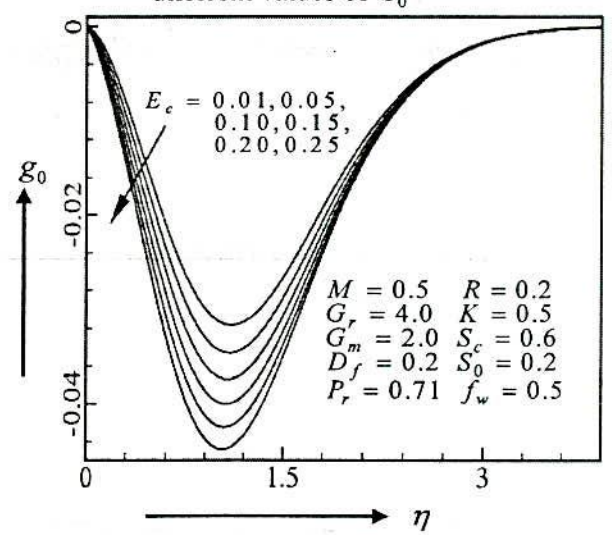

Figure 5.16: Secondary velocity profiles for different values of E_c

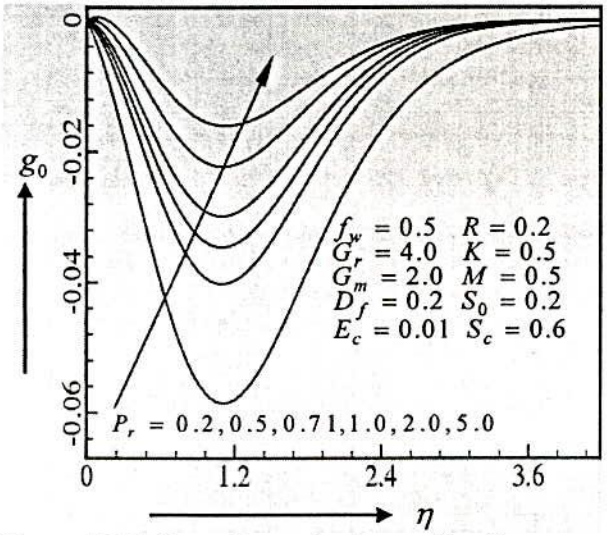

Figure 5.17. Secondary velocity profiles for different values of P_r

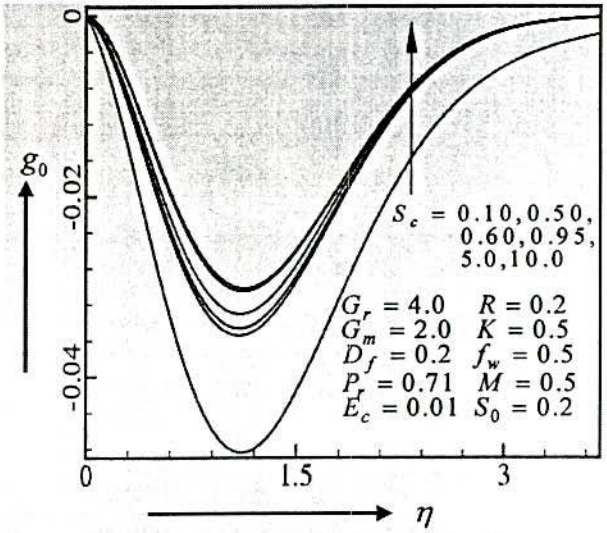

Figure 5.18. Secondary velocity profiles for different values of S_c

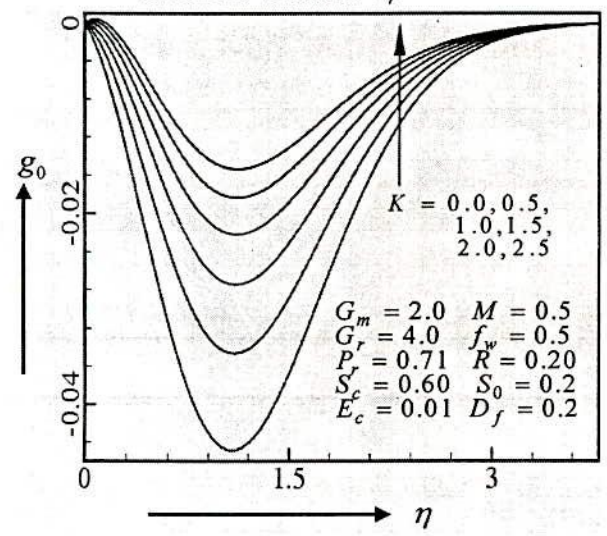

Figure 5.19. Secondary velocity profiles for different values of K

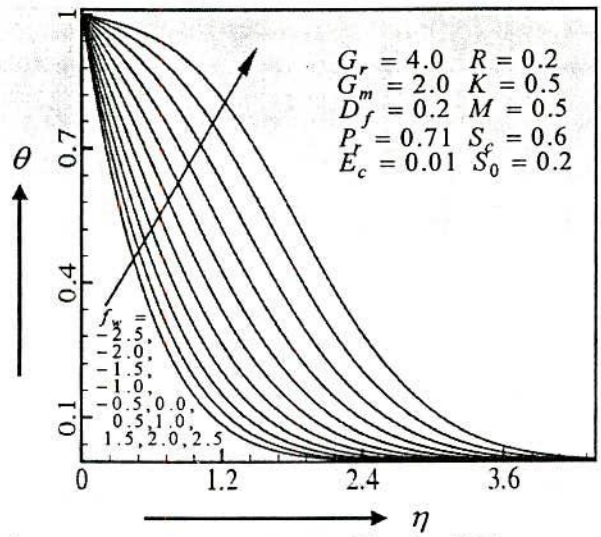

Figure 5.20. Temperature profiles for different values of f_w

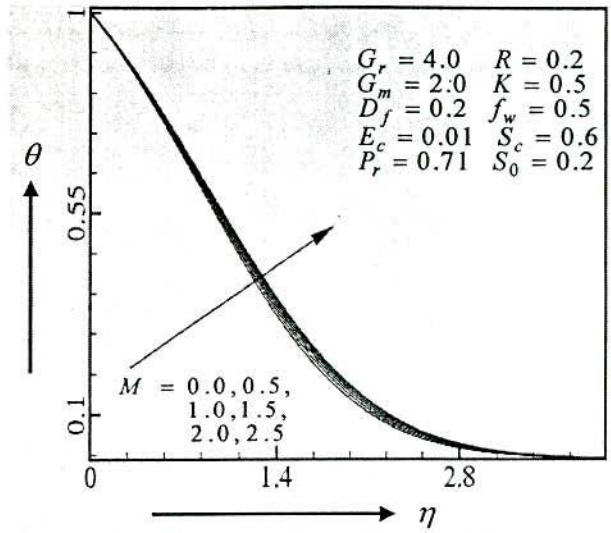

Figure 5.21. Temperature profiles for different values of M

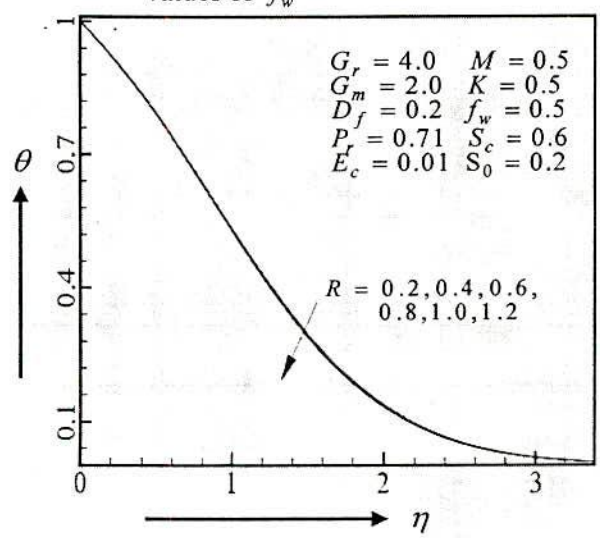

Figure 5.22. Temperature profiles for different values of R

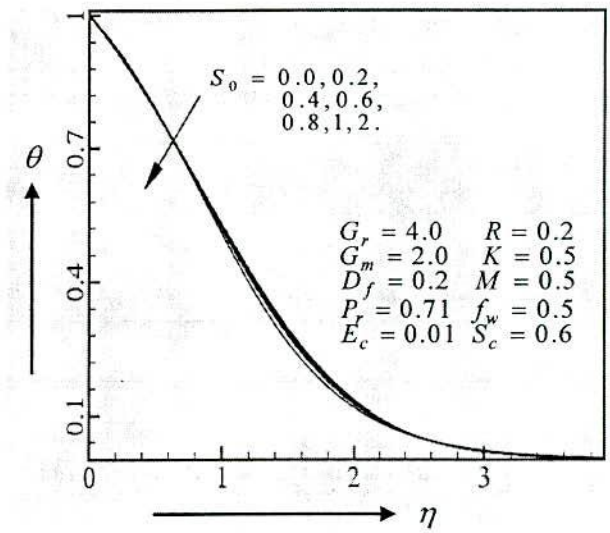

Figure 5.23. Temperature profiles for different values of S_0

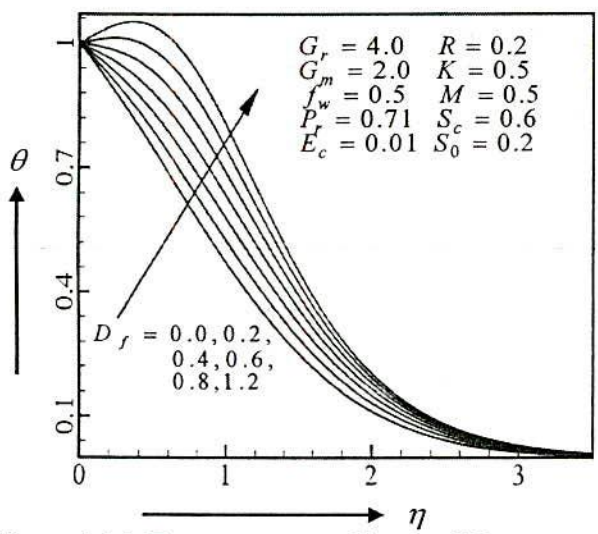

Figure 5.24. Temperature profiles for different values of D_f

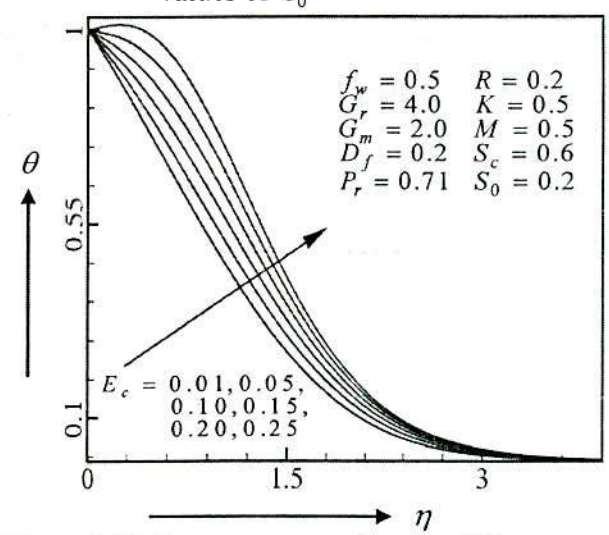

Figure 5.25. Temperature profiles for different values of E_c

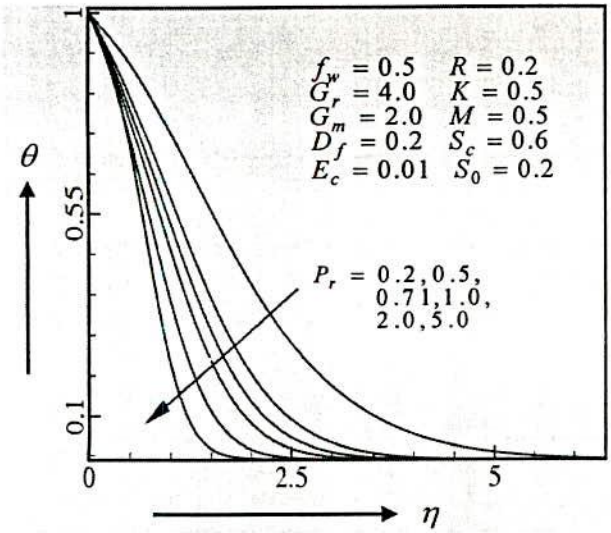

Figure 5.26. Temperature profiles for different values of P_r

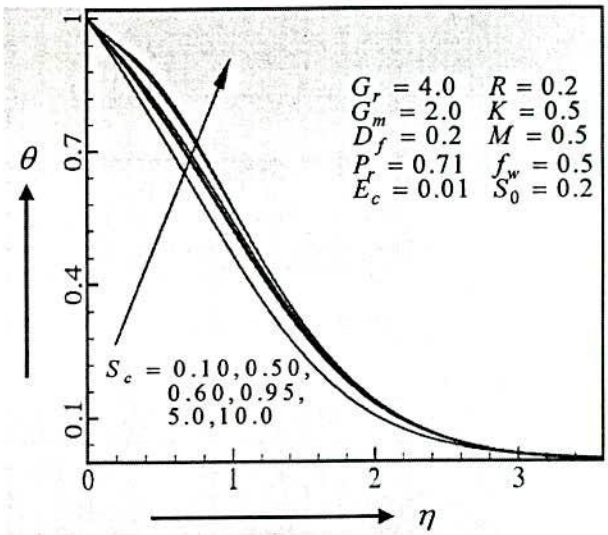

Figure 5.27. Temperature profiles for different values of S_c

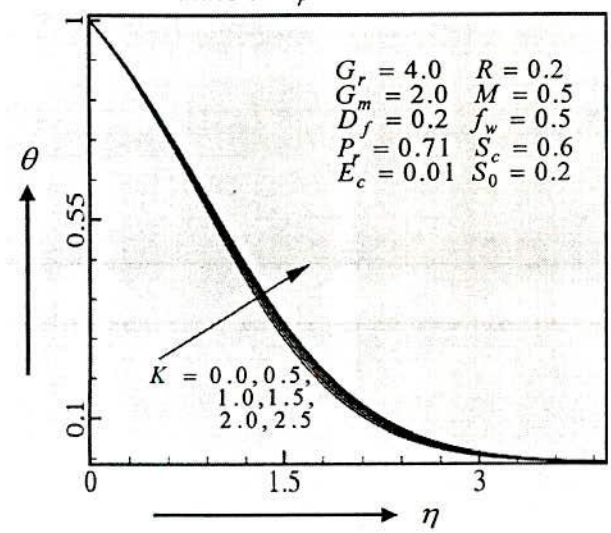

Figure 5.28. Temperature profiles for different values of K

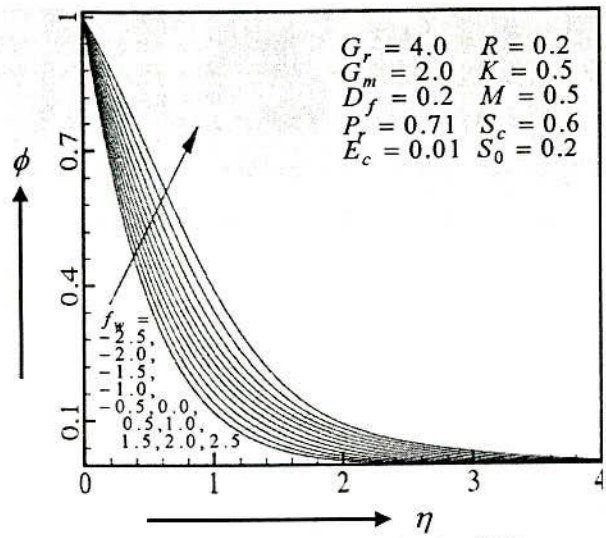

Figure 5.29. Concentration profiles for different values of f_w

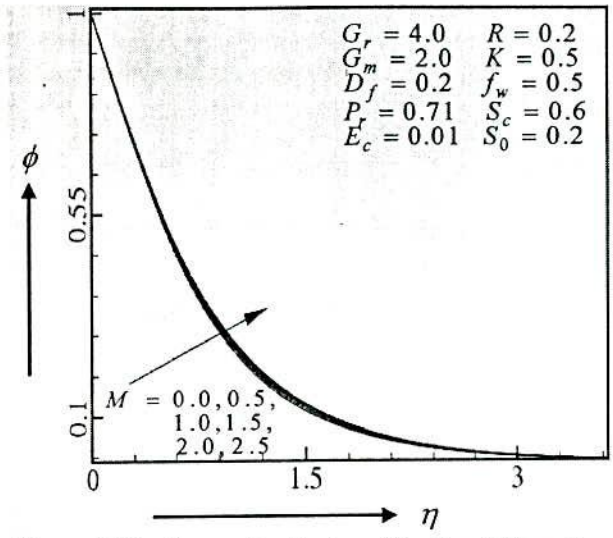

Figure 5.30. Concentration profiles for different values of M

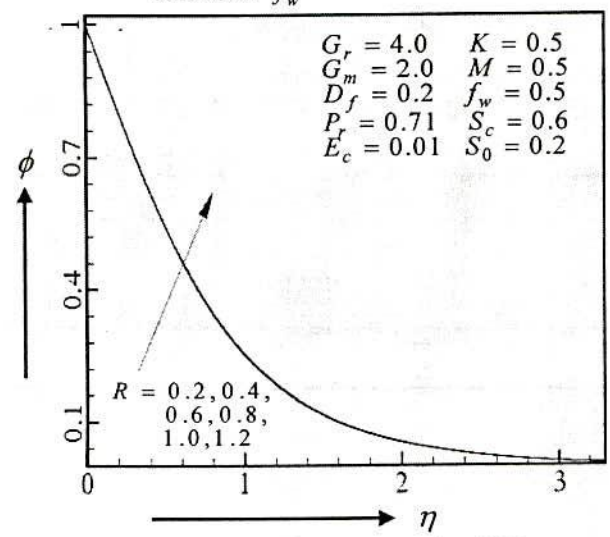

Figure 5.31. Concentration profiles for different values of R

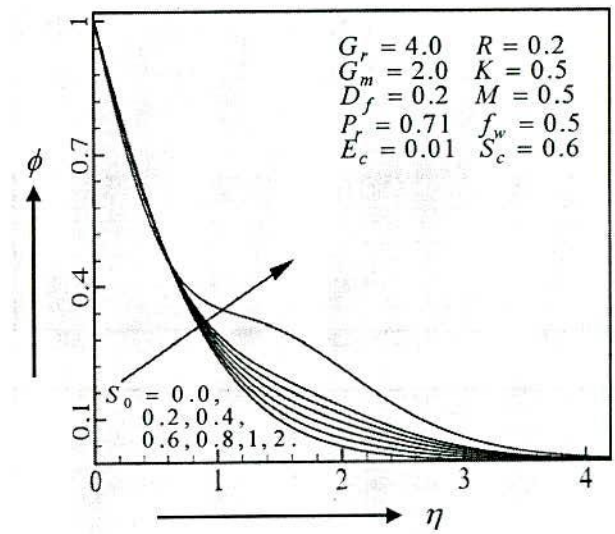

Figure 5.32. Concentration profiles for different values of S_0

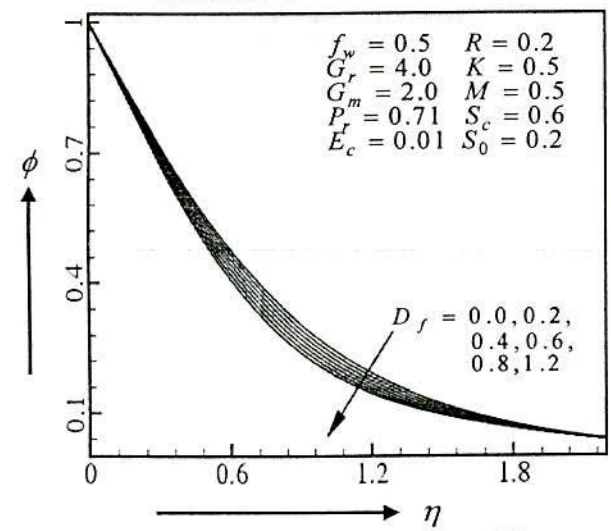

Figure 5.33. Concentration profiles for different values of D_f

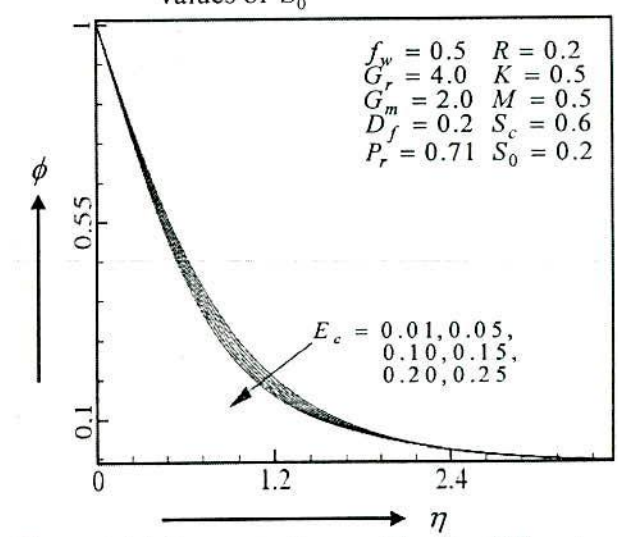

Figure 5.34. Concentration profiles for different values of E_c

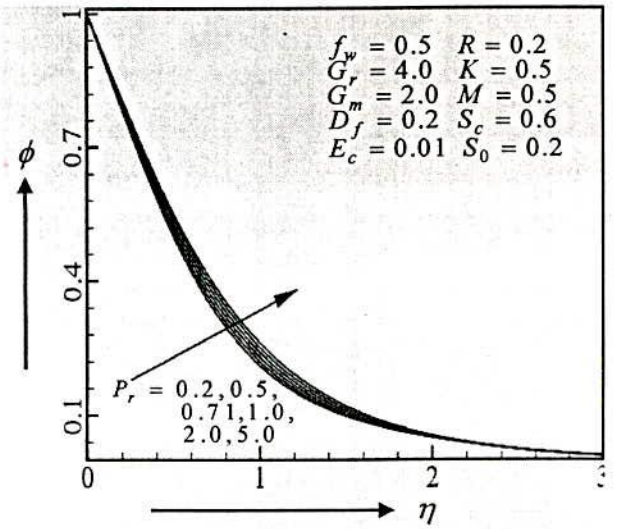

Figure 5.35. Concentration profiles for different values of P_r

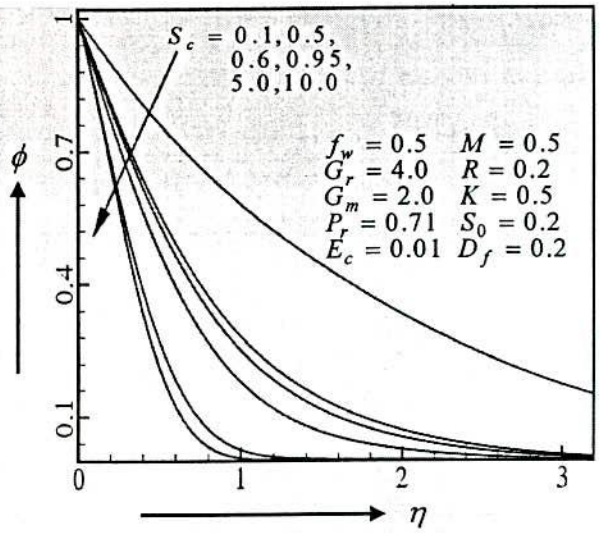

Figure 5.36. Concentration profiles for different values of S_c

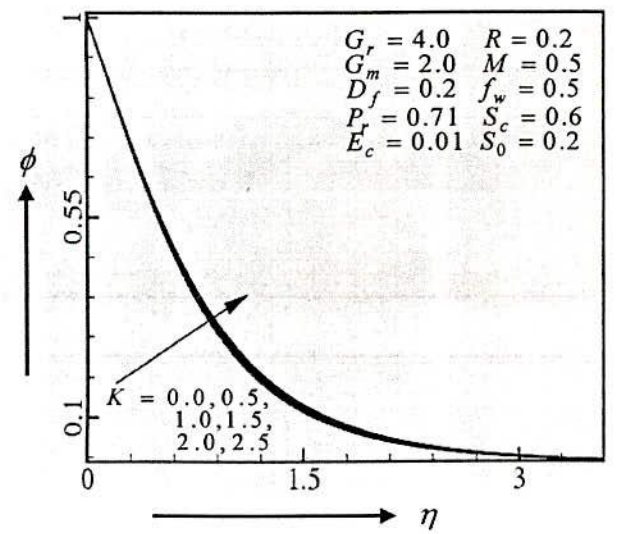

Figure 5.37. Concentration profiles for different values of K

Finally, the values proportional to skin friction coefficients τ_x, τ_z, the *Nusselt* number N_u and the *Sherwood* number S_h are tabulated in Tables 5.1-5.5 to indentify the effects of various nondimensional parameters and numbers on them. From Table 5.1, we observe that the skin friction component τ_x increases whereas the *Nusselt* number N_u, the *Sherwood* number S_h and the skin friction component τ_z decreases with the increase of suction parameter f_w. From Table 5.2, we observe that the skin friction component τ_x, the *Nusselt* number N_u and the *Sherwood* number S_h decreases while the skin friction component τ_z increases with the increase of Magnetic parameter M. It is also observed from this table that the skin friction component τ_z, the *Nusselt* number N_u and the *Sherwood* number S_h decreases on the other hand the skin friction component τ_x increases with the increase of rotation parameter R. We observe from Table 5.3 that the skin friction components τ_x, τ_z and the *Nusselt* number N_u decreases while the *Sherwood* number S_h increases with the increase of *Soret* number S_o. It is also seen from this table that the skin friction components τ_x, τ_z and the *Sherwood* number S_h increases while the *Nuselt* number N_u decreases with the increase of *Schmidt* number S_c. From Table 5.4, we observe that the skin friction components τ_x, τ_z, and the *Nusselt* number N_u decreases while the *Sherwood* number S_h increases with the increase of *Dufour* number D_f. It is also observed from this table that the skin friction components τ_x, τ_z and the *Nusselt* number N_u increases while the *Sherwood* number S_h decreases with the increase of *Prandtl* number P_r. From Table 5.5, we observe that the skin friction component τ_x, the *Nusselt* number N_u and the *Sherwood* number S_h decreases and the skin friction component τ_z increases with the increase of permeability parameter K. It is also observed from this table that the skin friction components τ_x, τ_z, the *Nusselt* number N_u decreases and the *Sherwood* number S_h increases with the increase of *Eckert* number E_c.

Table 5.1. Numerical values propotional to τ_x, τ_z, N_u and S_h taking $G_r = 4, G_m = 2$, $R = 0.2$, $M = 0.5, P_r = 0.71, S_o = 0.2, S_c = 0.6, D_f = 0.2, K = 0.5$ and $E_c = 0.01$ with f_w to vary.

f_w	τ_x	τ_z	N_u	S_h
-2.5	-5.3970229	.0095642	1.6758812	1.8607977
-2.0	-5.1216523	.0052565	1.4084526	1.6964478
-1.5	-4.8538308	.0003204	1.1544840	1.5418072
-1.0	-4.5853473	-.0046324	.9184907	1.3960458
-0.5	-4.3070914	-.0086552	.7053785	1.2573834
00	-4.0104591	-.0105361	.5201109	1.1232665
0.5	-3.6917408	-.0113294	.3663491	.9914265
1.0	-3.3536806	-.0137340	.2458710	.8607047
1.5	-3.0067006	-.0155478	.1577621	.7319121
2.0	-2.6667044	-.0179716	.0983641	.6079297
2.5	-2.3505682	-.0187566	.0618422	.4930417

Table5.2. Numerical values propotional to τ_x, τ_z, N_u and S_h taking $f_w = 0.5$, $G_r = 4, G_m = 2$, $P_r = 0.71, S_o = 0.2$, $S_c = 0.6$, $D_f = 0.2$, $K = 0.5$ and $E_c = 0.01$ with M and R to vary

M	R	τ_x	τ_z	N_u	S_h
0.0	0.2	-3.5022917	-.0220123	.3742230	1.0036013
0.5	,,	-3.6917408	-.0093294	.3663491	.9914265
1.0	,,	-3.6980711	-.0008342	.3597538	.9818533
1.5	,,	-3.7164723	.0050039	.3541684	.9742727
2.0	,,	-3.7435833	.0091054	.3493845	.9682283
2.5	,,	-3.7770366	.0120398	.3452420	.9633798
0.5	0.2	-3.6917408	-.0093294	.3663491	.9914265
,,	0.4	-3.6860095	-.0179782	.3658385	.9904204
,,	0.6	-3.6766617	-.0252933	.3650000	.9887717
,,	0.8	-3.6639933	-.0306751	.3638521	.9865216
,,	1.0	-3.6483983	-.0336014	.3624201	.9837260
,,	1.2	-3.6303484	-.0336476	.3607351	.9804528

Table 5.3. Numerical values propotional to τ_x, τ_z, N_u and S_h taking $f_w = 0.5, G_r = 4$, $G_m = 2$, $P_r = 0.71, R = 0.2$, $M = 0.5$, $D_f = 0.2, E_c = 0.01$ and $K = 0.5$ with S_o and S_c to vary.

S_o	S_c	τ_x	τ_z	N_u	S_h
0.0	0.6	-3.6863470	-.0087116	.3686189	.9793709
0.2	,,	-3.6917408	-.0093294	.3663491	.9914265
0.4	,,	-3.6970671	-.0099420	.3637905	1.0049244
0.6	,,	-3.7023847	-.0105583	.3608885	1.0200427
0.8	,,	-3.7075551	-.0111624	.3576506	1.0369413
1.0	,,	-3.7126155	-.0117608	.3540188	1.0558461
2.0	,,	-3.7355230	-.0146655	.3280050	1.1907625
0.2	0.10	-3.9076176	-.0253921	.4499665	.5033741
,,	0.50	-3.7102878	-.0104183	.3754558	.9377720
,,	0.60	-3.6917408	-.0093294	.3663491	.9914265
,,	0.95	-3.6490389	-.0070213	.3439702	1.1239821
,,	5.00	-3.5444672	-.0024614	.3052763	1.3840714
,,	10.00	-.3.267398	-.0010966	.2906047	1.5218182

Table5.4. Numerical values propotional to τ_x, τ_z, N_u and S_h taking $f_w = 0.5, G_m = 2$, $G_r = 4$, $K = 0.5, R = 0.2$, $M = 0.5, S_0 = 0.2$, $E_c = 0.01$ and $S_c = 0.6$ with D_f and P_r to vary.

D_f	P_r	τ_x	τ_z	N_u	S_h
0.0	0.71	-3.6099163	-.0049333	.4575134	.9688530
0.2	,,	-3.6917408	-.0093294	.3663491	.9914265
0.4	,,	-3.7758098	-.0136408	.2693714	1.0144665
0.6	,,	-3.8622569	-.0178842	.1662347	1.0380500
0.8	,,	-3.9510433	-.0220521	.0566285	1.0622193
1.0	,,	-4.0423218	-.0261582	-.0598571	1.0870546
1.2	,,	-4.1362128	-.0302091	-.1836539	1.1126291
0.2	0.2	-4.0427357	-.0372245	.2040620	1.0529437
,,	0.5	-3.7811806	-.0160653	.3275896	1.0068981
,,	0.71	-3.6917408	-.0093294	.3663491	.9914265
,,	1.0	-3.6124076	-.0035178	.3938730	.9787620
,,	2.0	-3.4827098	.0058550	.3973896	.9651949
,,	5.0	-3.3913691	.0134775	.3994546	.9543460

Table 5.5. Numerical values propotional to τ_x, τ_z, N_u and S_h taking $f_w = 0.5, G_r = 4, G_m = 2$, $P_r = 0.71, R = 0.2$, $M = 0.5$, $S_0 = 0.2$, $D_f = 0.2$ and $S_c = 0.6$ with K and E_c to vary.

K	E_c	τ_x	τ_z	N_u	S_h
0.0	0.01	-3.6831492	-.0220644	.3732633	1.0038458
0.5	,,	-3.6917408	-.0093294	.3663491	.9914265
1.0	,,	-3.6975916	-.0008105	.3605262	.9816772
1.5	,,	-3.7157276	.0050371	.3555876	.9739627
2.0	,,	-3.7426961	.0091411	.3513642	.9678111
2.5	,,	-3.7760778	.0120748	.3477206	.9628722
0.5	0.01	-3.6917408	-.0093294	.3663491	.9914265
,,	0.05	-3.7218309	-.0105303	.2683589	1.0117531
,,	0.10	-3.7612753	-.0120986	.1403502	1.0382299
,,	0.15	-3.8029588	-.0137484	.0055945	1.0660079
,,	0.2	-3.8471337	-.0154884	-13666883	1.0952283
,,	0.25	-3.8940949	-.0173282	-.2873339	1.1260564

References

1) Acrivos,A.(1958). *Trans ACICHE*, **4**, 285-289.

2) Alfven, H. (1942). *On the existence of electromagnetic Hydromagnetic waves, Arkiv F.Mat. Astro. O. Fysik. Bd.*, **295** No. 2.

3) Adams, J. A. and Lowell, R. L. (1968). *Int. J. Heat Mass Transfer,* **11**, 1215.

4) Adams, J. A. and McFadden, P.W. (1966). *Amer. Inst. Chem. Eng. J.*, **12**, 642.

5) Agrawal, H. L., Ram, P. C. and Singh, S. S.(1977). *Acta, Phys. Acad. Sci.Hung.*,**42**,49.

6) Agrawal, H. L., Ram, P. C. and Singh, S. S. (1980). *Can. J. Chem. Engng.* **58**, 131.

7) Agrawal, H. L., Ram, P. C. and Singh, V. (1987). *Proc. Nat. Acad. Sci.*, **57(II)**,329.

8) Anghel, M., Takhur, H. S. and Pop, I. (2000). *Studia Universitatis Babes-Bolyai. Mathematica, Mathematica*, **XLV (4),** pp. 11-21.

9) Alam, M. S. and Rahman, M. M. (2006). *Nonlinear analysis: Modeling and Control, Vol.* **11**, No. 1, 1-10.

10) Batchelor,G. K.(1970). *An Introduction to fluid dynamics, Cambridge University Press.*

11) Bathaiah, D. (1978). *Int. J. Pure Appl. Math.*, **9(10)**, 996.

12) Bestman, A. R. (1990 a). *Astrophys. Space Sci.*, **173**, 93.

13) Bestman, A. R.(1990 b). *Int.l J. Energy Resch.* **14**, 389.

14) Bhat, J. P. (1982). *Czech. J. Phys.*, **B 32(9)**, 1050.

15) Bhattacharya, S. P. and Jain, S. K. (1977). *Proc. Ind. Nat. Sci. Acad. A*, **43(3)**, 201.

16) Boura, A. and Gebhart, B. (1976). *.Amer. Inst. Chem. Eng., J.* **22**, 94.

17) Cobble, M. H. (1977). *J. Engg. Maths.* **11**, 249.

18) Debnath, L. (1972). *ZAMM,* **52**, 623.

19) Debnath, L. (1975). ZAMM **55**, 141.

20) Debnath, L. and Mukherjee, J. (1977). *Lett. Appl. and Eng. Sci.,* **5(5)**, 371.

21) Debnath, L., Roy, S. C. and Chatterjee, A. K. (1979). *SAMM,* **59**, 469.

22) Eshghy, S. (1964). *J. Heat Transfer (Tr. ASME)*, **86** (Ser. C), 290-291.

23) Eckert, E. R. G, and Drake, R. M. (1972). *Analysis of Heat and Mass Transfer, McGraw-Hill Book Co., New York.*

24) Faraday, M. (1832). *Experimental Researches in electrically Phill, Trans.* **15**, 175.

25) Gebhart, B. and Pera, L. (1971). *Int. J. Heat Mass Transfer,* **14**, 2025.

26) Georgantopoulos, G. A., Koullias, J., Goudas, C. L, and Couragenis, C. (1981). *Astrophys. Space Sci.,* **74**, 359.

27) Georgantopoulos, G. A, and Nanousis, N. D. (1980). *Astrophys. Space Sci.,* **67(1)**, 229.

28) Gill, W. N., Casel, A. D. and Zeh, D. W. (1965). *Int, J. Heat Mass* Transfer, **8**,1131.

29) *Greenspan, H. P. and Howard, L. N.* (1963). **17**, 385.

30) Greenspan, H. P. (1968). *The theory of rotating fluids, Cambridge University Press.*

31) Gupta, A. S. (1972). *J. Phys. Fluids,* **15**, 930.

32) Gupta, A. S. and Soundalgekar, V. M. (1975). *ZAMM,* **55**, 762.

33) Hasimoto, H. (1957). *J. of the Physical Society of Japan,* **12(1)**, 68.

34) Haldavnekar, D. D. and Soundalgekar, V. M. (1977). *Acta. Phys. Acad. Sci. Hung.* **43**, (3/4), 243.

35) Hossain, M. A.(1990). *ICTP, Internal Print no* IC/**90**/265.

36) Hubbel, R. H. and Gebhart, B. (1974). *Proceedings of 24th Heat Mass Transfer and Fluid Mech.Inst. Corvallis, Oregon (USA).*

37) Inger, G. R. and Swearn, T. F. (1975). *AIAA, J.* **13(5)**, 616.

38) Jha, B. K. and Singh, A. K. (1990). *Astrophys. Space Sci.* **173**, 251.

39) Kafoussias, N. G. and Williams, E. M. (1995). *Int. J. Eng. Sci.,* **33**, 1369-1384.

40) Light foot, E. N. (1968). *Chem. Eng. Sci.,* **23,** 931.

41) Lowell, R. L. and Adams, J. A. (1967). *AIAA, J.,* **5**, 1360.

42) Mathers, W. G., Maddan, A. J. and Piret, E. L. (1957). *Ind. Eng. Chem.,* **49,** 961.

43) Mazumder, B. S. (1977). *Int. J. Eng. Sci.,* **15(910)**, 601.

44) Mazumder, B. A., Gupta, A. S. and Datta, N. (1976a). *Int. J. Heat Mass Transfer,* **19**, 523.

45) Mazumder, B. S., Gupta, A. S. and Datta, N. (1976b). *Int. J. Eng. Sci.,* **14**, 258.

46) Mayer, R. C. (1958). *J. Aerospace Sci.,* 25, 561.

47) Merkin, J. H. (1969). *J. Fluid Mechanics,* **35**, 439-450.

48) Metais, B., and E.R.G.Eckert (1964). *J. Heat Tranfer, (Ser. C), vol.* **86**, 295.

49) Mori, Y. (1961). *J. Heat Transfer (Tr. ASME,* **83** *(Ser. C),* 479-482.

50) Mollendrof, J. C. and Gebhart, B. (1974). *Proceedings of 5th International Heat Transfer Conference, Tokyo.*

51) Murty, S. N. and Prabhakar Ram, R. K. (1978). *Nuovo Cimento B, 64B Series* **2(l)**, 189.

52) Nanousis, N. D. and Goudas, C. L. (1979). *Astrophys. Space Sci.,* **66(1)**, 13.

53) Nanbu, K. (1971). *AIAA, J.,* **9**, 1642.

54) Ostrach, S. (1953). *NACA Rept.,* 1111.

55) Pai, S. I. (1962). *Magnetogasdynamics and Plasma dynamics, Springier Verlag, New York.*

56) Pera, L. and Gebhart, B. (1972). *Int. J. Heat Mass Transfer,* **15**, 269.

57) Pohlhausen, E. (1921). *Zait. Angew. Math. Mech.,* **1**, 115.

58) Postelnicu A. (2004). *Int. J. Heat Mass Transfer,* **47**, 1467-1472.

59) Raptis, A. A., Kafoussias, N. G., Massalas, C. V. and Tzivanidis, G. J. (1980). *Indian J. of Pure Appl.Math.* **12(2)**, 253.

60) Raptis, A. A. (1983). *Aatrophys. Space Sci.,* **92(1)**, 135.

61) Raptis, A. A., Perdikis, C. P. and Tzivanidis, G. J. (1981). *Lett. Heat and Mass Transr,* **8(2)**,137.

62) Raptis, A. A. and Kafoussias, N. G. (1982). *Rev. Roum. Sci. Tech. Mech. Appl.,* **27(1)**, 37.

63) Raptis, A. A. and Tzivanidis, G. J. (1983). *Astrophys. Space Sci.* **94(2)**, 311.

64) Raptis, A. A. (1985). *Z. Appl. Math. Mech.,* **65**, 314.

65) Raptis, A. A. and Perdikis, C. P. (1982). *Astrophys. Space Sci.* **94(2),** 311

66) Raptis, A. A. and Perdikis, C. P. (1985a). *Int. Comm. Heat Mass Trans.* **12**, 697.

67) Raptis, A. A. and Perdikis, C. P. (1985b). *Int. J. Eng. Sci.* **23**, 51.

68) Raptis, A. A. and Perdikis, C. P. (1988). *Int. J. Energy Res.* **12**, 557.

69) Sattar, M. A. (1992). *Astrophys. Space Sci.* **191**, 323-328.

70) Sattar, M. A. (1993), International Journal of Energy Research, 17, p.1-7.

71) Sattar, M.A. and Alam, M.M.(1994). *Ind. J. of Pure and Applied Mathematics,* **25(6),** 679.

72) Saville, D. A. and Churchill, S. W. (1970). *Amer. Inst. Chem. Eng. J.* **16**, 268.

73) Schlichting, H. (1968). *Boundary Layer theory, McGraw-Hill, New york.*

74) Seth,G.S, and Jana, R.N.(1981).*Rev. Roum, des. Sci. Tech. series, de Mech.Appl.* **26(3)**,383

75) Seth, G. S., Jana, R. N, and Maiti, M. K. (1982). *Int. J. Eng. Sci.* **20(9)**, 989.

76) Siegel, R. (1958). *Trans. Amer. Soc. Mech. Eng.,* **80,** 347.

77) Singh, A. K. and Dikshit, C. K. (1988). *Astrophysics and Space Sci.* **148**, 249.

78) Singh, A. K. (1980). *Astrophys. Space Science,* **115**, 387.

79) Soundalgekar, V. M, and Rarnanarnurthy, T. V. (1980). *J. Engg. Maths.,* **14**, 155.

80) Soundalgekar, V. M, Vighnesam, N. V. and Pop, I. (1981). *Int. J. Energy Res.,* **5**, 215-226.

81) Soundalgekar, V. M., Gupta, S. K. and Birajdar, N. S. (1979). *Nucl. Eng. Des.,* **53(3)**, 339.

82) Soundalgekar, V. M. and Pop, I. (1979). *Acia Phys. Acad. Sci. Hung.,* **47**, 317.

83) Sparrow, E.M., and Gregg, J. L. (1959). *J. Appl. Mech. (Tr. ASMED),* **26E,** 133-134.

84) Szewczyk, A. A. (1964). *J. Heat Transafer (Tr. ASME),* **86C**, *501-507.*

85) Tenner, A. R. and Gebhart, B. (1971). *Int. J. Heat Mass Transfer,* **14**, 2051.

86) Yamamoto, K. and Iwamura, N. (1976). *J. Eng. Math.* **10**, 41.